DOCTOR DISSERTATION

Impact of Anodic Respiration on Membrane Fouling in Electrode-assisted Membrane Bioreactor

by

So ISHIZAKI

GRADUATE SCHOOL OF ENGINEERING
HOKKAIDO UNIVERSITY

DOCTOR DISSERTATION

Impact of Anodic Respiration on Membrane Fouling in Electrode-assisted Membrane Bioreactor

by

So ISHIZAKI

GRADUATE SCHOOL OF ENGINEERING
HOKKAIDO UNIVERSITY

DOCTOR DISSERTATION

Impact of Anodic Respiration on Membrane Fouling in Electrode-assisted Membrane Bioreactor

by

So ISHIZAKI

GRADUATE SCHOOL OF ENGINEERING
HOKKAIDO UNIVERSITY

TABLE of CONTENTS

CHAPTER 1

Introduction

1.1. Background

It is essential to fulfill various water demands with lower operational energy for future wastewater treatment system. An integrated system of microbial fuel cell (MFC) and membrane bioreactor (MBR) has been introduced as a promising energy-efficient approach for wastewater treatment (Wang et al., 2011b;Yuan and He, 2015). Since MFC could achieve poor effluent quality, installation of post-treatment system is necessary to fulfill water quality standards for wastewater treatment (Wang et al., 2011b). In while, MBR is capable of achieving high effluent quality, but its operation requires enormous energy for such as aeration (Gil et al., 2010;Kraume and Drews, 2010). Thus far, a variety type of the integrated system has been proposed (Yuan and He, 2015), and it is likely that the system in which membrane modules were installed in or equipped simultaneously to anode chamber is available for a net energy generation (Katuri et al., 2014;Li et al., 2016;Ren et al., 2014).

A reduction of membrane fouling is important for an increase in the net energy generation. Membrane fouling is recognized to be main obstacle for widespread utilization on MBR since it requires exceed operational energy and cost for air-scrubbing, membrane exchange, and/or frequent membrane cleaning (Judd, 2008;Meng et al., 2009b). It should be of greater concern for the integrated system to maximize the net energy generation due to no aeration for air-scrubbing and biological oxidation (Malaeb et al., 2013a). However, the effect of anodic respiration on membrane fouling has not been yet investigated.

Besides, identification and characterization of the bacteria causing severe membrane fouling (fouling-causing bacteria (FCB)) is essential for better understanding

of membrane fouling (Malaeb et al., 2013b). Although extensive studies were addressed to reveal FCB by using pure culture and/or actual MBR, FCB has not been identified on the basis of direct measurement of their fouling potential. The identification and characterization of FCB should be also helpful for the evaluation of membrane-fouling mitigation and elucidation of its detail mechanism.

1.2. Research objective

On the basis of this background, the main objective of this research was to reveal the effect of anodic respiration on fouling potential of bacteria responsible for membrane fouling. In order to achieve it, various specific objectives were established as follows:

1. To investigate the effect of anodic respiration on membrane fouling with MFC established by mixed population.
2. To evaluate fouling potential of bacteria isolated from MBR treating municipal wastewater and identify FCB and characterize their cellular property.
3. To evaluate the influence microbial interaction on fouling potential of FCB.
4. To investigate the effect of electron acceptor involving anodic respiration on fouling potential of FCB.

1.3. Structure of this thesis

This thesis comprises seven chapters as shown in **Figure 1**. Background information, research objective, and the structure of this thesis were described in Chapter 1. Chapter 2 provides basic information regarding this thesis as literature reviews.

In Chapter 3, the effect of anodic respiration on membrane fouling was investigated. Four MFC reactors with different value of external resistance to regulate the degree of anodic respiration were constructed, and subjected to measurements of fouling potential, bacterial secretion, and microbial community in the reactors.

Chapter 4 and 5 focused on the bacteria responsible for membrane fouling. In

Chapter 4, Forty-one bacterial strains were isolated from MBR treating municipal wastewater, and subjected to measurements of fouling potential with cross-flow membrane filtration system (CFMFS) and cellular properties to characterize FCB. In Chapter 5, the fouling potential of the bacterial strains as single-culture and co-culture to evaluate the influence microbial interaction on fouling potential of FCB.

In Chapter 6, the effect of electron acceptor on fouling potential of FCB was investigated. FCB was cultured with electrode, oxygen, nitrate as sole electron acceptor, and subjected to measurements of fouling potential and the secretion in the reactors. Conclusion remarks and recommendation topics for future were shown in Chapter 7.

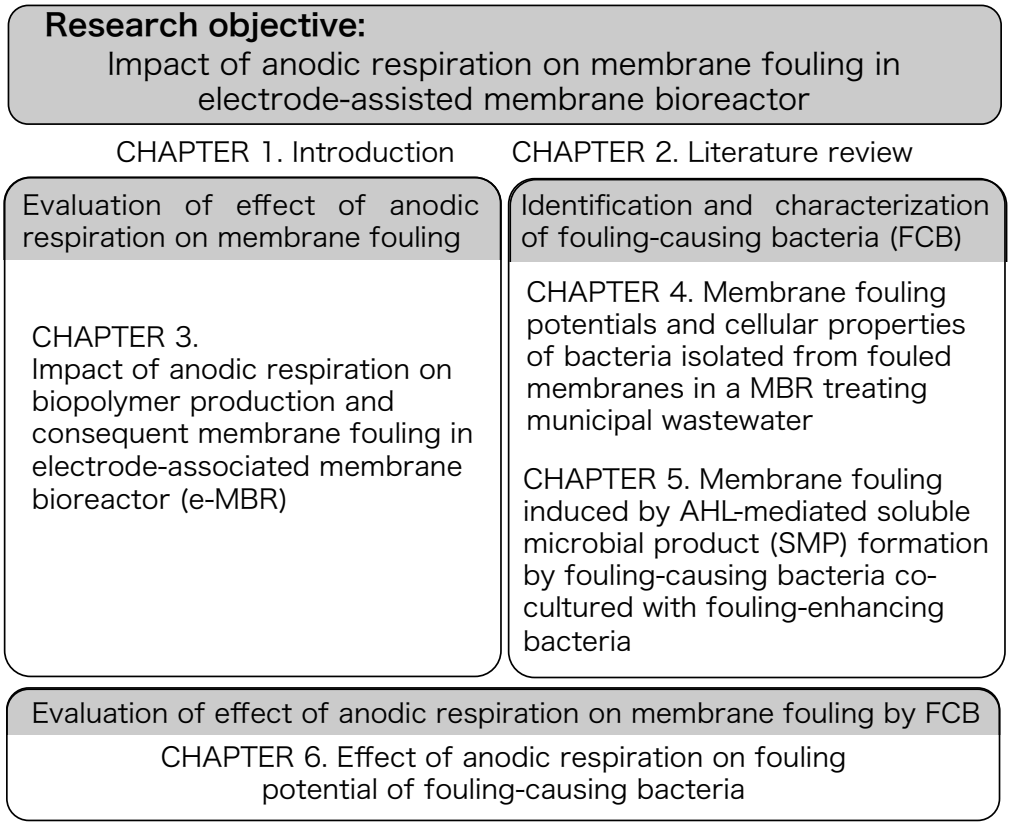

Figure 1.1 An overhead view of the structure of this thesis.

CHAPTER 2

Literature review

2.1. Microbial fuel cell (MFC)

2.1.1. Advantages for wastewater treatment

MFC is the device that is able to convert chemical energy to electrical energy through exoelectrogenic bacteria (Davis and Higson, 2007;Logan et al., 2006). As compared with conventional activated sludge (CAS) and the other energy recovery systems from wastewater (i.e. methane fermentation), MFC has several advantages for wastewater treatment as following: Higher energy efficiency (*vs.* methane fermentation) (Pham et al., 2006), no need for aeration(Rozendal et al., 2008), lower sludge production (Liu et al., 2005;Rabaey and Verstraete, 2005;Wang et al., 2012b).

Methane fermentation requires storage and combustion process for generating electricity, suggesting that energy loss and extra cost occur during electricity generation. In while, MFC allow to generate electricity directly by exoelectrogenic bacteria. In addition, as mentioned below, MFC does not required to be heated as like methane fermentation. This should help to increase net energy recovery (Pham et al., 2006).

Exoelectrogenic bacteria can oxidize organic compounds by reducing electrode instead of oxygen. This suggests that aeration does not required in MFC. Besides, MFC is known to produce lower volume of sludge as compared with CAS (Brown et al., 2015;Rabaey and Verstraete, 2005;Zhang et al., 2013). Since aeration and sludge treatment required enormous cost and energy (25-65% of cost and 45-75% of energy for operation of CAS were occupied by sludge treatment and aeration, respectively (Brown et al., 2015)), these advantages also work for energy-saving wastewater treatment.

2.1.2. Reactor configuration

1) Reactor

MFC comprises mainly three parts: Reactor, anode electrode, and cathode electrode. Separator is also important part, but its pattern and role is dependent on the configuration of reactor. Reactor configuration of MFC can be classified into three types; Separated, non-separated, and packed and fluidized bed reactor (Krieg et al., 2014). In terms of topological view, it can be categorized into single-chamber and double-chamber reactor (Single-chamber type reactor contains non-separated, and packed and fluidized bed reactor).

Single-chamber type reactor is available for higher generation of electricity and feasibility. As one of the configurations of this type reactor, cassette-electrode MFC has been well investigated (Miyahara et al., 2013;Shimoyama et al., 2008). This is available configuration for the practical utilization, because it is able to generate high cell voltage by connecting some modules and the modification of the configuration of CAS can be minimize to install.

In while, double-chamber type reactor is available for sustainable construction and operation, because bio-cathode has been recently developed (Jafary et al., 2015;Zhang et al., 2014a). As mentioned below, cathode electrode is known to main cause for expensive capital cost of MFC (Rozendal et al., 2008). In bio-cathode, instead of chemical catalyst for cathode electrode, bacteria which is capable of reducing cathode electrode was used as the catalyst (Jafary et al., 2015). Several papers succeeded long-term operation of MFC equipped with bio-cathode involving the integrated system (Liu et al., 2014;Wang et al., 2011b).

2) Electrode

Carbon-based material was mainly used as anode and cathode electrode (Krieg et al., 2014). As anode electrode, a variety of carbon-based electrode was developed; Carbon felt, cloth, brush, foam, nanotube, and fabric. As cathode electrode, aside from

carbon-based material, stainless steel mesh was frequently used as cathode electrode (Liu et al., 2014;Wang et al., 2011b).

For higher production of electricity, cathode-reaction limitation is crucial problem for enhancement of the production of electricity (Rismani-Yazdi et al., 2008;You et al., 2009). Cathode-reaction limitation can be classified into three parts; Activation loss, ohmic loss, and mass transport loss (Rismani-Yazdi et al., 2008). Ohmic loss is derived from ion transport through separator. Occurrence of mass transport loss is due to lower electric conductivity (Fan et al., 2007;Rozendal et al., 2008).

Proton shortage on cathode electrode is relevant to both ohmic resistance and mass transport loss. Proton shortage leads high cathodic pH, which results in a shift in the reaction mechanism of cathode reactions (Popat and Torres, 2016). As mentioned below, this problem is well related to the separator of MFC.

3) Separator

For separators, cation-exchange membrane (CEM), anion-exchange membrane (AEM), bipolar membrane were used as ion exchange membrane. In MFC, cation species consists mainly of sodium, potassium, ammonium, and proton. In while, anion species consists mainly of organic compounds (i.e. acetate and propionate), carbonate, and phosphate ion. As compared with CEM, AEM is superior to reduce pH value on cathode electrode and generate higher electricity (Sleutels et al., 2009). Since cation and anion species can pass through the bipolar membrane, MFC equipped with it achieved to generate higher electricity than that equipped with CEM or AEM (Harnisch et al., 2008).

Moreover, since wastewater contains much amount of cation species other than proton (i.e. sodium and potassium ions) as compared with proton, it is difficult to increase electrical conductivity and proton concentration simultaneously (Harnisch et al., 2009;Rozendal et al., 2006). As one way of increasing electrical conductivity and

proton concentration simultaneously, the external supply of carbon dioxide (Fornero et al., 2010;Ishizaki et al., 2014;Torres et al., 2008b) and water (Ishizaki et al., 2014) to cathode electrode (chamber) were proposed. External water supply is expected to enhance water ionization and carbonate dissolution on the cathode electrode (Harnisch and Schröder, 2009;Ishizaki et al., 2014).

2.1.3. Development of MFC-integrated system

The characteristics of MFC such as electrical driving force can deliver other benefit as mentioned below. Microbial desalination cell (MDC) is able to generate electricity and desalinate simultaneously (Cao et al., 2009b). Seawater will flow between anode and cathode chamber and cation and anion species will be transferred to each chamber through CEM and AEM by electrical potential between the electrodes (Cao et al., 2009b). Valuable resources recovery and production (i.e. Phosphorus and caustic) also utilized the electrical driving force in previous studies (Ichihashi and Hirooka, 2012;Rabaey et al., 2010). In addition, carbon dioxide produced by exoelectrogenic during the process of electricity generation by was also utilized as algae cultivation and methane production (Cheng et al., 2009b;Ruiz-Martinez et al., 2012).

Improvement of effluent water quality is also the motivation for integrating the other technology to MFC. It seems that MFC required further treatment technology for practical utilization to treat wastewater (Wang et al., 2011b). In particular, the integration with MBR has been highlighted to achieve high effluent water quality. The integration system was reviewed in CHAPTER 2.9.

2.2. Operational condition of MFC

The performance of MFC varies with the operational condition, such as external resistance, operational temperature, SRT and HRT (Li et al., 2013b;Penteado et al., 2016). In particular, the researches regarding the relation to external resistance and operational temperature were markedly focused, because these parameters also

influence on MBR and the integration system of MFC and MBR.

2.2.1. External resistance

1) Electrical power generation

The value of external resistance determines the degree of electrical current and cell potential on the basis of Ohm's low. There is an optimum value of external resistance to maximize the performance of MFC in terms of power density, suggesting that MFC could not generate higher power density when equipped too lower or higher value of external resistance.

Theoretically, MFC could accomplish maximum power density when equipped the external resistance whose value is equal to the value of internal resistance, which is the loss due to the ionic transport between anode and cathode compartment. Pinto *et al.* demonstrated that MFC whose external resistance value changed automatically to similar value to the internal resistance could achieve higher power density and CE than the other reactor equipped with lower value of external resistance (Pinto et al., 2011). However, it was also mentioned that the performance of MFC was independent of the influence of the history: Only small difference was observed in the polarization-curves (Lyon et al., 2010).

2) Energy efficiency

The value of external resistance also influence on anodic potential, implying that the energy gained by exoelectrogenic bacteria was dependent on the value of external resistance (See equation 3). According to the equation, the energy gained by exoelectrogenic bacteria increased as the value of external resistance decrease, resulted in enrichment of exoelectrogenic bacteria. This indicates that the microbial community in anodic biofilm is susceptible to the value of external resistance decrease. In fact, suppression of methane emission was also observed with lower value of external resistance (Jung and Regan, 2011) and higher CE could accomplish as the value of

external resistance is small (Pinto et al., 2011;Ren et al., 2011b;Rismani-Yazdi et al., 2011).

3) Biomass and microbial community

Microbial community in anodic biofilm varied with the value of external resistance, probably due to anodic potential (Jung and Regan, 2011;Katuri et al., 2011;Lyon et al., 2010;Ren et al., 2011b;Rismani-Yazdi et al., 2011). Katuri *et al.* observed that the microbial community structure differed from the sludge inoculated in MFC and the degree of their diversity became smaller as the value of external resistance was lower (Katuri et al., 2011). This is agreement with the MFC whose anode potential was regulated using potentiostat (Torres et al., 2009). The microbial community was affected by the change in the value of external resistance, it was affected by the influence of the history of the change (Lyon et al., 2010). In order to compare the structure matured at different external resistance, Lyon *et al.* switched the external resistance equipped on two MFC reactors operated for 18 days each other (10,000 to 470 ohm and 470 to 10,000 ohm, respectively), continued to operate again for 10 days, and thereafter analyzed the structure (Lyon et al., 2010). As the results, the structures generated after the exchange was not similar to each other before the exchange, suggesting that the structure was not independent of the value of external resistance and was affected by the influence of the history of the exchange. Using too lower value of external resistance might induce acidification inside the anodic biofilm, because exoelectrogenic bacteria produce the same amount of proton with the electron (Torres et al., 2008a). In order to inhibit the acidification, several techniques were provided as following: Addition of cathodic solution into the anode chamber and alternation of the role as anode and cathode electrode by the control of their potential (Cheng et al., 2009a;Pinto et al., 2011;Qu et al., 2012). According to the direct observation of anodic biofilm using SEM, anodic biofilm in MFC equipped lower value of external resistance has pores to encourage diffusion inside the biofilm (Zhang et al., 2011).

2.2.2. Temperature

1) Electrical power generation

MFC generally produces lower electrical power generation at lower temperature (Cheng et al., 2011;Li et al., 2013a;Min et al., 2008;Patil et al., 2010;Zhang et al., 2014b). Moreover, it generally takes more time to develop anode biofilm for electrical generation (Cheng et al., 2011;Michie et al., 2011b;Patil et al., 2010). Cheng et al. reported that MFC operated at 15℃ required 210 hours to attain a stable power generation while one at 30℃ could achieve maximum power generation within 50 hours (Cheng et al., 2011). In particular, it seems like that further longer incubation time was required to established MFC at 10℃ or lower. Several reports mentioned that MFCs operated at 10℃ or lower could generate no electricity although they were incubated over 500 hours, but a stable power generation was achieved about one year after the beginning of the incubation (Cheng et al., 2011;Ma et al., 2015;Michie et al., 2011b).

2) Energy efficiency

In while, many studies observed higher CE at lower temperature (Cheng et al., 2011;Jadhav and Ghangrekar, 2009;Michie et al., 2011a). Cheng et al. confirmed that there was a high correlation between CE and temperature ($R^2 > 0.99$) (Cheng et al., 2011). This would be attributable to inhabitation of the activities of non-exoelectrogenic bacteria including methanogenesis. This causes a decrease in chemical oxygen demand, and subsequently CE also decrease (Michie et al., 2011a). Michie et al. show that the MFCs developed at 20℃ and 30℃ produced methane at flow rates of 1.03 and 0.006 mmol/d (Michie et al., 2011a). In particular, no methane was detected from MFC operated at 10℃.

3) Biomass and microbial community

Several papers mentioned that the anodic biofilm developed at lower temperature was

superior to generating more electricity at lower temperature as compared with one at higher temperature (Liu et al., 2012;Michie et al., 2011a;b). Michie *et al.* developed MFCs at 10℃ and 30℃ for 47 weeks and switched the operational temperature to verify their performance at different temperature (Michie et al., 2011a). Surprisingly, the MFCs developed at 10℃ and 30℃ achieved greater electrical generation when operated at 10℃ and 30℃, respectively. In particular, significant drop was observed in cell voltage of MFC developed at 30℃ when the operational temperature turned 10℃ (Michie et al., 2011a). Several papers also show similar outcome (Liu et al., 2012;Michie et al., 2011b).

Exoelectrogenic bacteria seems to become more active than the other bacteria including with methanogenesis. It was observed the diversity and growth of non-exoelectrogenic bacteria including methanogenesis became smaller at lower temperature became lower (Michie et al., 2011a;b). On the other hand, relative abundance of *Geobacteraceae*, which is a famous exoelectrogenic family, was confirmed in MFC operated at lower temperature (Liu et al., 2012;Zhang et al., 2014b). *Geobacter* was well known to tolerant at low temperature as lower as 4℃ (Sharma and Kundu, 2010), in particular, *Geobacter psychrophilus* was found in MFC at lower temperature as relative predominant species (Liu et al., 2012).

Unlike the value of external resistance, anodic biofilm might be affected irreversibly by operational temperature. Irreversible change was observed in the level of electrical generation when the operational temperature was changed (Liu et al., 2012;Michie et al., 2011a;b;Patil et al., 2010). This might be due to which the anodic biofilm developed at low temperature is superior to generating electricity such as exopolymer matrix composition, and/or the activity of individual exoelectrogenesis, and/or microbial community (Patil et al., 2010). Lower level of internal resistance was observed in MFC developed at lower temperature (Michie et al., 2011b). Liu et al. revealed that operational temperature variation influenced on anodic resistance rather than cathodic resistance on the basis of electrochemical impedance spectrometry

analysis although it should increase with a decrease in temperature, because the resistance originated from substrate utilization, which is expected as major resistance, increases with a decrease in temperature (Liu et al., 2012). They suggested that this was resulted from the significant decrease in the resistance originated from extracellular electron transfer provided by conductive polymer (i.e. nanowire). These mean that the understanding of the composition and the mechanism to transfer electron in anodic biofilm is essential to gain much electricity from MFC. These previous studies suggest that MFC demonstrates greater performance at the temperature at which it was developed and is capable of tolerating lower temperature as compared with higher temperature.

2.3. Exoelectrogenic bacteria

2.3.1. Gained energy through anodic respiration

Heterotrophic bacteria generally gain energy from the free energy of substrate oxidation. The free energy was determined by the amount of electrons transferred and the difference in the redox potential between electron donor (substrate) and electron acceptor as following equation:

$$\Delta G^\circ = nF(E^\circ_{donor} - E^\circ_{acceptor}) \text{ ...equation 1}$$

Where, ΔG° is the free energy; n represents the amount of electron delivered to anode electrode; F is Faraday's constant; E°_{donor} is the potential required to degrade the substrate, and $E^\circ_{acceptor}$ is the anodic potential (Schröder, 2007). In the case of MFC employing air-cathode and fed with glucose as carbon source, the electron donor and acceptor are glucose and oxygen, respectively (Logan et al., 2006). ΔG° could be described as below:

$$\Delta G^\circ = \Delta G^\circ_{biol} + \Delta G^\circ_{elec.} \text{ ...equation 2}$$

Where, $\Delta G°_{biol}$ denotes the free energy for their survival and reproduction involving biofilm maintenance; $\Delta G°_{elec.}$ represents the energy which we can collect as electrical power. Furthermore, $\Delta G°_{biol}$ and $\Delta G°_{elec.}$ can be calculated as below:

$$\Delta G°_{biol} = nF(E°_{substrate} - E°_{anode}) \text{ ...equation 3}$$

$$\Delta G°_{elec.} = nF(E°_{anode} - E°_{acceptor}) \text{ ...equation 4}$$

These equations indicate that the substrate with more negative potential provides more energy to exoelectrogenic bacteria and higher electrical power generation can be achieved when the oxidant having more positive potential is utilized for the cathode reaction (Schröder, 2007;Torres et al., 2009).

2.3.2. Transport of electron from exoelectrogenic bacteria to anodic electrode

The mechanism of the electron transport by exoelectrogenic bacteria can be categorized as direct electron transfer (DET) and mediated electron transfer (MET) (Schröder, 2007). In the case of DET, exoelectrogenic bacteria transfer electron to the anodic electrode via outer membrane redox protein and/or through extracellular biofilm matrix (Torres et al., 2010). Outer membrane redox protein and conductive pili are used to transfer electron from bacterial cell to electrode. In particular, the pili plays important role to deliver electron when the bacteria presents away from the electrode. Several species (*Geobacter sulfurreducens* and *Shewanella oneidensis*) are found to transfer electron with the pili (Malvankar and Lovley, 2014). In while, in the case of MET, exoelectrogenic bacteria transfer electron with mediators (e.g. pyocyanine), which comes and goes between bacterial cells and solid oxidant involving anodic electrode (Schröder, 2007). As compared with DET, MET has lower redox potential than DET (While most of the DET possess around 0 V (vs. SHE), pyocyanine has -0.03 V (vs. SHE)), suggesting that electron transfer via MET provides much electrical power than DET. However, MET might not be suitable way to transfer electron to anodic electrode,

because slowly diffusion flux was well observed and the continuous production of the shuttle required expensive energy (Torres et al., 2010). Furthermore, discarding electron via the outer membrane protein directly to the electrode also seems inefficient way, because limit numbers of cells can attach on the electrode (Torres et al., 2010). Thus, establishment of anodic biofilm matrix involving conductive pili is likely primary way to achieve higher electrical generation.

2.3.3. Development of anodic biofilm

1) Microbial community

Anodic biofilm was developed by attaching anodic microorganisms, such as *Geobacter sulfurreducens* and *Shewanella Oneidensis*, on the anode electrode surface and form thick biofilm (Logan, 2009;Lovley, 2012). Although exoelectrogenic bacteria was found in diverse phyla, such as *Alpha-, Beta-, Gamma-,* and *Delta-Proteobacteria, Firmicutes, Acidobacteria* (Logan, 2009), high electrical generation was achieved at high abundance of *Deltaproteobacteria,* especially in *Geobacter sulfurreducens* (Ishii et al., 2013;Torres et al., 2009). Most of these bacteria could consume simple fermentation products (e.g. Acetate and hydrogen) (Torres et al., 2010). Although the other high-molecular carbon source was consumed by the exoelectrogenic bacteria which was capable of generating high electricity, further higher coulomb efficiency was achieved at which acetate was used as substrate (Chae et al., 2009;Pant et al., 2010).

Anodic biofilm tends to generate much electrical current as they develop. *Geobacter sulfurreducens* was known to establish their biofilm on anode electrode and the degree of electrical current was proportional to its thickness (Reguera et al., 2006). The anode biofilm was also known to generate much electrical current as they matured in terms of per biomass (Ishii et al., 2012). Ishii *et al.* revealed that the performance of anodic biofilm at 105 days after starting the operation was greater than that at 28 days after starting the operation (1002 *vs.* 374 μmol-electron/g-protein/min) (Ishii et al., 2012). This increase was due to the abundance of *Geobacter sulfurreducens* (32% to

70%). In addition, it might takes time that anodic biofilm could function as anode electrode, because the occurrence of lag phase in current variation was observed and regulation of gene encoding specific protein related to electrical generation was suggestive as the cause of the lag phase (McLean et al., 2010).

2) Anodic biofilm composition

Viability of anodic biofilm is also important factor to generate much electrical current. As well as general biofilm, the viability of anodic biofilm also gradually declines (Reguera et al., 2006;Ren et al., 2011a;Sun et al., 2016). Sun *et al.* observed the growth of anodic biofilm using CLSM and characterized it using electrochemical impedance spectrometry (EIS) related to the variation of electrical current (Sun et al., 2015). They observed the anodic biofilm was clearly divided into 2 parts; live outer-layer and dead inner-layer. They revealed the thickness of live outer-layer increased and reached at stable thick ness (<15 μm) while the thickness of dead inner-layer increased gradually during the operation. The variation of electrical current was consistent with the increase in the thickness of live outer-layer, suggesting that only viable bacteria are relevant to increase electrical current. Dead inner-layer acted as the path of electron generated in live outer-layer in this study (Sun et al., 2015). Sun *et al.* also displayed that the maximum electrical current was observed when the thickness of the anodic biofilm reached 25 μm, and the electrical current decline with the increase in electrical current thereafter (Sun et al., 2016). This result also shows clearly that only viable bacteria are relevant to increase electrical current.

The spatial composition in the viability might be dependent on the microbial community in anodic biofilm. In contrast to Sun *et al.* (Sun et al., 2015;Sun et al., 2016), Yang *et al.* observed the outer layer of anodic biofilm established by only *Shewanella decolorationis* comprised mainly dead cells (Yang et al., 2014). This conflict was in agreement with the previous reports regarding the characteristics of anodic biofilm developed by *Geobacter sulfurreducens* and *Shewanella oneidensis*. While *Geobacter*

sulfurreducens develop the anodic biofilm over several hundred micrometers, the thickness of the anodic biofilm of *Shewanella oneidensis* was less than ten meters (Dolch et al., 2014;Malvankar et al., 2011). The reason why *Geobacter sulfurreducens* has the ability to increase the thickness of anodic biofilm is that they are able to conductive pili, called nanowire. In addition, in mixed-culture MFC, occurrence of filamentous bacteria was confirmed as anodic biofilm developed (Ren et al., 2011a). It is known that filamentous bacteria are able to transport electrons over centimeters (Pfeffer et al., 2012). Consequently, it is likely that there is a limitation to the thickness of anodic biofilm and pili (nanowire) and filament were key factors to determine the height of the biofilm, because they function as the network of conductor between the surface of solid electrode and living cells (Liu and Bond, 2012;Snider et al., 2012).

2.4. Membrane fouling and bacterial secretion

2.4.1. Brief introduction of membrane bioreactor (MBR)

MBR is a technology which provides biological treatment with membrane separation and increasingly used to fulfill various water demand such as water reuse (Judd, 2008;Malaeb et al., 2013b;Meng et al., 2009b). Owing to membrane separation, MBR does not require to discriminate primary sedimentation and subsequent biological treatment parts unlike CAS (Judd, 2008). MBR has several advantages for wastewater treatment as following: Excellent effluent water quality (Judd, 2008;Meng et al., 2009a), independent control of SRT and HRT (Judd, 2008), operation at higher mixed liquor suspended solids (MLSS) concentration (Judd, 2008;Kraume and Drews, 2010), and smaller footprint (Le-Clech et al., 2006). Longer HRT is required for the operation of MBR, because a growth of floc is essential for the removal by sedimentation (Judd, 2008). CAS is not also operated at exceed high MLSS concentration due to the same reason. In while, for the operation of MBR, membrane filtration prevents an outflow of smaller particles than pore size of the membrane. It is thus that MBR has been developed for household wastewater treatment and enhanced nutrient removal

(Abegglen et al., 2008;Kraume and Drews, 2010), allow to treat wastewater in rural areas and prevent from eutrophication (Abegglen et al., 2008;Zuthi et al., 2013).

It is widely accepted that membrane fouling is a main obstacle for its wider application. Occurrence of sever membrane fouling cause several problems; Increase in filtration pressure, frequent membrane exchange, and additional process to mitigate the fouling. These consequently cause increases in energy and cost, and complexity of its operation (Guo et al., 2012;Judd, 2008;Le-Clech et al., 2006). MBR operation requires two to four fold much energy as compared with CAS (Gil et al., 2010). In particular, aeration is a major energy consuming process, often exceeding 50% of total energy consumption (Gil et al., 2010;Kraume and Drews, 2010).

As described below, although extensive studies have been conducted to understand the detailed mechanisms of membrane fouling in MBRs and to develop its effective mitigation strategies (Huang and Lee, 2015;Lin et al., 2014;Malaeb et al., 2013b), improvement of fouling control and management is still remarkably slow in practice.

2.4.2. Membrane fouling

Membrane fouling is the undesirable deposition and accumulation of microorganisms, colloids, solutes, and cell debris within/on membranes in MBR (Meng et al., 2009b). On the basis of the degree of hard-to-remove, membrane fouling is classified into three parts; Removable, irremovable, and irreversible fouling (Meng et al., 2009b). The foulants causing removable fouling can be washed by physically cleaning such as backwash. While removable fouling is a main contributor for membrane fouling (Cake resistance accounted for 80% of filtration resistance (Lee et al., 2001)), it can be eliminated easily as compared with the other fouling (Meng et al., 2009b;Miyoshi et al., 2012). Irremovable fouling requires chemical cleaning to be removed and the foulants which are not eliminated by both physical and chemical cleaning cause irreversible fouling (Meng et al., 2009b). It is considered that chemical cleaning should not be

frequently treated, because it delivers damages to membrane and the chemical agents causes environmental problem (Yamamura et al., 2007). This suggests that reduction of irremovable and irreversible fouling is crucial for continuous operation of MBR. Thus, membrane fouling is also defined in terms of whether it can be removed physically or not, and irreversible fouling, which involves both irremovable and irreversible fouling, has intensively studied (Kimura et al., 2009;Miyoshi et al., 2012).

In addition, membrane fouling can be divided into three parts on the basis of the characteristics of foulants; Biofouling, organic fouling, and inorganic fouling (Guo et al., 2012;Meng et al., 2009b). Biofouling is caused by particles including with bacterial cells, and organic fouling is caused by soluble microbial products and colloids (Guo et al., 2012). These are primary cause of sever membrane fouling of microfiltration (MF) and loosely ultrafiltration (UF) membranes (Meng et al., 2009b). In while, the effect of inorganic fouling (precipitation and crystallization of inorganic matter) on membrane fouling of these membrane is smaller, but it is known that organic matter matter cross-linked by inorganic matter may cause severe membrane fouling due to change in the characterization (Al-Halbouni et al., 2008).

2.4.3. Contribution of bacterial secretion on membrane fouling

1) Soluble microbial product

It is well accepted that soluble microbial product (SMP) and extracellular polymeric substances (EPS) are main contributor for membrane fouling occurring in MBR equipped with MF and UF membrane (Guo et al., 2012;Rosenberger et al., 2005). In particular, it is likely that SMP primarily contributes membrane fouling (Meng et al., 2009b;Tang et al., 2010).

SMP are soluble organic compounds that are released during normal biomass metabolism and decay, and can be classified as utilization-associated products (UAP) and bio- mass-associated products (BAP) on the basis of the production processes (Ni et al., 2011). UAP and BAP are SMP produced directly as part of electron-donor oxidation

and produced from the hydrolysis of biomass, in particular from EPS (Ni et al., 2011). In the other words, UAP and BAP are originated from unfinished substrate and debris of cell or EPS. The SMP related to membrane fouling was likely produced in and originated from EPS of bacteria in MBR (Meng et al., 2009c). The effect of UAP and BAP on membrane fouling is described as following.

Much many researches quantified the amount of SMP in TOC, carbohydrate, and protein concentrations. Although they concluded membrane fouling became severe with increases with carbohydrate and/or protein (Guo et al., 2015;Sweity et al., 2011;Tang et al., 2010;Tian et al., 2011b), some studies also concluded there is no correlation between the degree of membrane fouling and the quantity of SMP (Drews, 2010;Kimura et al., 2009;Ma et al., 2015). The reason for the discrepancies in the relationships between membrane fouling and SMP is that its composition is important factor to determine its fouling potential (Drews, 2010). In addition, the surrounding physico-chemical environment also affects the fouling potential of SMP (Drews, 2010). Taken together, not only quantitative information such as carbohydrate and protein concentrations but also qualitative information is essential for finding the fouling potential.

In previous reports, fourier transform infrared (FTIR) spectroscopy and excitation-emission matrix (EEM) fluorescence spectroscopy were well utilized to gain qualitative information of SMP (Drews, 2010;Tran et al., 2015). FTIR spectrum provides information on functional groups involved in SMP and EEM can yield a fingerprint of SMP contained in the sample, respectively (Chen et al., 2003;Drews, 2010;Kimura et al., 2009;Miyoshi et al., 2009). Io order to identify the specific polysaccharides and protein, further examination has been conducting by using matrix-assisted laser desorption/ionization time-of-flight mass spectrometry analysis (Kimura et al., 2012;Kimura et al., 2015) and metaproteomic analysis (Zhou et al., 2015b). In addition, particle size distribution, hydrophobicity and molecular weight are also well investigated for the characterization of SMP: However, particle size

distribution and hydrophobicity seems not to be relevant to fouling potential (Tran et al., 2015). Hydrophilic and neutral SMP likely to cause severe membrane fouling potential as compared with hydrophobic SMP (Ishizaki et al., 2016a;Tang et al., 2010;Tran et al., 2015), some studies also mentioned that hydrophobic SMP also cause severe membrane fouling by adsorption on membrane and/or hydrophobic interaction (Tran et al., 2015). In while, molecular weight is likely relevant in fouling potential of SMP. As mentioned below, biopolymer, which has >10 kDa of molecular weight, can be a promising indicator for the fouling potential.

2) Biopolymer

Biopolymer is the hydrophilic organic compounds having high molecular weight (>10 kDa) detected by liquid chromatography – organic carbon detection (LC-OCD) (Huber et al., 2011;Tran et al., 2015). Biopolymer is contains not only polysaccharides but also nitrogen-containing material such as protein or amino sugars (Huber et al., 2011;Tran et al., 2015). Importance of biopolymers for membrane fouling in MBRs and biopolymers accumulation on membranes have been reported by some researchers recently (Jiang et al., 2010a;Meng et al., 2009c;Tian et al., 2013). Rosenberger *et al.* revealed that biopolymer fraction was trapped by membrane and cause severe membrane fouling (Rosenberger et al., 2006). Moreover, the concentration of biopolymer was strongly correlated with the degree of membrane fouling by surface water (Kimura et al., 2014;Yamamura et al., 2014) and wastewater (Tian et al., 2013), respectively. Ishizaki *et al.* also exhibited the correlation between the concentration of biopolymer in ML and fouling potential(Ishizaki et al., 2016a).

Much biopolymer seems to be produced during decline phase rather than exponential growth phase, because BAP contained much biopolymer than UAP (Jiang et al., 2010a). In while, biopolymer contained in UAP likely have greater fouling potential than that in BAP in terms of the proportion of biopolymer trapped (Jiang et al., 2010a).

2.4.4. Effect of operational conditions on membrane fouling

Fouling potential was influenced on the operational condition such as hydraulic retention time (HRT), solid retention time (SRT), food to microorganism ratio (F/M), temperature, and dissolved oxygen (DO) concentration. Particularly, it can be seen that SRT and temperature are important parameters when MBR is integrated with MFC. Therefore, the effect of solid retention time (SRT) and temperature on the fouling potential was introduced as below.

1) Temperature

Almost all the papers which investigate the effect of temperature on fouling potential mentioned that membrane fouling aggravates at low temperature (Drews et al., 2007;Gao et al., 2013b;Ma et al., 2013b;Miyoshi et al., 2009;Rosenberger et al., 2006;Sun et al., 2014b;van den Brink et al., 2011;Wang et al., 2010). Several papers has addressed to operate MBR through the year and significant membrane fouling was observed in winter season (Miyoshi et al., 2009;Rosenberger et al., 2006;Sun et al., 2014b). van den Brink *et al*. introduces the detail mechanism as hypothesis why the fouling potential increased with a decrease in the temperature as follows (van den Brink et al., 2011): (i) Increased mixed liquor viscosity, reducing the stress generated by coarse bubbles; (ii) More severe deflocculation, reduction biomass floc-size and releasing EPS into the mixed liquor; (iii) Brownian diffusion was less affected; (iv) Reduced biodegradation of COD. Hypothesis ii suggests that the quantity of SMP increases in MBR at low temperature, in agreement with several studies (Gao et al., 2013b;Ma et al., 2013b;Miyoshi et al., 2009;Rosenberger et al., 2006;Sun et al., 2014b). In addition, hypothesis iv suggests that much foulant remains to be retained in MBR. Miyoshi *et al.* could not find any seasonal change in fouling potential of MBR operated at longer SRT, probably due to which retained foulant was biodegraded (Miyoshi et al., 2009).

According to the papers, the quantity of microbial secretions generated in the

MBRs tended to increase with the fouling potential (Gao et al., 2013b;Ma et al., 2013b;Miyoshi et al., 2009;Rosenberger et al., 2006;Sun et al., 2014b). In particular, an increase in protein content was observed in response to an increase in fouling potential at low temperature (Gao et al., 2013b;Sun et al., 2014b). Drew *et al.* monitored the percentage of carbohydrate and protein contents by membrane through the year, and confirmed the increase in the percent of protein content along with a decrease in the operational temperature (Drews et al., 2007). In contrast to these papers, several papers observed an increase in carbohydrate contents in response to the increase in fouling potential (Miyoshi et al., 2009;Rosenberger et al., 2006).

As well as the effect of SRT on fouling potential, the characteristics of bacteria and the microbial community structure in MBRs plays important roles on a generation of microbial secretion (Gao et al., 2013b;2014b). In addition, Gao *et al.* analyzed microbial community related to the variation in fouling potential of and the quantity of microbial secretion in the MBRs operated at 10, 20, and 30℃ (Gao et al., 2013b). While the membrane fouling was significant in order of 10, 20, and 30℃, the quantity of SMP maximized at 30℃ and minimized at 20℃. Although the carbohydrate contents increased along with the temperature, significant increase in protein content was observed at 10℃ (Gao et al., 2013b). The microbial community structures were different in the MBRs and beta-Proteobacteria was abundant in the mixed liquor and biocake in MBR operated at 10℃ (Gao et al., 2013b). They concluded that the conflict on the composition of microbial secretion was affected to the variation in the microbial community, in particularly the pioneer-bacteria attaching initially on the membrane. Ma *et al.* observed relative abundance in alpha-Proteobacteria and Firamentous in mixed liquor (Ma et al., 2013b). These studies also mentioned absence of the bacteria reducing fouling potential at lower temperature, such as *Zoogloea* and *Saprospiraceae* (Gao et al., 2013b;Ma et al., 2013b). The absences of *Zoogloea* and *Saprospiraceae* were considered to inhibit the generation of fine-partical flocs and degradation of protein contents in MBRs. Moreover. bacteria is

known to likely generate microbial secretion in response to environmental stress (Barker and Stuckey, 1999;Rosenberger et al., 2006), in agreement with the observations in previously studies (Gao et al., 2013b;Ma et al., 2013b;Miyoshi et al., 2009;Rosenberger et al., 2006;Sun et al., 2014b). The proportion of carbohydrate or protein contents in the secretion might also influence on the characteristics of bacteria.

2) Solid retention time

Unlike in the case of the effect of temperature on membrane fouling, the effect of SRT is not agreed with each other in previous papers. It seems that membrane fouling aggravates when SRT excessively shortened and prolonged, suggesting the existence of optimum SRT to minimum the degree of fouling potential. Meng *et al*. suggested that membrane fouling seemed to be mitigated when MBR was operated at the range of 20 to 50 d of SRT (Meng et al., 2009b). Several papers mentioned that the quantity of microbial secretion (SMP) increased when membrane fouling aggravated regardless of SRT (Duan et al., 2014;Lee et al., 2003;Yu et al., 2016). Moreover, the ratio of protein contents to carbohydrate contents in microbial secretion (SMP) was prone to increased with SRT (Lee et al., 2003;Ng et al., 2006). An increase in the ratio was observed in MBR operated as batch-mode (Zhou et al., 2012). That in extracellular polymeric substances (EPS) was also likely to increased with SRT (Duan et al., 2009;Malamis and Andreadakis, 2009;Sweity et al., 2011).

These phenomena were considered to related to the mechanisms of the generation of microbial secretion at different SRTs. When SRT is shortened, the quantity of microbial secretion likely tends to increase since the majority of the secretion did not be degraded in MBR. As introduced above, the secretion at shorter SRT comprised mainly carbohydrate contents, which is known to be more biodegradable substances than protein contents (Zhang and Bishop, 2003). Sweity *et al.* examined the percentage of carbohydrate in microbial secretion and its viscosity using QCM-D related to fouling potential (Sweity et al., 2011). In addition, UAP was known

to have greater fouling potential as compared with BAP (Jiang et al., 2010b). The microbial secretion at shorter SRT was composed of higher proportion of UAP than that at longer SRT. They revealed that the viscosity increased with the percentage of carbohydrate, and consequently the fouling potential increased as SRT shortened. In contrast, when SRT is prolonged, endogenous decay and cell lysis seems to increase the quantity of microbial secretion (Jarusutthirak and Amy, 2006;Pribyl et al., 1997). The secretion originated from endogenous decay and cell lysis was considered to consist of BAP and be high molecular weight (Jarusutthirak and Amy, 2006;Jiang et al., 2010b). The quantity of BAP was further larger than UAP so that the membrane fouling caused by BAP was more significant than that by UAP (Jiang et al., 2010b). Zhou et al. operated lab-scale MBR operated as batch-mode to examine the microbial secretion generated during exponential growth phase, stationary growth phase, and deceleration growth phase (Zhou et al., 2012). Higher fouling potential was observed during exponential and stationary growth phase, and a generation of secretion having high molecular weight occurred during stationary growth phase. In addition, Kimura *et al.* observed the increase in humic substances in microbial secretion as SRT prolonged (Kimura et al., 2009). This also suggests the progression of endogenous decay and cell lysis because a generation of humic substances was derived from endogenous decay of bacteria (Tian et al., 2011a).

Besides the characteristics of bacteria, microbial community also plays important roles to lead membrane fouling. It has been found that the microbial community structure can vary with DO concentration and ratio food to microorganisms, which likely depends on SRT (Wu et al., 2011). Recently, it was reported that the activities of quorum sensing (QS) and quorum quenching (QQ) bacteria was also dependent on SRT (Yu et al., 2016).

2.5. Identification of the role of bacteria on membrane fouling

2.5.1. Elucidation of mechanism of membrane fouling with actual MBR

1) Techniques for microbial community analysis

One of research approaches is to identify key players (microbial strains) of membrane fouling and subsequently to control and inhibit their activity by any means (Calderón et al., 2011;Ma et al., 2013b;Miura et al., 2007c). As mentioned above, since the organic matters causing sever membrane fouling was produced by bacteria living in MBR, the microbial community structure should contain valuable information for better understanding of membrane fouling. Much many researched have addressed to analyze the microbial community in mixed liquor and biocake in MBR and some of the researches revealed that change in the microbial community influences on the composition of bacterial secretion, which affects the degree of membrane fouling (Gao et al., 2014b;Guo et al., 2015;Silva et al., 2016). In the other words, microbial community is a leading factor to determine the fouling potential.

Although extensive studies have been conducted to reveal microbial communities in pilot-scale MBRs treating real municipal wastewater using several molecular biological techniques, our understanding is still largely limited to identify key bacteria responsible for membrane fouling (Kim et al., 2013;Lim et al., 2012;Miura et al., 2007c;Pang and Liu, 2007;Wu et al., 2011;Xia et al., 2010).

Microbial community is known to be sensitively influenced on the operational parameters and membrane; Shear force including with aeration intensity (Ma et al., 2013a;Rickard et al., 2004), DO concentration(Gao et al., 2011a), temperature(Gao et al., 2013b;2014b;Ma et al., 2013b), SRT(Farias et al., 2014;Silva et al., 2016), influent water(Miura et al., 2007a), salinity (Guo et al., 2015), and membrane material (Gao et al., 2011b). In addition, microbial community differs by whether in mixed liquor or in biocake (Gao et al., 2013a;Gao et al., 2014a;Huang et al., 2008;Wu et al., 2011). The similarity of the microbial community was dependent on the permeate flux (Huang et al., 2008) and shear force (Wu et al., 2011) due to the driving force from mixed liquor to the membrane surface (Thomas et al., 2000; Wang et al., 2005).

2) Identification of key bacteria responsible for membrane fouling

Identification of key players for membrane fouling is mainly focused on the basis of predominant species; Dominant species in mixed liquor (Yu et al., 2016) and biocake (Calderón et al., 2011;Pang and Liu, 2007), and the species increasing gradually in response to membrane fouling (Lee et al., 2014;Lim et al., 2012;Miura et al., 2007c). Moreover, pioneer bacteria, which initially attached on membrane surface, is also considered to play important role on membrane fouling (Vanysacker et al., 2014a;Zhang et al., 2006). The pioneer bacteria is assumed to colonize easily and condition the membrane surface to facilitate subsequent bacterial attachment (Vanysacker et al., 2014a;Xiong and Liu, 2010). Gao *et al.* assumed the process for the membrane fouling evolution with the pioneer-bacteria as three stages on the basis of empirical data; i) Pioneer bacteria adhere on the membrane surface and produce secretion, ii) Other bacterial subsequently attach on the conditioned membrane, colonize, and form biocake, and iii) bacterial cells and secretion produced in mixed liquor and/or biocake accumulate on the membrane (Gao et al., 2013a). Furthermore, conditioning film likely plays important role for the initial adhering of the pioneer bacteria (Lorite et al., 2011;Vanysacker et al., 2014a;Zaky et al., 2012).

Proteobacteria well appeared in both mixed liquor and biocake in MBR and considered as the bacteria responsible for membrane fouling (Miura et al., 2007c;Vanysacker et al., 2014a;Xia et al., 2010). In particular, *alpha-Proteobacteria* (Calderón et al., 2011;Gao et al., 2013b;Ma et al., 2013b), *beta-Proteobacteria* (Miura et al., 2007c), and *gamma-Proteobacteria* (Lim et al., 2012) were well reported as dominant species. In addition, *Actinobacteria* (Ma et al., 2013b;Xia et al., 2010) and *Firmicutes* (Calderón et al., 2011;Lim et al., 2012;Xia et al., 2010) were reported to be relatively abundance in MBR. Ma *et al.* observed that the decrease in relative abundance of *beta-* and *gamma-Proteobacteria* was correlated to the reduction of fouling potential (Ma et al., 2013a).

Table 2.1 Advantages and problems in pure culture-based and actual MBR-based studies

	Model bacteria	Isolated bacteria	Actual MBR (Mixed population)
Advantages	・Available for purchase ・Genetic information is available ・Easily genetic modification ・Repeatable ・Ease to experiment involving setup ・Available for genetic information	・Possible to test for many bacteria ・Possible to fill the gap to use model bacteria	・High certainty (More appicative information can be gained)
Problems	・Lower certainty (Gap between actual MBR) ・Unknown whether key bacteria	・Need to fill the Gap between actual MBR	・Complexity of phenomena ・Low repeatability and reliability ・Difficult to compare with the other papers

2.5.2. Elucidation of mechanism of membrane fouling with pure culture

As another approach to identify key players of membrane fouling and to understand the role of bacteria on membrane fouling, the researches of membrane fouling with pure-culture have been conducted. The study with pure-culture have several advantages as compared with that with actual MBR (**Table 2.1**). It is certain that the study with actual MBR delivers more certain and applicative knowledge which is easily reflected for the effective operation of MBR. The size of reactor (Lab- or full-scale) and influent water (Synthetic or real wastewater) also seems to influence on the outcome (Shen et al., 2012;Villain et al., 2014). However, unanticipated events involving a temporal change of influent water quality likely influence on the outcome in the study with actual MBR. Moreover, the study with actual MBR is also difficult to be carried out many times simultaneously and repeated, suggesting that repeatability and reliability of the results are lower. These suggest that it is difficult to evaluate the effect of what you are focusing on membrane fouling in actual MBR. Furthermore, it is also difficult to compare the gained result with the other papers, because each MBR must started to be operated with different sludge and influent, that is, different microbial population (Drews, 2010).

As compared the study with actual MBR, that with pure culture have high

repeatability, can be performed easily, and utilize genetic information. Although there is still gap between the study between with actual MBR and with pure culture, the study with pure culture is recognized to be important for understanding of key bacteria responsible for membrane fouling (Drews, 2010;Lade et al., 2014a;Malaeb et al., 2013b). In particular, it is necessary for understanding bacterial specific role on severe membrane fouling such as quorum-sensing (Lade et al., 2014a).

1) Elucidation of mechanism of membrane fouling with model bacteria

Model bacteria is a powerful tool for evaluating the specific role on membrane fouling, because accurate genetic information can be available and the genome information can be easily modified. It is also the advantage to be available for purchase, because it is easy to compare the result with the other studies. *Escherichia coli* and *Pseudomonas aeruginosa* were well used as model bacteria (Chao and Zhang, 2011;Vanysacker et al., 2014b;Yoshida et al., 2015). Vanysacker *et al*. used *P. aeruginosa* labeled by green fluorescent protein to observe the spatial location in biocake (Vanysacker et al., 2014b). This study reveals that *P. aeruginosa* distributed on the bottom of the biocake and acted as pioneer-bacteria to develop the biocake (Vanysacker et al., 2014b). Yoshida *et al*. used *E. coli* modified to produce much/less amount of specific extracellular polysaccharides, and examined for the effect of the polysaccharides on membrane fouling (Yoshida et al. 2015). In addition, the effect of biofilm formation (Pang et al. 2005) and the growth behavior in mixed liquor and on membrane (Chao et al. 2011) on membrane fouling were investigated with the model bacteria. However, there is enormous gap between using model bacteria and actual MBR, because it is unknown whether these bacteria were key bacteria for membrane bacteria or have similar characteristics to the key bacteria. Actually, *E. coli* K-12, which was used in previous study (Yoshida et al. 2015), shows smaller fouling potential as compared with strain S05, the fouling-causing bacteria isolated in my previous study (Ishizaki et al., 2016a) (**Fig. 2.1**).

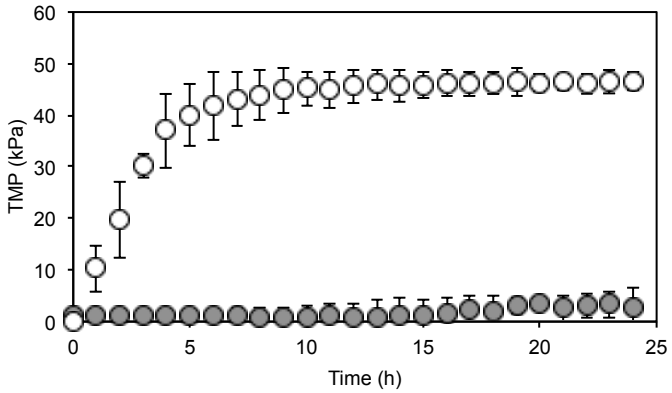

Fig. 2.1 Time variation of trans-membrane pressure (TMP) of *E. coli* K-12 and strain S05. Open and closed circles represent S05 and K-12, respectively. S05 is one of fouling-causing bacteria (FCB) identified in my previous study and their fouling potentials were measured with bench-scale cross-flow membrane filtration system (CFMFS) (see CHAPTER 4).

2) Elucidation of mechanism of membrane fouling with isolated bacteria

Use of environmental isolates is effective to fill the gap mentioned above. Several papers have addressed to reveal membrane surface colonization (Choi et al. 2006), biocake formation (Feng et al., 2009;Juang et al., 2010b;Pang et al., 2005b), detail mechanism of membrane fouling (Juang et al., 2008a;b). In addition, the identification of bacteria responsible for membrane fouling has been also carried out by several papers (Choi et al., 2006) (Juang et al., 2010b;Pang et al., 2005b). However, to date, only a few environmental isolates were subjected for the measurement of the fouling potential with a unified method (Choi et al., 2006;Feng et al., 2009;Juang et al., 2008b). Moreover, there is still gap between using isolated bacteria and using actual MBR regarding the influence on microbial interaction. Although several papers pointed out the effect of the interaction on membrane fouling (i.e. quorum-sensing), limited information can be available on the microbial interaction (Lade et al., 2014a;Shrout and Nerenberg, 2012;Yeon et al., 2008).

2.6. Integration system of MFC and MBR

Recently, the integration system of MFC and MBR has been well studied and developed (**Table 2.2**). Since MFC could achieve poor effluent quality, post-treatment was necessary to fulfill water quality standards for wastewater treatment (Wang et al., 2011b). In while, as mentioned above, MBR is capable of achieving high effluent quality, but its operation requires enormous energy for such as aeration (Gil et al., 2010;Kraume and Drews, 2010). The integration of MFC and MBR was thus expected to be able to compliment their bottlenecks each other.

2.6.1. Reactor configuration

The reactor configuration could be categorized roughly into five types: The reactor integrated membrane module inside anode chamber (inside-Anode) and cathode chamber (inside-Cathode), included both anode and cathode electrode and membrane module in a reactor (One-chamber), the reactor equipped membrane module in parallel (Parallel) or as subsequent reactor (Post-treatment). The performance of the integration system varied with the configuration in terms of COD removal, power density, and coulomb efficiency (**Fig. 2.2** and **Table 2.2**). Briefly, inside-Anode shows the ability of much lower COD removal as compared with the other systems, but it facilitates to increase the generation of electricity and CE (**Fig. 2.2**). In while, inside-Cathode shows higher COD removal and lower maximum power density and CE (**Fig. 2.2**). One-chamber seems to have similar characteristics to inside-Cathode (**Fig. 2.2**). Post-treatment achieves the greatest COD removal and maximum power density, because all the reactor configurations of MFC as former part were air-cathode MFC, which is known better configuration to generate high electricity (Du et al., 2007). Since the performance of Parallel and Post-treatment have dependent on the configuration of MFC (**Table 2.2** and **Fig. 2.2**), the degrees of COD removal, power density, and coulomb efficiency were categorized again on the configuration basis and then compared (**Fig. 2.3**). Similar to the result shown in **Fig. 2.2**, Anode shows lower COD

removal and higher power generation and CE as compared with Cathode. Cathode has advantage on the ability to nitrogen removal, which is one of the topics paid attention to (Gajaraj and Hu, 2014;Sun et al., 2014a;Zhang et al., 2014a;Zhou et al., 2015a), it may be however required much energy to operate due to pumping wastewater from anode chamber to cathode chamber as mentioned below. On the other hand, One-chamber achieves the greatest COD removal and CE (**Fig. 2.3**). The reason why the CE of One-chamber is further higher is that some One-chamber were applied for voltage, and consequently higher electrical current were generated (Wang et al., 2013) (Katuri et al., 2014) (Werner et al., 2016). Although external power supply was required to operate it, net energy generation was positive since biogas (e.g. methane and hydrogen) can be produced as mentioned below (Katuri et al., 2014).

As membrane module, stainless steel mesh (SS) and PVDF membrane were well used in the system. In addition, the mixture of polyether sulfone and polyvinylpyrrolidone (Katuri et al., 2014;Werner et al., 2016), polytetrafluoroethylene, (Ishizaki et al., 2016a), polyester (Malaeb et al., 2013a;Xu et al., 2015), pyrrole-modified polyester (Liu et al., 2013), nylon (Wang et al., 2012a), carbon nanotube (Zuo et al., 2016), and carbon felt (Zhang et al., 2014a). The average pore size of SS and PVDF used in previous studies ranged from 13-48 μm and 15 kDa-0.1 μm, respectively (**Table 2.2**). Whereas only a hollow-fiber membrane was equipped in inside-Anode, both hollow-fiber and flat membranes were used for inside-Cathode. Many of inside-Cathode used flat membrane as membrane cathode. The ability of COD removal was independent of membrane material, because SS was installed only in cathode chamber, indicating that further organic matters were treated as compared with inside-Anode. In while, PVDF membrane was used not only in cathode chamber, but also anode chamber and One-chamber. The degree of COD removal by SS was roughly correlated with pore size (R^2 = -0.84), while that by PVDF was independent of the size (R^2 = 0.23).

Table 2.2 Summary of the performance of integration system of MFC and MBR

Reference	aReactor configuration	bMembrane type	How to install membrane	Membrane material	Effective filtration area (cm2)	Pore size (μm)	Anode electrode	Cathode electrode	Aerobic/Anaerobic in cathode (MBR)	cVolume (l)	dCOD removal (%)	Maximum power generation	Permeate flux (L/m2/h)	eCE (%)	fHRT (d)	SRT (d)	Temperature (℃)	Fouling mitigation
Wang et al. (2011)	inside-Cathode	Tubular	Submerge	SS mesh+non woven cloth	494	40	Graphite rod and granular graphite	SS mesh	Aerobic	2.3(4.2)	91.4-93.9	4.35 W/m3	18.6(18.6-93.1)	8.2(0.51-8.2)	2.5 h (0.5-2.5 h)	-	25±1	-
Wang et al. (2012)	inside-Cathode	Flat	Submerge	Nylon mesh	1,000	74	Self-fabricated activated carbon fiber	Carbon felt	Aerobic	(20)	89.6	6 W/m3	23.3	1.5	8.6 h	-	-	-
Ge et al. (2013)	inside-Anode	Hollow-fiber	Submerge	PVDF	110	0.02	Carbon brush	Carbon cloth loaded Pt	Anaerobic (Air-cathode)	~0.92	45.3 (45.3-57.8)	36-38 W/m3	33.8	36.4 (29.8-36.4)	19-27 h	-	~20	-
Li et al. (2013)	inside-Cathode	Hollow-fiber	Submerge	PVDF	51	150 kDa	Carbon clot	Carbon cloth loaded Pt	Aerobic	-	86.9 (86.9-90.2)	3-25 W/m3	33.8	17.1 (10.8-17.1)	26 h	-	~20	-
				PVDF							90.4±5.9	39.0±2.0 W/m3	<7.1	31.2±1.6	6, 10	-	~22	-
				PVDF							91.9±0.0	64.0±0.0 W/m3	<2.9	11.5±0.0	18, 24	-		-
Liu et al. (2013)	One-chamber	Flat (MC)	Submerge	Pyrrole-modified polyester filter cloth	800	50	Iron plate	Pyrrole-modified polyester filter cloth	Aerobic	14.6(18.2)	<100	2.6 mW/m2	15	-	0.5	-	18±2	Yes
Malaeb et al. (2013)	inside-Cathode	Flat (MC)	Submerge	Polyester	7	40	Graphite brush	Membrane dispersed carbon nanotube	Anaerobic (Air-bio-cathode)	~0.04	97.3±1.1	6.8 W/m3	0.8-1.2	8.5±4.5	2-3	-	23±3	Yes
		Flat	Air-cathode	Polyester				Carbon cloth loaded Pt			96.9±0.9	14.5 W/m3		47.3±1.5		-		-
Su et al. (2013)	Parallel	Hollow-fiber	Submerge	PVDF	1,000	0.1	Carbon cloth	Carbon cloth loaded Pt	Aerobic	-	86.7	51 mW/m2	10	5.9	8.2	-	22±3	Yes
Wang et al. (2013)	inside-Cathode	Flat (MC)	Submerge	SS mesh	32	48	Graphite felt	SS mesh	Aerobic	1.25	85.5 ± 5 (81.0-92.8)	8.56 W/m3	10 (10-20)	12.3 (1.9-12.3)	12.3 min	-	25±1	-
Wang et al. (2013)	Parallel	Tubular	Crossflow	PES	37.7	30 kDa for separator and 0.1 μm for filtration	Carbon felt	Carbon felt	Aerobic	2.2	94	40 mW/m2	10.5	5.84	10	-	14-22	Yes
Wang et al. (2013)	One-chamber	Flat (MC)	Submerge	SS mesh	494	40	Graphite rod and granular graphite	SS mesh	Aerobic	2.3(4.2)	93.7	0.76-1.43 W/m3	13.8	4.5 (0.9-4.5)	3.6 h	-	-	Yes
Gajaraj and Hu (2014)	inside-Cathode	Hollow-fiber	Submerge	PVDF	470	0.1	Graphite cloth	Titanium mesh	Aerobic	7.2	84.4-91.9	0.09-0.16 V	4.8	<0.05	1	20	-	Yes
Huang et al. (2014)	inside-Cathode	Flat (MC)	Submerge	SS mesh	32	48	Graphite felt	SS mesh	Aerobic	1.29	86.1	8.6 W/m3	-	1.9-12.3	-	-	25±1	-
Katuri et al. (2014)	One-chamber	Hollow-fiber (MC)	Submerge	PES + PVP	14	1	Graphite fiber brush	Nickel-based hollow fiber membrane	Anaerobic	0.35	>95	-	6.9	81±8.8 (53-81)	-	-	25	Yes
Li et al. (2014)	inside-Anode Post-treatment	Hollow-fiber	Submerge	PVDF	210	0.02	Carbon cloth supported by SS mesh	Carbon cloth loaded Pt	Anaerobic (Air-cathode)	0.7(1.0)	<91.6	14.6 W/m3	2.3	-	8 h (5-24 h)	-	~20	-
										1.7(2.0)	95	47 W/m3	2.3		19.6			
Liu et al. (2014)	inside-Cathode	Flat (MC)	Submerge	SS mesh	800	15	Graphite graphite	SS mesh	Aerobic	(24.1)	95.1(94.2-95.1)	~0.13 W/m3	13.8	0.28(0.19-0.28)	2 h	-		Yes
Ren et al. (2014)	Post-treatment	Hollow-fiber	Submerge	PVDF	8	0.1	Graphite fiber brush	Carbon cloth loaded Pt	Anaerobic (Air-cathode)	(0.59)	92.5	19.7 W/m3	16	6-29	4 h	-	~25	-
Tian et al. (2014)	inside-Cathode	Hollow-fiber (Covered by SS mesh)	Submerge	-	90	0.4	Carbon brush	SS mesh	Anaerobic	0.33	91.6	1.16 W/m3	6.7	10.3±1.8	17 h	-	-	Yes
Wang et al. (2014)	Parallel	Flat	Crossflow	PVDF	37.7	0.1	Carbon felt	Carbon felt	Aerobic	2.2	92	60 W/m2	8.0 (5.3-9.3)	6.5 ± 0.3 (5.5-6.5)	7.3 (6.3-11)	-	25±3	-
Zhang et al. (2014)	inside-Cathode	Flat (MC)	Submerge	SS mesh Carbon felt	30	13	Graphite rod and granular graphite	SS mesh	Aerobic	0.52(0.96)	96.4	0.12 W/m3	11	1.8	9.6 h (whole)	-	20-25	-
										0.96	95.5	1.25 W/m3		8.5	11.7 h (whole)			
Li and He (2015)	inside-Cathode	Hollow-fiber	Submerge	PVDF	-	15 kDa	Carbon brush	Carbon cloth loaded Pt	Aerobic	(2)	91.3	20.6±3.0 A/m3	-	-	21.7 h	-	-	-
											84.5	3.5±2.1 A/m3			27.4 h			
Ma et al. (2015)	Post-treatment	Flat	Submerge	-	4,800	0.1	Carbon felt	Carbon fiber brush	Aerobic	30	<100	55.0 mW/m2	4.1	0.24	15.3 h	220	<15	Yes
												98.4 mW/m2					15-36	No
Tian et al. (2015)	One-chamber	Hollow-fiber	Submerge	PVDF	2,000	0.03	Carbon brush	Carbon fiber	Aerobic	12	95.1	2.18 W/m3	7.5	1.9	-	-	-	Yes
Werner et al. (2015)	One-chamber	Hollow-fiber	Submerge	PES + PVP	14	1	Carbon cloth	Nickel-based hollow fiber membrane	Anaerobic	0.17(0.35)	83.4 ± 7.7 (83.4-89.5)	49±5 A/m3	6.9	79±30	17.6	-	25	Yes
Xu et al. (2015)	inside-Cathode	Flat (MC)	Submerge	Polyester	32	9.8	Graphite fiber brush Graphite rod and granular graphite	Anthraquinone-disulphonate/polypyrrole	Aerobic	0.72(1.24)	99.7 ± 0.5	10±1 A/m3	3.9 (2.0-3.9)	57±7	11.6 h (5.8-11.6 h (whole))	-	-	Yes
											92.5	0.35 W/m3		4.58				
Zhou et al. (2015)	inside-Cathode	Flat (MC)	Submerge	SS mesh	62	38	Carbon felt	SS mesh	Aerobic	-	92.6	0.56-0.63 W/m3	0.5	0.41-1.03	4.2-16.9 h	-	35	Yes
Ishizaki et al. (2016)	Parallel	Flat	Cross-flow	PTFE	20	0.2	Carbon felt	Carbon cloth loaded Pt	Anaerobic	0.25	77±7(71-77)	2.83 W/m3	12.5	8.9 (0.2-11.7)	10 h	-	25±2	Yes
Li et al. (2016)	Post-treatment	Hollow-fiber	Submerge	PVDF	-	15 kDa	Carbon brush	Carbon cloth loaded Pt	Anaerobic (Air-cathode)	0.9	<100	7.1 A/m3	6<	-	10	-	RT	-
Zuo et al. (2016)	inside-Cathode	Flat	Submerge	Nitrogen-doped carbon nanotube	35.9	0.095	conductive activated carbon guranule	Carbon cloth loaded Pt and nitrogen-doped carbon nanotube	Anaerobic (Air-cathode)	>(1.26)	98.3	-	5.4 L/m2/h/kPa	-	12 h	-	-	-
											88.7-97.2	5.8±0.3 mA		9.1	12 h			

[a]Reactor configuration was categorized into five types: inside-Anode, inside-Cathode, One-chamber, Parallel, and Post-treatment as

descrived elsewhere.

[b]MC; Membrane cathode

[c]Reactor volume without electrodes or the other materials were shown in parentheses.

[d-f]The range of COD removal and coulomb efficiency at various operational conditions were shown in parentheses, respectively (COD removal and coulomb efficiency, and HRT at the highest electrical generation was shown outside the parehteses, respectively)

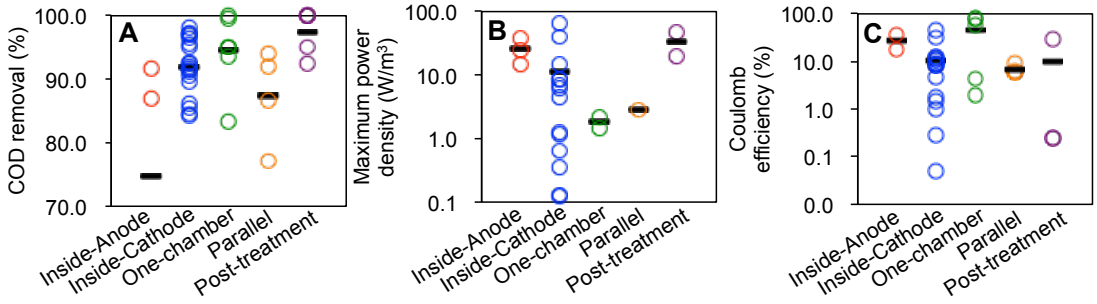

Fig. 2.2 A) COD removal, B) Maximum power density, and C) Coulomb efficiency in the integrated systems categorized into inside-Anode, inside-Cathode, One-chamber, Parallel, and Post-treatment. Maximum power generation expressed as watt over cubic meter was only referred in **Fig. 2.2B**.

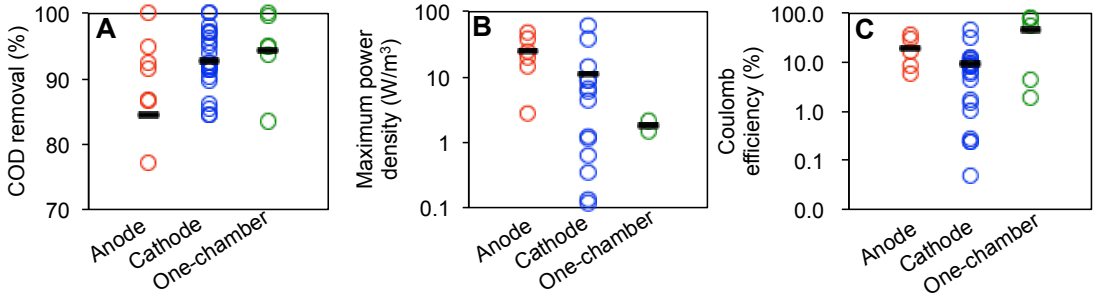

Fig. 2.3 A) COD removal, B) Maximum power density, and C) Coulomb efficiency in the integrated systems categorized into Anode, Cathode, and One-chamber. Maximum power generation expressed as watt over cubic meter was only referred in **Fig. 2.3B**.

Table 2.3 Energy balance in the integration system

Reference	Reactor configuration	Aeration	Net generated energy (kWh/m3)	Generated energy (kWh/m3)	Required energy (kWh/m3)
Katuri et ai. (2014)	One-chamber	No	0.24±0.10	0.74±0.03	0.51±0.07
Li et al. (2016)	Post-treatment	No	0.003±0.002	0.004±0.002	0.001
Ren et ai. (2014)	Post-treatment	No	0.001	0.020	0.019
Li et al. (2015)	inside-Cathode	Yes	-0.09	0.03	0.12

2.6.2. Energy balance

An estimation of energy balance of the system is addressed by several researchers (Ge et al., 2013;Katuri et al., 2014;Li and He, 2015;Li et al., 2016;Ren et al., 2014) (**Table 2.3**). While inside-Cathode shows smaller net energy generation (-0.09 kWh), Post treatment (connected to anode chamber) shows positive energy balance (Li and He, 2015;Li et al., 2016;Ren et al., 2014) (**Table 2.3**). This was due to which the energy required to operate the Cathode is much larger than the other reactors (0.12 kWh/m^3 *vs.* 0.001 and 0.0186 kWh/m^3), which is probably attributable to pumping water from anode to cathode chamber. Furthermore, One-chamber shows much positive net generated energy (0.24±0.10 kWh/m^3) (Katuri et al., 2014). Although it required enormous energy to operate to apply potential to anode electrode, much more energy can be generated as biogas comprising mainly methane (Katuri et al., 2014). In conclusion, to maximize net generated energy, single-chamber reactor should be used to minimize required energy as much as possible. Although biogas collection facilitates to increase energy recovery, it requires temperature control, proper strategy, and additional systems (Li et al., 2016). It is likely that energy-free high-quality wastewater treatment can be achieved by the system integrated single-chamber air-cathode MFC and MBR (Li et al., 2016;Ren et al., 2014).

2.6.3. Membrane fouling

1) Membrane cathode

It was recently found that the integrating MFC allow to mitigate membrane-fouling. In particular, cathode reaction and compartment involving membrane cathode have been well studied. Cathode compartment enable to mitigate membrane fouling by electric repulsion force and a generation of hydrogen peroxide (H_2O_2) on the surface of membrane cathode (Liu et al., 2013;Liu et al., 2014;Wang et al., 2013). Membrane cathode is the membrane integrated with cathode electrode so that it has negative charge on its surface. Since suspended solid generally also have negative charge, the membrane

could inhibit to attach the suspended solid on its surface, and subsequently membrane-fouling is mitigated (Liu et al., 2013;Liu et al., 2014). Indeed, although the effect of electric repulsion force on membrane surface on membrane fouling mitigation was already known previously (Akamatsu et al., 2010;Chen et al., 2007), Liu et al. introduced to make the electric repulsion force with the electricity generated by MFC (Liu et al., 2013;Liu et al., 2014). Furthermore, Wang et al. revealed that hydrogen peroxide generated on the membrane surface could oxidize and degrade the foulant attached on the surface, which is also effective to mitigate membrane fouling (Wang et al., 2013). A generation of H_2O_2 was proportional to electrical generation and the characteristic of sludge was observed in the integrated system, implying that the fouling potential of the ML might be also changed (Wang et al., 2013). SS is also effective to mitigate membrane fouling when used as cover of hollow-fiber membrane (Tian et al., 2014). Electric repulsion force was confirmed on the membrane not made by SS. Gajaraj et al. observed membrane fouling mitigation on titanium-modified membrane (Gajaraj and Hu, 2014). Moreover, anthraquinone-modified membrane could generate not only electric repulsion force but also H_2O_2 generation (Xu et al., 2015).

2) Bacterial secretion

Several papers observed a reduction in SMP (Su et al., 2013;Tian et al., 2015b) and EPS (Tian et al., 2015b;Zhou et al., 2015a) by integrated MFC. Particle size distribution was also reported to shift and the fouling potential was reduced (Tian et al., 2014;Tian et al., 2015b). H_2O_2 was reported to influence on characteristics of sludge, and might subsequently mitigate membrane fouling (Zhou et al., 2015a). In while, there is little information on the effect of anodic respiration on fouling potential. In these papers, cathode electrode was also contained in biological treatment chamber: However, the effect of anodic respiration on fouling potential and bacterial secretion is still unknown.

CHAPTER 3

Impact of anodic respiration on biopolymer production and consequent membrane fouling in electrode-associated membrane bioreactor (e-MBR)

3.1. Background and Objectives

Although membrane bioreactors (MBRs) have several advantages over conventional activated sludge system such as superior effluent water quality (complete removal of suspended solids) and small footprint, high energy requirement for aeration and membrane fouling are the remaining major challenges for wider practical application (Judd, 2008;Meng et al., 2009a). Aeration is a major energy consuming process, often exceeding 50% of total energy consumption (Gil et al., 2010;Kraume and Drews, 2010). Membrane fouling in MBRs is generally controlled by continuous air-scrubbing and periodical chemical cleaning, which also increases the operational cost. In addition to continuous air-scrubbing, aeration is needed to supply oxygen as electron acceptor for biological oxidation. Therefore, aeration must be optimized or minimized to reduce the energy consumption (Gil et al., 2010).

Microbial fuel cells (MFCs) have been considered as a promising wastewater treatment technology with renewable energy recovery (Logan et al., 2006;Wang et al., 2015). In MFCs, bacteria use anode electrodes as electron acceptor for substrate oxidation in the absence of any dissolved electron acceptors. MFCs also have several advantages, including no requirement of aeration and sludge reduction. However, the MFC effluents usually need post-treatment to meet the effluent discharge standards due to poor effluent water quality (Wang et al., 2011b).

In order to reduce the energy consumption of MBRs and improve the MFC effluent water quality simultaneously, here, we propose an electrode-assisted membrane bioreactor (e-MBR). This e-MBR system takes advantages of both MFC and MBR, in

which the aeration for oxygen supply is omitted and anode electrode is installed in MBR as alternative electron acceptor instead. Namely, organic matter is oxidized using a solid anode electrode as electron acceptor under anoxic conditions (anodic respiration) (Logan, 2009;Torres et al., 2009). The e-MBR could simultaneously achieve reduction of energy consumption, high effluent water quality, sludge reduction, and recovery of renewable energy (*i.e.*, electrical power) without aeration. Therefore, e-MBR is expected as a promising net energy positive or neutral wastewater treatment.

Some MFC and MBR integrated systems have been proposed for wastewater treatment, energy recovery, and membrane fouling mitigation (Liu et al., 2014;Ma et al., 2015;Su et al., 2013;Tian et al., 2014;Tian et al., 2015b;Wang et al., 2011b;Wang et al., 2013). In these integrated systems, stainless steel meshes were submerged in aerated chambers and used as membrane bio-cathode for simultaneous oxygen reduction reaction and filtration. High removal efficiencies of chemical oxygen demand (COD) and ammonia nitrogen were observed with sludge reduction and electricity recovery (Ma et al., 2015;Wang et al., 2011b). Furthermore, the integrated systems were able to mitigate membrane fouling by degrading microbial metabolites such as soluble microbial products (SMP) and loosely-bound extracellular polymeric substances (EPS) (Su et al., 2013;Tian et al., 2014;Tian et al., 2015b) and generating electric field that modifies sludge properties including the average floc size (Tian et al., 2014;Tian et al., 2015b) and membrane (*i.e.*, stainless steel mesh) surface charge (Wang et al., 2013). However, these integrated systems use membrane bio-cathodes and thus still require aeration for biological oxidation of organic matter and air-scrubbing. Furthermore, it takes a relatively long time to establish bio-cathods (*i.e.*, cathode biofilms).

One of concerns of e-MBR that we propose is membrane fouling because e-MBR does not have aeration for air-scrubbing and biological oxidation. However, the impact of anodic respiration by exoelectrogens on membrane fouling has not been investigated yet (Yuan and He, 2015).

In this study, we therefore constructed MFC reactors equipped with different

external resistances that regulate the degree of anodic respiration and measured the membrane-fouling potential of each MFC anode effluent by using cross-flow membrane filtration systems to investigate the impact of anodic respiration on membrane fouling. Furthermore, to explain why membrane fouling was mitigated, we investigated biopolymer (a main membrane foulant) production by exoelectrogens. The results demonstrated that a dominant exoelectrogen such as *Geobacter sulfurreducens* produced less biopolymer under anodic respiration condition than fumarate (anaerobic) respiration condition, which consequently leads to membrane fouling mitigation.

3.2. Materials and Methods

3.2.1. MFC configuration and operation

MFCs equipped with different external resistances (100 - 10,000 Ω) (MFC A - C) were constructed (**Table 3.1**) to evaluate the impact of anodic respiration on MFC performance and membrane-fouling potential of anode effluents. An open circuit MFC (MFC D) was operated as a control (without any dissolved electron acceptor and anode electrode in the anode chamber). The double-chamber MFC consisted of an anode chamber (250 ml) and a cathode chamber (250 ml). The porous carbon (6 cm × 5 cm, Somerset; NJ, USA) and carbon cloth loaded with 0.5 mg/cm^2 of platinum (3 cm × 5 cm, E-TEK, Somerset; NJ, USA) were used as an anode electrode and a cathode electrode, respectively. Each chamber was separated with a Nafion membrane (Nafion^{TM} 117, Dupont Co., DE, USA). Each MFC reactor was operated at room temperature (25 ± 2˚C).

Each anode of MFC was inoculated with biomass from a MFC fed with glucose as sole energy source in our laboratory, and incubated for 7 days as a batch mode. Thereafter, a synthetic medium containing 200 μM $(NH_4)_2SO_4$, 200 μM NaCl, 500 μM $CaCl_2$, 500 μM $MgCl_2$•$6H_2O$, 27 mM K_2HPO_4, 55 mM KH_2PO_4 and 2.8 mM glucose (a sole energy source) was continuously fed with peristaltic pumps (MP-1100; EYELA; Tokyo, Japan) at a hydraulic retention time (HRT) of 10 hr as previously

described (Chung and Okabe, 2009). After 4-month operation (first run), the cross-flow filtration experiments were conducted to measure the membrane-fouling potentials of anode effluents. Subsequently, the operational condition of each MFC reactor was changed as described in **Table 3.1** (second run) and incubated for 8 weeks to stabilize the reactor performance. After the incubation, the cross-flow filtration experiments were conducted to confirm the reproducibility of the results of the first run. In the second run, ambient air was continuously supplied into the anode chamber of MFC D at a flow rate of 250 ml/h. Each cathode chamber of closed-circuit MFC (MFC A - D) was filled with the catholyte containing 100 mM potassium ferricyanide, 27 mM K_2HPO_4, and 55 mM KH_2PO_4, which was not aerated during operation of both runs.

Cell voltage and electrical current were continuously monitored using a multimeter and a data acquisition system (Agilent HP 34970). The anode effluent pH was measured using a pH meter (F-51; Horiba, Ltd.; Tokyo, Japan). COD concentration was measured following HACH COD method 8000 by using a HACH COD reactor and spectrophotometer DR/2400 (HACH Co.; CO, USA). The OD_{600} was measured by using an optical absorbance meter (Smart Spec Plus; Bio-Rad; CA, US). Coulombic efficiency (CE) was calculated with the equation described elsewhere (Logan et al., 2006).

3.2.2. Membrane-fouling potential

Membrane-fouling potential (trans-membrane pressure (TMP)) was measured for 3 hr using bench-scale cross-flow filtration systems (CFMFS) (Ishizaki et al., 2016a). Filtration experiments were carried out with a constant permeate flux of 0.3 m/d using peristaltic pumps (MP-1100; EYELA; Tokyo, Japan) without aeration. Flat membrane filters (100 mm× 20 mm, 0.2 μm, hydrophilic PTFE; Advantec Toyo; Tokyo, Japan) were used for all filtration experiments. More detailed information on dimension and operation of the CFMFS can be found in elsewhere (Ishizaki et al., 2016a). The cross-flow filtration tests were performed in triplicates for each MFC before and after

the external resistances were changed as described in **Table 3.1** (**Fig. 3.1A** and **3.1B**).

Each filtration test was carried out for 3 hr and the trans-membrane pressure (TMP) at 3 hr (TMP_3) was measured. After filtration tests, the mixed liquor (ML) and biocake (BC) on fouled membranes were collected to characterize the soluble microbial product (SMP) as below. Dead-end filtration experiment was also carried out to determine the fouling potential of soluble microbial product (SMP) as described in previous study (Ishizaki et al., 2016a) (Ramesh et al., 2007). In order to estimate the percentage of SMP trapped on membrane to SMP in ML, TOC concentrations of SMP before and after the dead-end filtration was measured.

3.2.3. Extraction of SMP and EPS

In this study, SMP was defined as total organic carbon (TOC) in the supernatant after centrifugation of ML at 4°C, 6000 × *g* for 15 min (Eboigbodin and Biggs, 2008). The SMP contained in BC was collected as follows: the BC on fouled membrane was removed and resuspended in 25 ml of 0.05% NaCl solution by vortexing for 1 min, and then centrifuged as described above (Ishizaki et al., 2016a). Loosely-bound and tightly-bound extracellular polymeric substances (LB-EPS and TB-EPS) in ML and BC were extracted as described previously with minor modifications (Li and Yang, 2007). The biomass pellet was resuspended with 15 ml of 0.05% NaCl solution and the suspension was mixed with 25 ml of 0.05% NaCl solution of 70 °C, and thus resuspended by vortexing for 1 min. After the centrifugation at 4°C, 6000 × *g* for 15 min, the supernatant gained was regarded as LB-EPS. The pellet was resuspended with 40 ml of 0.05% NaCl solution and heated at 60 °C for 30 min. After the centrifugation with the same condition, the supernatant gained was regarded as TB-EPS.

3.2.4. Chemical analysis

TOC concentration of the supernatant was measured using a TOC analyzer (TOC-V CSH; Shimadzu; Kyoto, Japan). Protein concentration was determined by using an

excitation-emission matrix (EEM) fluorescence spectrometer (Aqualog; Horiba, Ltd., Tokyo, Japan) and parallel factor analysis (PARAFAC) with BSA as the standard. There was a clear correlation between the score obtained by PARAFAC and the protein concentration (R^2 > 0.99). Carbohydrate concentration was determined with the phenol-sulfonic acid method with glucose as the standard. Glucose concentration was measured with a Dionex DX 500 HPLC equipped with a pulsed amperometric detector (Dionex ED40) (Dionex Co., CA, US) (Kimura et al., 2009). Particle size distributions of ML were measured by using a Nano Sight NS500 (SALD-7100; Shimadzu Co., Kyoto, Japan). Biopolymer concentration in the supernatant was determined by using a Liquid chromatography with organic carbon detection (LC-OCD Model 8, DOC-LABOR; Karlsruhe, Germany) after filtration with 0.45 μm hydrophilic PTFE membranes (Advantec Toyo; Tokyo, Japan) as described previously (Huber et al., 2011) (Yamamura et al., 2014). The mixed liquor suspended solid (MLSS) concentration in each MFC reactor was measured according to the Standard Methods (Apha, 1998).

3.2.5. Microbial community analysis

The microbial communities in the ML, BC, and inner and outer part of anode biofilms (AB_{in} and AB_{out}) were analyzed by applying Illumina Miseq analysis (Illumina; Hayward, CA, USA) (Caporaso et al., 2012). The ML (3 ml) was centrifuged at 4°C, 8000 × *g* for 5 min. The BC on fouled membrane (20 mm × 20 mm) was cut into quarters with a sterile scissor, resuspended in 0.05% NaCl solution by vortexing for 1 min, and then centrifuged as above. The anode electrode (ca. 5 mm × 5 mm) was cut with a sterile scissors, suspended into 0.05% NaCl solution (10 ml), and vortexed for 10 sec. The loosely attached biofilm was regarded as the outer part of anode biofilm (AB_{out}) and the remaining biofilm on the anode electrode after vortexing was regarded as the inner part of biofilm (AB_{in}). The biomass was harvested by centrifugation (8000 × *g* for 5 min) and total community DNA was extracted using a Fast DNA Spin kit for soil (Bio101, Vista; CA, USA). The DNA of AB_{in} was extracted directly from the anode

electrode after collecting the AB_{out}. The partial 16S rRNA genes including v3 and v4 regions were amplified with Bakt_341F and Bakt_805R primers (Miura et al., 2013). Illumina Miseq 16S rRNA gene analysis was performed as described elsewhere (Rathnayake et al., 2015). The sequence reads were analyzed by using QIIME 1.8.0 with the Silva 119 database, respectively (Caporaso et al., 2012). The qPCR assays were performed using SYBR Green chemistry to quantify the bacterial populations in ML, BC, AB_{out}, and AB_{in} samples as based on the number of 16S rRNA gene (Kobayashi et al., 2013). In SYBR Green assays, each PCR mixture (10 µl) was composed of 1× SYBR Premix Ex Taq II (Takara Bio, Otsu, Japan), 50× ROX Reference Dye (Takara Bio, Otsu, Japan), 400 nM each of forward and reverse primers, and 2 µl of template DNA. The set of primers of Eub338f (5'-CCTACGGGAGGCAGCAG-3') and Eub518r (5'-GWATTACCGCGGCKGCTG-3') were used to quantify the total bacteria numbers in MFCs (Elshahed et al., 2008).

3.2.6. *Geobacter sullferreducens* strain PCA

Geobacter sulfurreducens strain PCA was grown in the double-chamber MFC as mentioned above with anode electrode (anodic respiration) or fumarate (fumarate respiration) as a sole electron acceptor, and tested for biopolymer production and consequent membrane-fouling potential, respectively. Furthermore, foulant degradation ability of the strain PCA was investigated. The pure culture of strain PCA was pre-incubated for 4 days, washed twice with and inoculated into a medium containing 200 µM $(NH_4)_2SO_4$, 200 µM NaCl, 500 µM $CaCl_2$, 500 µM $MgCl_2 \cdot 6H_2O$, 27 mM K_2HPO_4, 55 mM KH_2PO_4 and 20 mM acetate (a sole energy source) (OD_{600} = approximately 0.1). For fumarate respiration study, 40 mM disodium fumarate was added to the medium (Nevin et al., 2009). The strain PCA was incubated for 4 days as a batch mode, and the MLs were sampled every day for measurement of membrane-fouling potential and biopolymer concentration. Membrane-fouling potential was evaluated by dead-end filtration, and biopolymer concentration was determined as

Table 3.1 Performance of MFCs before and after external resistance was changed

First run

	MFC A-1	MFC B-1	MFC C-1	MFC D-1
Electron acceptor	Anode electrode (Anodic respiration)	Anode electrode (Anodic respiration)	Anode electrode (Anodic respiration)	Non
External resistance	100 ohm	1,000 ohm	10,000 ohm	-
Electrical current (mA)	2.78 ± 0.02	0.60 ± 0.01	0.07 ± 0.00	-
Cell voltage (mV)	246.2 ± 1.0	634.7 ± 1.1	750.6 ± 0.6	-
Power density (W/m^3)	2.83 ± 0.01	1.62 ± 0.00	0.21 ± 0.00	-
Coulombic efficiency (%)	8.9	2	0.2	-
pH value in	6.9 ± 0.0	7.0 ± 0.0	6.9 ± 0.1	7.0 ± 0.0
ML OD600	0.19 ± 0.01	0.18 ± 0.02	0.21 ± 0.02	0.17 ± 0.01
COD removal (mg/l/h)	38.5 ± 3.5	35.5 ± 0.5	35.5 ± 0.5	39.0 ± 2.0
COD removal rate (%)	77 ± 7	71 ± 1	71 ± 1	78 ± 4

Second run

	MFC A-2	MFC B-2	MFC C-2	MFC D-2
Electron acceptor	Anode electrode (Anodic respiration)	Anode electrode (Anodic respiration)	Anode electrode (Anodic respiration)	Oxygen
External resistance	10,000 ohm	1 ohm	100 ohm	-
Electrical current (mA)	0.07 ± 0.00	3.54 ± 0.03	2.42 ± 0.01	-
Cell voltage (mV)	785.4 ± 0.7	5.9 ± 0.0	246.8 ± 0.8	-
Power density (W/m^3)	0.23 ± 0.01	0.08 ± 0.00	2.40 ± 0.01	-
Coulombic efficiency (%)	0.2	11.7	7.8	-
pH value in	7.1 ± 0.1	7.0 ± 0.0	7.1 ± 0.1	7.0 ± 0.1
ML OD600	0.20 ± 0.01	0.21 ± 0.02	0.20 ± 0.02	0.22 ± 0.01
COD removal (mg/l/h)	32.5 ± 3.3	32.7 ± 1.8	32.6 ± 2.2	38.9 ± 1.1
COD removal rate (%)	72 ± 6	71 ± 3	71 ± 5	79 ± 2

described above. Furthermore, the entire ML of each MFC was exchanged with the same volume of the autoclave-sterilized anode effluent of MFC D-2 (aerobic). The membrane-fouling potential of the ML of MFC D-2 was monitored by dead-end filtration to evaluate the foulant degradation ability of the strain PCA. Acetate concentration of ML was measured using High-Performance Liquid Chromatography (LC-10AD; Shimadzu Co., Kyoto, Japan). Each MFC reactor was equipped with an external resistance of 100 ohm and operated at room temperature (25 ± 2˚C).

3.3. Results and Discussion

3.3.1. Performance of MFCs

The overall performances of MFCs are summarized in **Table 3.1**. The higher electrical current and lower cell voltage, resulting in higher power generation, were observed at lower external resistance (**Table 3.1**). There was no significant difference in COD and

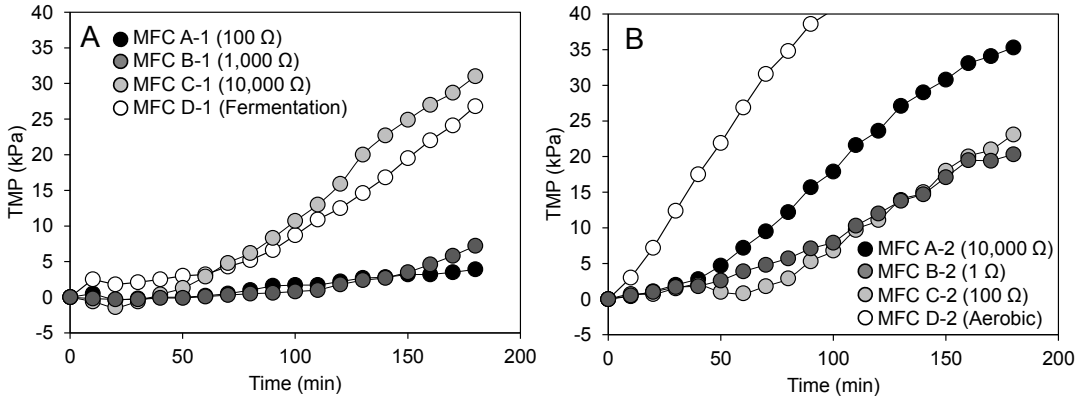

Figure 3.1 Time courses of trans-membrane pressure (TMP) of MFCs equipped with different external resistances (**A**) before and (**B**) after the external resistances were changed. The filtration tests were performed in triplicates and the reproducibility was confirmed. A typical time course of TMP is presented under each operational condition. The membrane-fouling potential of the MFC equipped with lower external resistance is lower than that of the MFC equipped with higher external resistance and control reactors (MFC D-1 (Fermentation) and D-2 (Aerobic)).

glucose removal efficiencies regardless of anodic and aerobic respiration. Glucose was not detected in any MFC anode effluents (data not shown). Coulombic efficiencies (CE) of closed-circuit MFCs were in a range of 0.2 – 11.7%, being similar with the values of the integrated MFC–MBR systems (Ma et al., 2015;Tian et al., 2014;Tian et al., 2015b;Wang et al., 2014;Wang et al., 2011b;Zhou et al., 2015a). Aerobic respiration (due to oxygen contamination), fermentation, and/or methanogenesis in the anode chamber would be possible reasons led to such low CE values (Ishii et al., 2013;Liu and Logan, 2004). In particular, glucose-fed MFC was likely to cause lower CE due to electron loss by competing the metabolisms such as fermentation and methanogenesis (Chae et al., 2009;Pant et al., 2010).

3.3.2. Impact of anodic respiration on membrane-fouling potential

The membrane-fouling potential of each MFC effluent was directly measured using

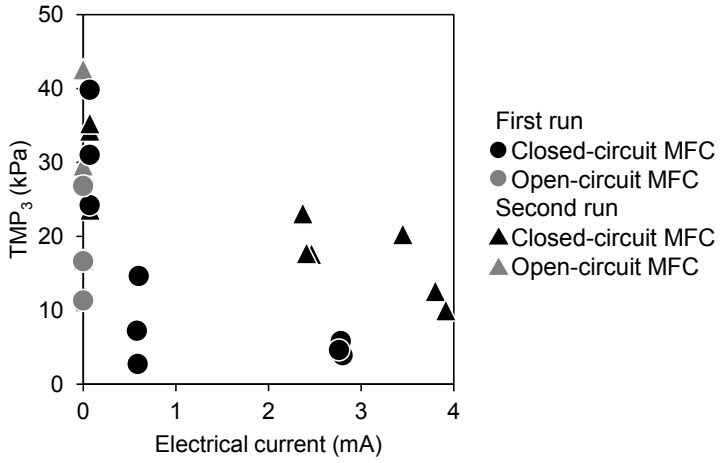

Figure 3.2 A relationship between TMP_3 and electrical current generation in each MFC. Closed-circuit MFC and open-circuit MFC indicated MFC A-C and MFC D in both first and second run, respectively. TMP_3 was lower at higher electrical current generation.

cross-flow membrane filtration system (CFMFS) and related to the characteristics of the soluble microbial product (SMP) and the microbial community in anode biofilms. The time courses of TMP revealed that membrane-fouling potentials of MFCs equipped with lower external resistances (*i.e.*, MFC A-1 (100 Ω) and B-1 (1,000 Ω)) were significantly lower than those of MFC C-1 equipped with 10,000 Ω and open circuit MFC D-1 (Fermentation), which clearly suggest that membrane fouling was mitigated at high current generation (active anodic respiration) (**Fig. 3.1**). To evaluate the reproducibility, the external resistances of closed-circuit MFCs were changed as described in **Table 3.1,** MFCs were operated for additional 8 weeks, and then the filtration tests were performed. As a result, similar results were obtained, indicating that the membrane fouling mitigation by active anodic respiration was reproducible (**Fig. 3.1B**). For example, the TMP_3 of MFC A-1 (100 Ω) was the lowest in the first run but became the second highest after the external resistance was changed to 10,000 Ω.

Based on these experimental results, it can be concluded that the membrane-fouling potential of MFCs with higher current generation was significantly lower than that of conventional MBR with aeration (MFC D-2 (aerobic)) and depends

on the degree of anodic respiration (current generation) (**Fig. 3.2**). Overall, fouling potentials in the second run were higher than those in the first run (**Fig. 3.2**). The second run was initiated with the high MLSS concentration caused by biofilm detachment from anode electrodes due to the long incubation.

The integrated MFC and MBR systems could potentially mitigate membrane fouling even though their CEs were low (in a range of 1.0% to 12.1%) (Ma et al., 2015;Tian et al., 2014;Tian et al., 2015b;Wang et al., 2014;Zhou et al., 2015a). For example, Tian *et al*. reported the mitigation of membrane fouling in an anaerobic membrane bio-electrochemical reactor (AnMBER) with CE of 10.3 ± 1.8% (Tian et al., 2014). However, the membrane fouling could not be mitigated when the CE was as low as 0.24% (Ma et al., 2015). This consists with our results that MFC C-1 (10,000 Ω) and MFC A-2 (10,000 Ω), whose CEs were about 0.2%, could not mitigate membrane fouling effectively (**Fig. 3.1A** and **3.1B**). In addition, the fouling potential of MFC A-1 (100 Ω) and MFC B-1 (1,000 Ω) was similar (**Fig. 3.1A**) even though the CEs were different (8.9% *vs*. 2.0%) (**Table 3.1**). These results suggest that there might be a threshold CE value for membrane fouling mitigation, above which the mitigation effect could be minimal. Further study is required to validate this speculation.

In order to better understand the mechanism of membrane fouling mitigation, electron balance, i.e., the distribution of electron sinks other than electrical current generation, must be determined. Biomass, EPS, SMP, and CH_4 are considered as dominant electron sinks and their distribution can vary with anodic potential (Freguia et al., 2008;Yu et al., 2015). It was also reported that inhibition of methanogenesis promoted the electron flow to biomass including SMP (Jiang et al., 2010b;Parameswaran et al., 2009), which is a main foulant in this study. In this study an exact electron balance could not be determined because CH_4 and organic acids were not quantified. However, the amount of SMP, especially biopolymers, was quantified, which was directly correlated with the membrane fouling (**Fig. 3.3C** and **3.3D**).

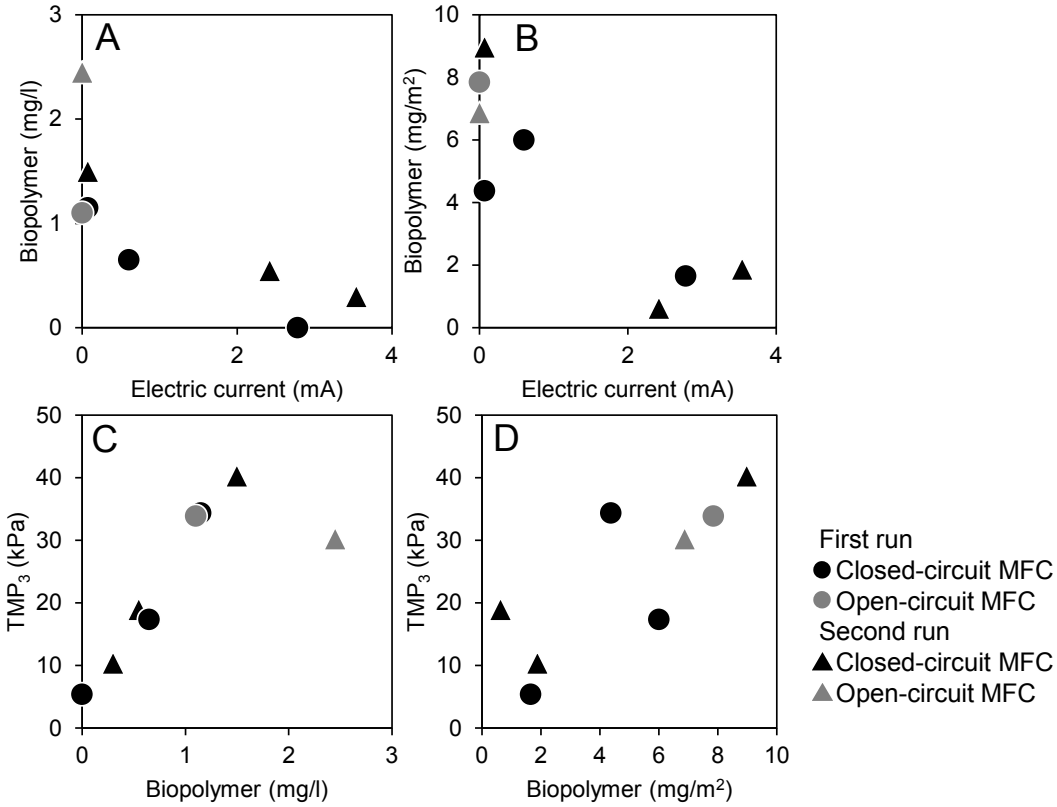

Figure 3.3 Biopolymer concentrations in mixed liquor (ML) and biocake (BC) were adversely correlated to electrical current generation (**A** and **B**), showing less biopolymer was produced and accumulated under high current generation. TMP_3 clearly increased with increasing biopolymer concentrations in the ML (**C**) and in BC (**D**), indicating biopolymer is a major foulant in this study. Closed-circuit MFC and open-circuit MFC indicated MFC A-C and MFC D in both first and second run, respectively.

3.3.3. Characterization of SMP

To investigate why membrane fouling was mitigated in MFCs with high current generation, SMP in the anode mixed liquor (ML) was characterized. Membrane fouling potential of SMP in each MFC reactor as determined by the dead-end filtration experiment was significantly different and closely correlated to the degree of fouling potential shown in **Fig. 3.1** (**Fig. 3.4A**) even though MLSS concentrations, particle size distributions, EPS concentrations and OD_{600} in the ML were basically similar with each

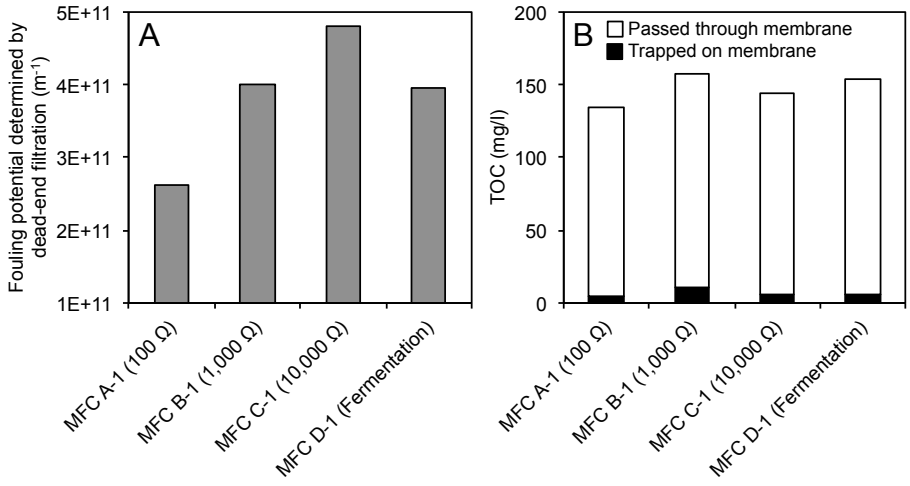

Figure 3.4 (A) Fouling potentials of SMP in each MFC anode effluent were tested by dead-end filtration experiment. (B) Percentage of SMP passed through and trapped on membrane in the dead-end filtration experiment, showing only a small fraction of SMP was trapped on the membrane.

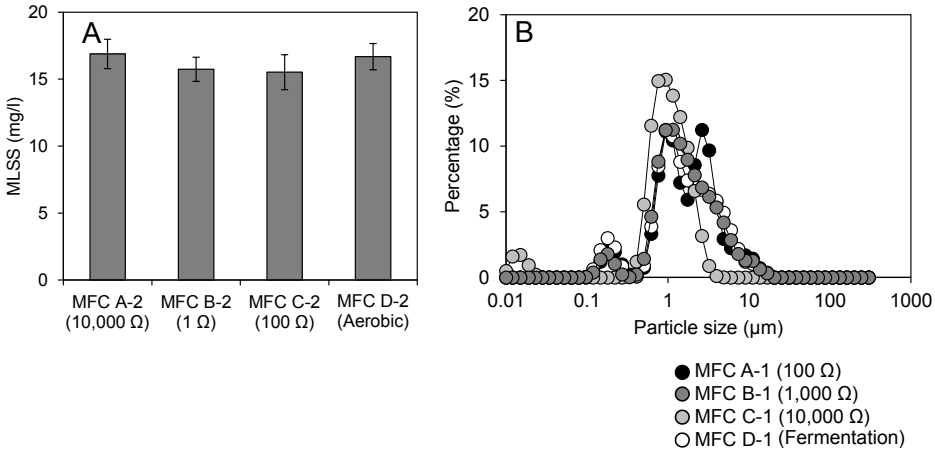

Figure 3.5 (**A**) MLSS concentration and (B) particle size distribution in each MFC anode effluent. There was nor significant difference among different MFC set-ups.

other (**Fig. 3.5 and 3.6**). These results indicated that SMP was a main cause of membrane fouling in this study as previously reported (Ishizaki et al., 2016a;Jiang et al., 2010b)**.**

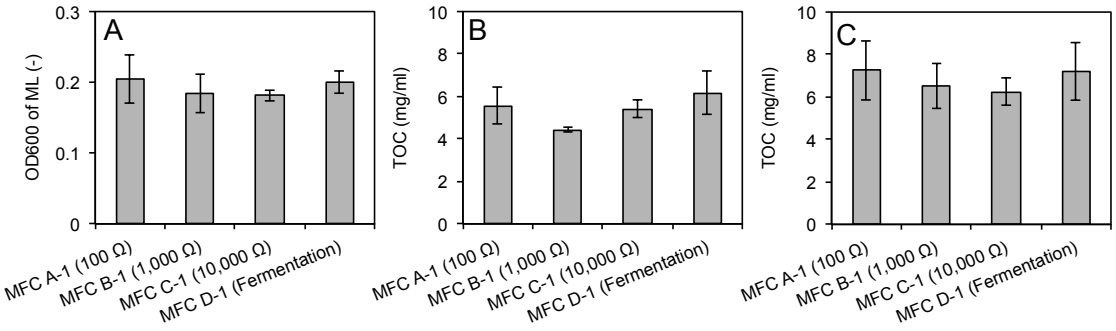

Figure 3.6 (**A**) OD_{600} of the ML and TOC concentrations of (B) loosely-bound EPS (LBEPS) and (C) tightly-bound EPS (TBEPS) in the first run. There was no significant difference among different MFC set-ups.

First, total organic carbon (TOC), carbohydrate and protein concentrations in the SMP of mixed liquor (ML) and biocake (BC) were measured and related to TMP_3 (**Fig. 3.7**). However, there was no clear correlation between TMP_3 and these concentrations, which is in agreement with previous reports (Gao et al., 2013b;Kimura et al., 2009). The peak intensity at Ex/Em = 270 nm/320 nm, which was recognized as protein-like substances in previous studies (Chen et al., 2003;Wang et al., 2009c), did not correlate with TMP_3 (**Fig. 3.8**).

Second, the concentrations of biopolymer, which is defined as a hydrophilic fraction with high molecular weight (>10 kDa) detected by LC-OCD (Haberkamp et al., 2007;Tran et al., 2015), were measured and related to the TMP_3 (**Fig. 3.3**). There were clear positive correlations between TMP_3 and the biopolymer concentrations in both ML and BC in both first and second run (**Fig. 3.3C** and **3.3D**), suggesting that membrane fouling was mainly caused by biopolymer. Although biopolymer accounted for small percentage of SMP (< 2.1%), only a small fraction of SMP (< 7.0%) was trapped on membrane and caused severe membrane fouling (**Fig. 3.4B**). Biopolymers have been paid attention recently and regarded as the main important foulant in MBRs treating real wastewater (Jiang et al., 2010b;Meng et al., 2009c;Tian et al., 2013).

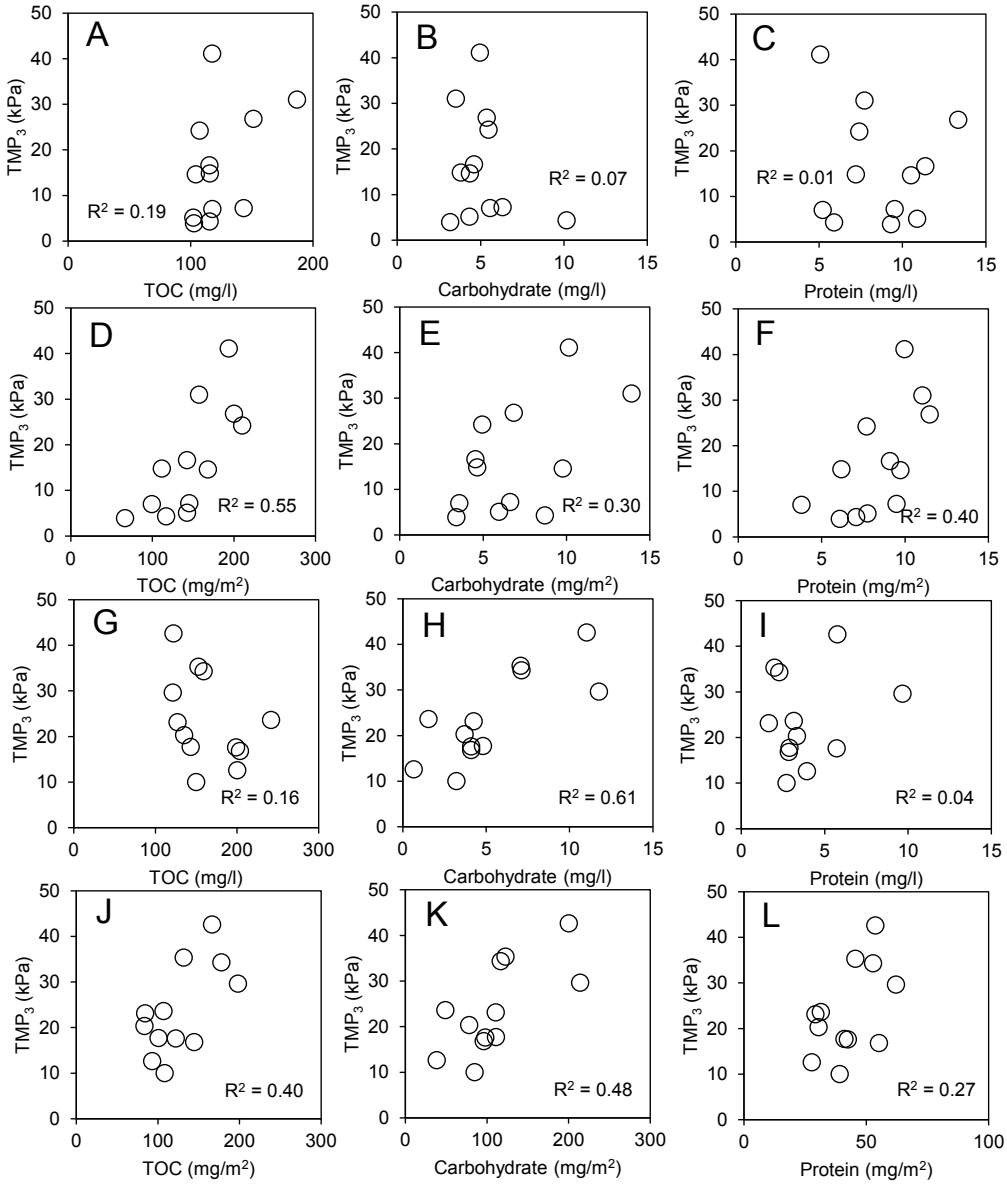

Figure 3.7 Correlations of TMP with the SMP in ML (**A** to **C**) before and (**G** to **I**) after and in biocake (BC) (**D** to **F**) before and (**J** to **L**) after the external resistance was changed. The concentrations of TOC, carbohydrate and protein contained in SMP were compared with TMP value at 3 hr (TMP_3) after the filtration was started. TOC, carbohydrate and protein contained in BC had correlation with TMP_3 compared with that in ML. These experiments were performed in triplicates.

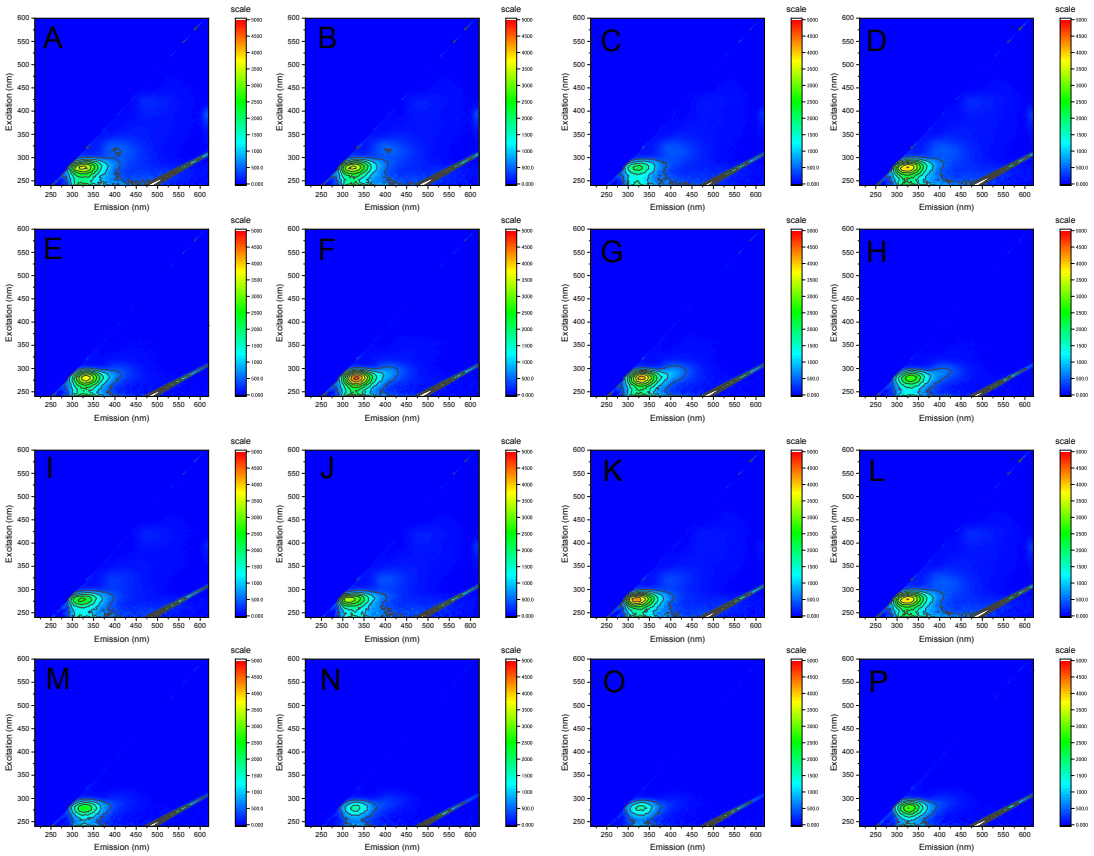

Fig. 3.8 Fluorescence excitation-emission matrix of SMP contained in ML (**A** to **D**) and BC (**E** to **H**) of MFC A-1 (100 Ω), MFC B-1 (1,000 Ω), MFC C-1 (10,000 Ω), and MFC D-1 (Fermentation), and in ML (**I** to **L**) and BC (**M** to **P**) of MFC A-2 (10,000 Ω), MFC B-2 (1 Ω), MFC C-2 (100 Ω), and MFC D-2 (Aerobic), respectively.

It is noteworthy that the biopolymer production was inversely related to the electrical current generation (*i.e.*, the degree of anodic respiration) in both first and second run (**Fig. 3.3A** and **3.3B**). The higher biopolymer concentrations were observed in MFCs equipped with higher external resistances (lower current generation) and open circuit MFC (MFC D-1 and D-2). This implies that more biopolymer is produced by aerobic respiration than anodic respiration.

It is a subject of great interest to investigate whether this difference in biopolymer production is attributed to different microbial community developed in

MFCs or respiration activity with different electron acceptors (fermentation *vs*. anodic respiration). Therefore, the microbial community structure of each MFC was analyzed based on 16S ribosomal RNA (rRNA) gene sequences using next-generation sequencing (Illumina MiSeq).

3.3.4. Microbial community analysis

Microbial population in the inner part and outer part of anode biofilms (AB) and mixed liquor (ML) were quantified based on 16S rRNA gene copy numbers (**Fig. 3.9A**). The majority of bacteria was associated with anode biofilms in this study. The copy numbers (i.e., biomass) in anode biofilms decreased in the second run, which was probably caused by the biofilm detachment due to the change in operational conditions. In general, anodic biofilms tended to increase with a decrease in external resistance (Aelterman et al., 2008;Zhang et al., 2011).

Microbial communities of the ML, BC and anode biofilms (inner part; AB_{in} and outer part; AB_{out}) were analyzed based on 16S rRNA gene sequences using next-generation sequencing (Illumina MiSeq) (**Fig. 3.10**). The microbial communities (*Proteobacteria* accounted for more than 70%) of the ML and BC were more or less similar each other in all MFCs (**Fig. 3.11**), indicating that the suspended biomass in the ML was directly entrapped and deposited on the membrane as biocake (BC). In contrast to the ML and BC, the microbial communities of anode biofilms, especially inner parts, were clearly diverse and distinct from those of ML and BC. The most distinct feature was that *Geobacteraceae* was detected at high percentage in the inner part of anode biofilms in MFCs equipped with lower external resistances (e.g., MFC A and B) (**Fig. 3.9B**). *Methanobacteriaceae*, hydrogenotrophic methanogens, were also detected in the inner part of anode biofilm (in a range of 1.6% – 4.1%) (**Fig. 3.9B**), which might indicate the possibility of CH_4 formation since fermentable glucose was used as a sole substrate in this study (however, CH_4 was not measured in this study) (Freguia et al., 2008;Yu et al., 2015). The electrical current generation was highly dependent on the

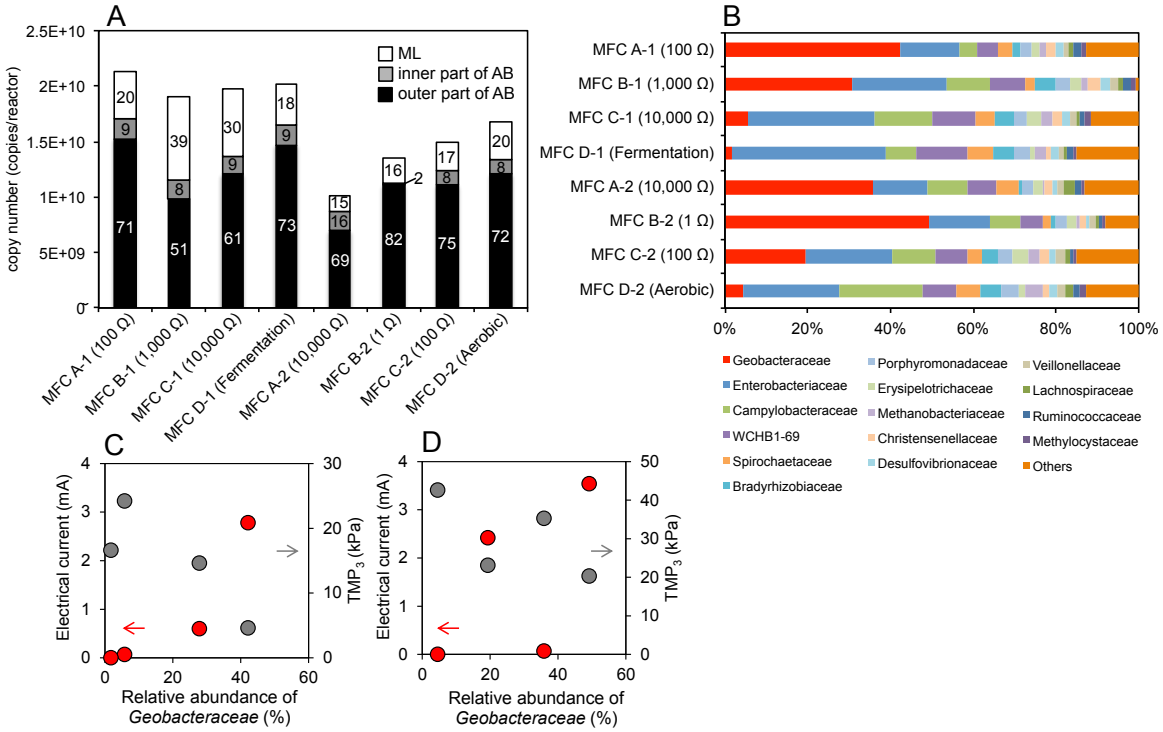

Figure 3.9 Microbial community analyses of MFCs. (**A)** Copy numbers of 16S rRNA genes in mixed liquor (ML) and in inner part and outer part of anode biofilms (AB). Biofilm bacterial communities account for 59 - 84% of total copy numbers. (**B**) Microbial community compositions of inner part of anode biofilms based on MiSeq 16S rRNA gene sequencing analysis, showing the higher abundance of *Geobacteraceae* in MFCs equipped with lower external resistances. Relationships among relative abundance of *Geobacteraceae* in inner part of anode biofilms, electrical current, and TMP_3 (**C**) before and (**D**) after the external resistances were changed. At higher abundance of *Geobacteraceae,* higher electrical current was generated, and lower TMP_3 was observed.

relative abundance of *Geobacter* (**Fig. 3.9C** and **3.9D**). The higher current generation and lower TMP_3 were observed at higher abundance of *Geobacter* (**Fig. 3.9C**). The relative abundance of exoelectrogens in anode biofilms increased with decreasing the external resistance due to increases in anodic potential and electrical current (Aelterman et al., 2008;Chae et al., 2009;Ishii et al., 2013;Liu and Logan, 2004). However, this

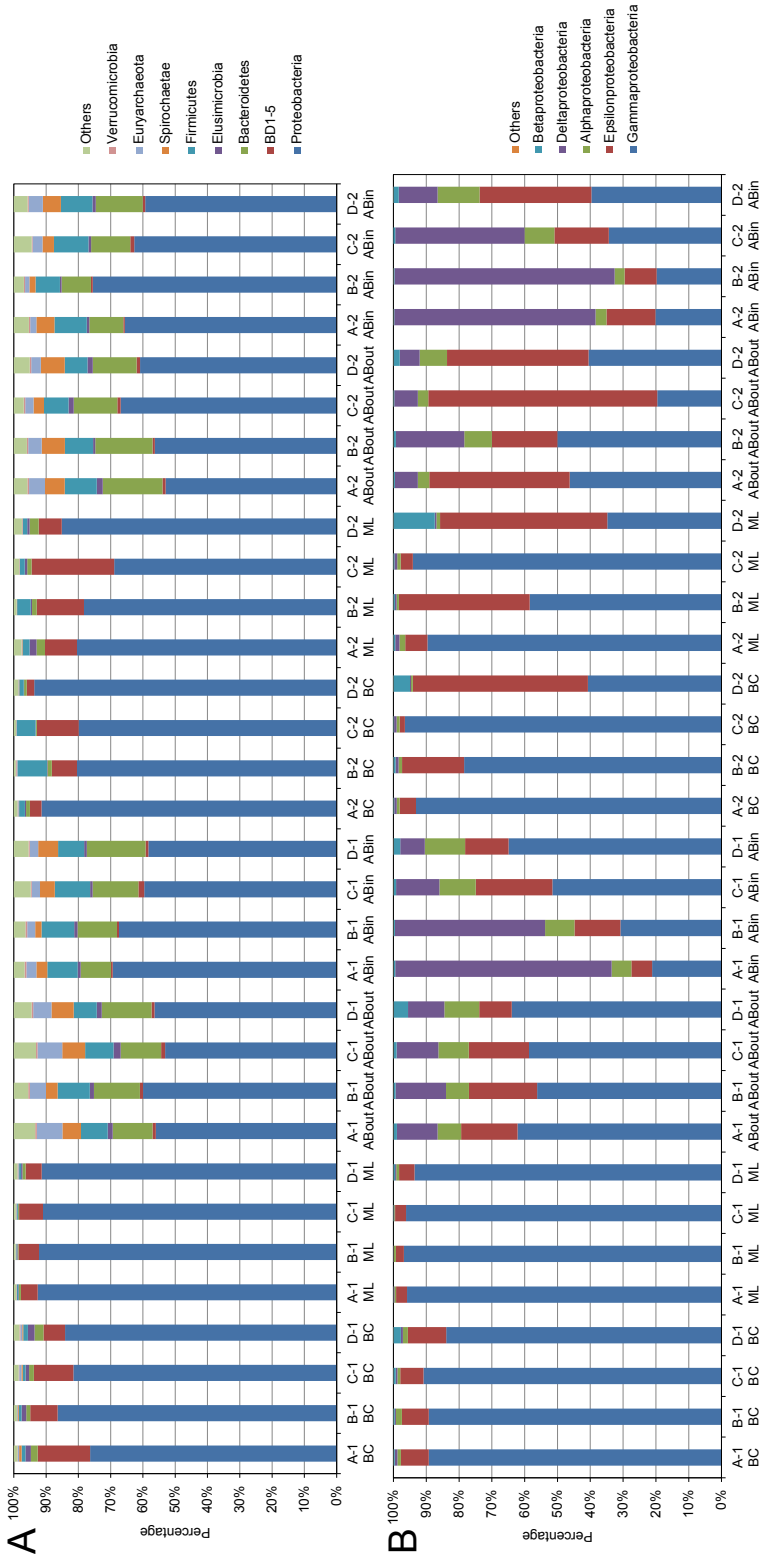

Fig. 3.10 Results of MiSeq 16S rRNA gene analysis in phylum level (**A**) and class level (**B**) in *Proteobacteria*

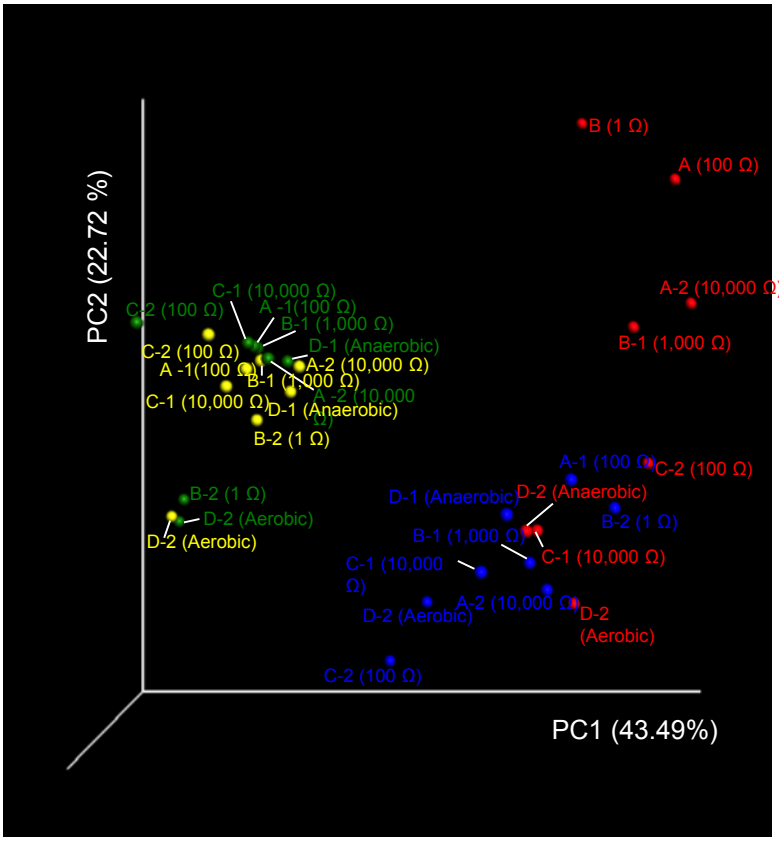

Fig. 3.11 Weighted principle compartment analysis (PCA) of microbial communities in ML, BC, and inside and outside of anodic electrode (AB_{out} and AB_{in}, respectively) of MFCs based on MiSeq 16S rRNA gene analysis.

general trend was slightly changed after the external resistance was changed (in the second run), because the anode biofilm community still did not reach steady state due to a short incubation time (8 weeks) (**Fig. 3.9D**).

Based on these results, it is speculated that the actively anode-respiring *Geobacter* dominated and produced less biopolymer, a main membrane foulant, in MFCs equipped with lower external resistances (MFC A-1 (100 Ω) and B-1 (1,000 Ω)), which consequently led to the mitigation of membrane fouling. However, it is not clear whether (1) the predominant *Geobacter* produce less biopolymer under anodic respiration than fumarate (anaerobic) respiration condition or (2) *Geobacter* can

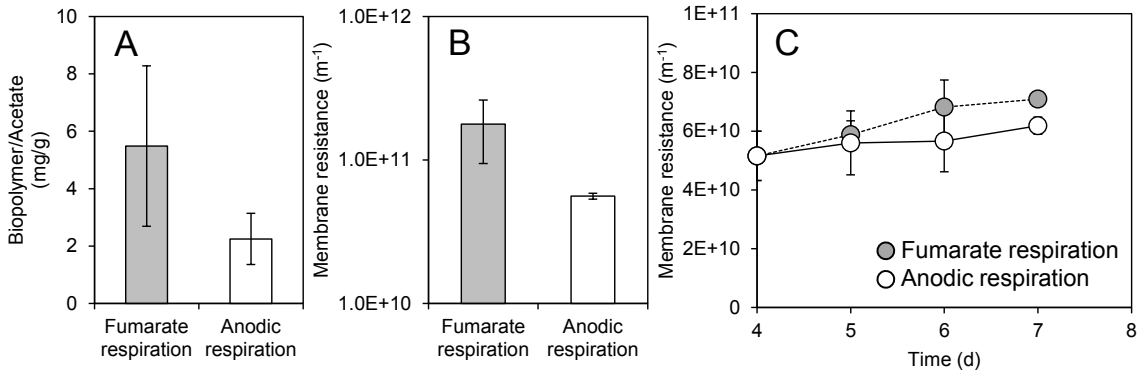

Figure 3.12 Impact of anodic respiration by *Geobacter sulfurreducens* strain PCA (PCA) on biopolymer production (**A**) and membrane fouling potential (**B**). The foulant degradation ability of the strain PCA was evaluated (**C**), showing no significant degradation of foulant. These experiments performed in duplicate and the error bars indicate the standard deviations.

degrade foulant including biopolymer generated by other bacteria. This speculation was clarified by the following study with a pure culture of *G. sulfurreducens* PCA as a model exoelectrogen.

3.3.5. Biopolymer production by *Geobacter sullferreducens* strain PCA

Geobacter sulfurreducens strain PCA was cultured with anode electrode (anodic respiration) or fumarate (fumarate respiration) as a sole electron acceptor for 4 days, and biopolymer concentrations and membrane resistance (fouling potential) were measured. More biopolymer was produced per consumed acetate under fumarate (anaerobic) respiration condition than anodic respiration condition (5.48 ± 2.79 *vs*. 2.25 ± 0.89 (mg-biopolymer/g-acetate)) (**Fig. 3.12**). As a consequence, membrane resistance (fouling potential) was higher under fumarate (anaerobic) respiration condition than anodic respiration condition (1.78 ± 0.84 *vs*. 0.56 ± 0.03 (10^{11} m^{-1})) (**Fig. 3.12B**). This result was in good agreement with the results of MFCs (**Fig. 3.3C** and **3.3D**). Furthermore, the ability of the strain PCA to mitigate membrane fouling (*i.e.*, to

degrade foulant) was tested under anodic or fumarate respiration conditions, because some bacteria (*e.g.*, *Chloroflexi*) were known to degrade foulant (Miura et al., 2007b) (Miura and Okabe, 2008). The strain PCA was incapable of degrading foulant accumulated in the ML of MFC under both respiratory conditions (**Fig. 3.12C**). Based on these results, the strain PCA produced less biopolymer (a main foulant in this study) under anodic respiration condition than fumarate (anaerobic) respiration condition, which can explain the lower membrane-fouling potential of MFC effluents under high current generation (**Fig. 3.1** and **Fig. 3.2**).

3.4. Conclusion

MFCs equipped different external resistances, which regulate anodic respiration rate, *i.e.*, current generation, were constructed and tested for membrane-fouling potential. It was found that although the COD removal efficiency was comparable, the fouling potential was significantly reduced due to less production of biopolymer at higher current generation (*i.e.*, lower external resistance) as compared with open circuit MFC (aerobic respiration or fermentation). This result indicated that membrane fouling of MBR could be mitigated by applying anodic respiration without air-scrubbing (*i.e.*, aeration), leading to development of an electrode-assisted MBR (e-MBR) without high energy-demanding aeration. To explain the reason for reduction of biopolymer production in MFCs, microbial community of anode biofilms was analyzed. *Geobacter sulfurreducens*-related bacteria were found to be dominant exoelectrogens in the inner part of anode biofilms. Furthermore, a pure culture of *Geobacter sulfurreducens* strain PCA produced less biopolymer under anodic respiration condition than fumarate respiration condition, resulting in lower membrane-fouling potential. Taken together, *Geobacter sulfurreducens*-related bacteria dominated in the anode biofilms produced less biopolymer using anode as electron acceptor, which consequently mitigated membrane-fouling potential of MFC anode effluent. However, since the biochemical pathway of biopolymer synthesis under anodic respiration condition is not known

presently, future study is essential to investigate the impact of anodic respiration on biochemical pathway of biopolymer synthesis and biopolymer production by other exoelectrogens.

CHAPTER 4

Membrane fouling potentials and cellular properties of bacteria isolated from fouled membranes in a MBR treating municipal wastewater

4.1. Background and Objectives

It is widely accepted that membrane fouling is a main obstacle for wider application of membrane bioreactors (MBRs). Although extensive studies have been conducted to understand the detailed mechanisms of membrane fouling in MBRs and to develop its effective mitigation strategies (Huang and Lee, 2015;Lin et al., 2014;Malaeb et al., 2013b), improvement of fouling control and management is still remarkably slow in practice. One of research approaches is to identify key players (microbial strains) of membrane fouling and subsequently to control and inhibit their activity by any means (Calderón et al., 2011;Ma et al., 2013b;Miura et al., 2007c). Although extensive studies have been conducted to reveal microbial communities in pilot-scale MBRs treating real municipal wastewater using several molecular biological techniques, our understanding is still largely limited to identify key bacteria responsible for membrane fouling (Kim et al., 2013;Lim et al., 2012;Miura et al., 2007c;Pang and Liu, 2007;Wu et al., 2011;Xia et al., 2010). The dominant species in MBRs (Calderón et al., 2011) and in biocake (biomass accumulated on the membranes) (Miura et al., 2007c;Pang and Liu, 2007), or the increasing species as membrane fouling (Lim et al., 2012) have been regarded as key bacterial groups responsible for membrane fouling. For example, *Proteobacteria* has been determined as a dominant phylum in MBRs and thus regarded as fouling causing bacteria (Lim et al., 2012;Ma et al., 2013a). It was also reported that *Proteobacteria* plays a pioneering role in biocake formation on membrane (Gao et al., 2014b;Miura et al., 2007c;Vanysacker et al., 2014a). This is, however, not always true because membrane fouling is known to be mainly caused by metabolites (i.e.,

extracellular polymeric substances (EPS) and soluble microbial products (SMP)) produced by or released from microorganisms and cellular materials (debris), which are highly dependent on microbial species and operational conditions (Guo et al., 2012;Lin et al., 2014). For examples, changes in operational conditions (i.e., DO and temperature) and environmental stress (i.e. salinity concentration) induced the changes in microbial community structures and microbial metabolisms (production rates and compositions of EPS and SMP) and consequently influenced membrane fouling (Gao et al., 2011a;Gao et al., 2013b;Guo et al., 2015;Ng and Ng, 2010).

Several papers have highlighted the relevance of cellular properties such as bacterial motility and cell surface properties of environmental isolates in biofilm formation, which was often overinterpreted to membrane fouling potential. For examples, a strain belonging to *Arthrobacter* sp. having a relatively small cell size in mixed liquor of an aerobic granular membrane bioreactor (AGMBR) can penetrate the microfiltration (MF) membrane and develop an internal biofilm that induce membrane fouling (Juang et al., 2010a). Furthermore, biofilm formation potentials of strains isolated from reverse osmosis (RO) membranes treating potable water were measured in microtiter plates and related to their cellular properties such as hydrophobicity, surface charge, and motility (Pang et al., 2005a). However, membrane fouling potentials of these isolates were not directly measured under filtration conditions in their studies.

Biofilm formation potentials determined in microtiter plates sometimes do not reflect membrane fouling potentials, because convective permeate flow is known to be a major mechanism that transports bacterial cells and EPS to membrane surfaces during filtration (Habimana et al., 2014). Therefore, biofilm formation and/or biomass deposition on membrane surfaces, furthermore membrane fouling, are more likely to be independent of bacterial cell surface properties and motility (Habimana et al., 2014;Juang et al., 2010b). Thus, membrane fouling potential must be directly evaluated for each bacterial strain under defined filtration conditions. However, membrane fouling potentials have been evaluated for only a few isolates and model bacteria (e.g.,

Escherichia coli and *Pseudomonas*) using dead-end or cross-flow filtration systems (Choi et al., 2006;Feng et al., 2009;Juang et al., 2008b;Vanysacker et al., 2014b). Therefore, there is very little information on fouling potentials of environmental isolates and the relevance to their cellular characteristics (Malaeb et al., 2013b).

The objectives of this study are to identify key fouling-causing bacteria (FCB) for microfiltration (MF) membranes in MBRs treating real municipal wastewater and characterize their cellular properties. To achieve these objectives, 41 bacterial strains were isolated from fouled MF membrane gel layers (biofilms) in the MBRs, and their fouling potentials were directly evaluated using bench-scale cross-flow membrane filtration systems (CFMFSs). FCB strains were phylogenetically identified, and their cellular properties such as cell surface properties (hydrophobicity and surface charge), and bacterial motility, biofilm formation potential and colony properties were analyzed in details to evaluate the relevance of these cellular properties in their membrane fouling potentials.

4.2. Materials and Methods

4.2.1. Isolation of bacterial strains

The firmly attached biomass (gel layer) on fouled microfiltration (MF) hollow-fiber membranes was collected from a pilot-scale MBR treating municipal wastewater located at Soseigawa Municipal Wastewater Treatment Plant, Sapporo, Japan (**Fig. 4.1**). The hollow-fiber polytetrafluoroethylene (PTFE) membrane with 0.3 μm nominal pore size was submerged in a reaction tank (175 L) of the MBR. The MBR was operated at a permeate flux of ca. 0.2 m/d and sludge retention time of 35 day. Average MLSS concentration in the reaction tank was ca. 50 g/l. Characteristics of the raw wastewater of this plant can be found elsewhere (Kimura et al., 2005).

The biomass was collected after washing loosely attached biomass with tap water in April, 2013. The biomass was serially diluted with sterilized MilliQ water, spread on R2A agar plates, and incubated at 30°C. The colonies grown on the plates

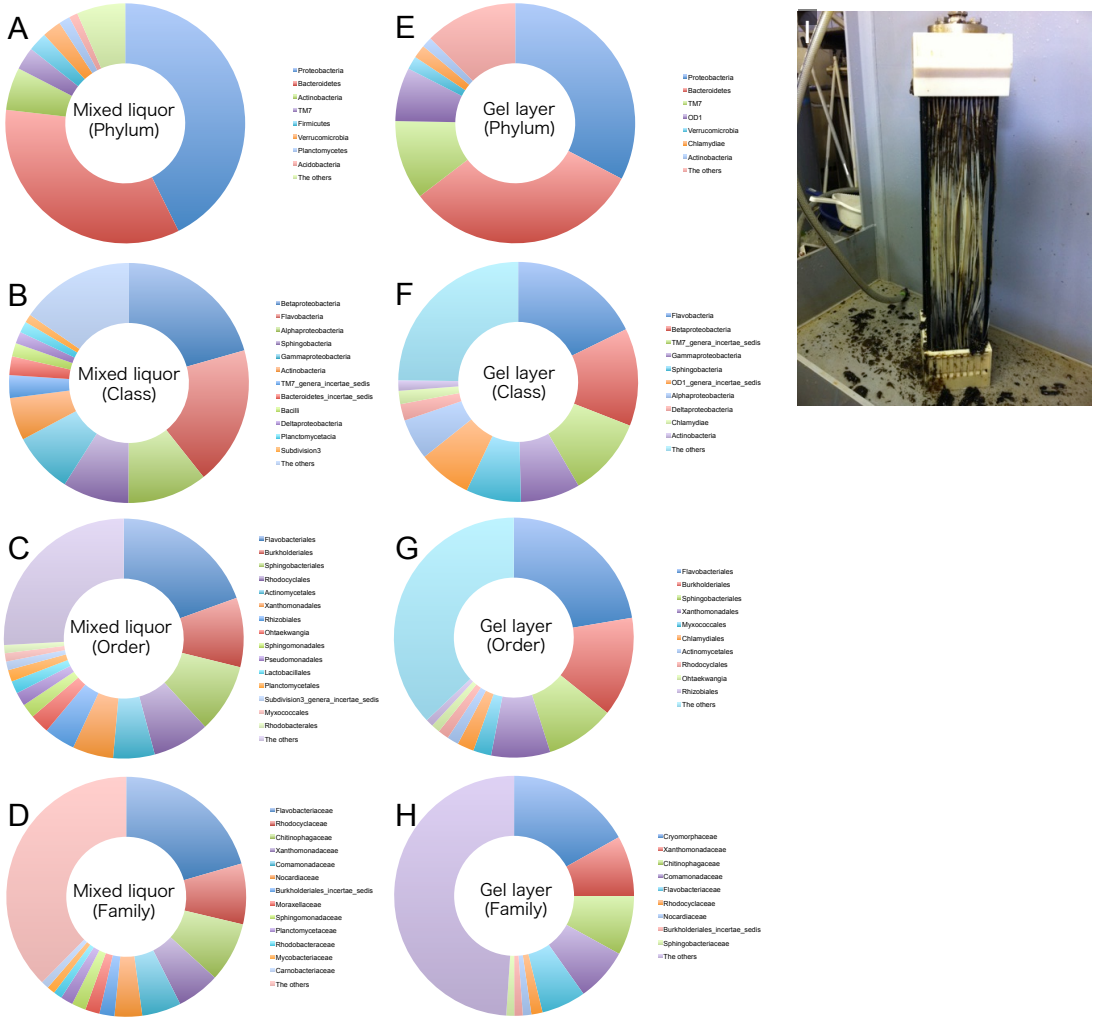

Figure 4.1 Bacterial community structures in the mixed liquor of a MBR (**A** to **D**) and gel layer (**E** to **H**) of fouled microfiltration (MF) hollow fiber membranes (**I**) in a pilot-scale MBR treating real municipal wastewater, from which 41 bacterial strains were isolated. The groups with relative percentages < 1% were complied in "The others". White membranes (in the middle part) were washed area by watering, from which the gel layers were sampled for isolation of bacterial strains.

were transferred to new R2A agar plates and the plates were incubated at 30°C again. Forty-one strains were obtained by repeating this process more than 3 times. These isolates were analyzed by 16S rRNA gene sequencing and repetitive sequence-based

PCR (rep-PCR) as described below. All 41 strains were subjected to the analyses of membrane fouling potential and cellular properties (**Table 4.1**). According to 16S rRNA gene sequencing data, OTUs were generated using identity cut-offs of 97%. When the isolates shear >97% 16S rRNA gene sequence identity, rep-PCRs were performed to further differentiate the isolated strains. Based on the results of these analyses, representative strains of each unique strain group were subjected to further analyses of colony water content and hydrophilic organic matter content. All isolated strains were cultivated on R2A agar plates in this study.

DNA was extracted from each isolate as described previously (Ashida et al., 2010). Briefly, the isolated bacterial colonies grown on R2A agar plates were suspended in 100 μl of 0.05 M NaOH, and then the suspension was heated at 95°C for 15 min. After centrifugation (1,000 rpm, 5 min), the supernatant was diluted 10-fold, which was used as template DNA for PCR amplification (Ashida et al., 2010). A primer set of 27F and 1492R was used to amplify 16S rRNA gene fragments for 16S rRNA gene sequence analysis (Goodfellow and Stackebrandt, 1991). The 16S rRNA gene sequences (ca. 1,352 bp) were compared to sequences available in the BLAST database (Altschul et al., 1997). For the phylogenetic analysis, a neighbor-joining tree (Saitou and Nei, 1987) was constructed (1,000 replicate bootstraps) by using MEGA 5.2. software. Rep-PCR fingerprinting was performed as described elsewhere (Ishii and Sadowsky, 2009).

4.2.2. Microbial community analysis

The microbial communities of the firmly attached biomass on fouled MF membranes (gel layer; Gel) and biomass in the mixed liquor (ML) were analyzed by applying next-generation sequencing (Illumina MiSeq) analysis (Illumina; Hayward, CA, USA). Total community DNA was extracted from the gel layer and the pellet of the mixed liquor by using a PowerSoil DNA Isolation Kit (MoBio Laboratories; CA, USA). The partial 16S rRNA gene including v3 and v4 regions were amplified with Bakt_341F and

Bakt_805R primers (Herlemann et al., 2011). Next-generation sequencing (Illumina MiSeq) 16S rRNA gene analysis was performed as described elsewhere (Rathnayake et al., 2015). In total, 58,134 and 76,354 sequence reads were analyzed for the ML and Gel samples by using QIIME 1.8.0 with the Silva 119 database, respectively (Caporaso et al., 2012).

4.2.3. Membrane fouling potential

Membrane fouling potential of each isolated strain was determined using a bench-scale cross-flow membrane filtration system (CFMFS). The CFMFS consists of a reactor (75 mL), which was operated as chemostat, and a cross-flow membrane filtration cell (CFMFC) (**.2**). The dimension of the CFMFC was 0.5 mm (height) by 20 mm (width) by 100 mm (length), corresponding to a volume of 1,000 mm^3 and effective filtration surface area of 2,000 mm^2, respectively. Flat membrane filter (0.2 μm, hydrophilic PTFE; Advantec Toyo; Tokyo, Japan. The detail information was shown in **Fig. 4.3**) was used for all filtration experiments in this study. Cross-flow velocity was set at 1 cm/s. Hydraulic retention time (HRT) and solid retention time (SRT) were adjusted at 2.5 hr and 12.5 day, respectively.

Overnight grown cultures (75 ml, OD_{600} was adjusted to approximately 0.3 with fresh R2A broth medium (3.2 g/L)) of each isolated strain were prepared and inoculated into the reactor. The fresh R2A broth medium was then continuously fed to the reactor at a flow rate of 0.71 L/d. Growth rates of isolates can be controlled by changing the flow rate (i.e., dilution rate). Feeding substrate to the reactor was accomplished with a peristaltic pump (MP-1100; EYELA; Tokyo, Japan). The feed cell suspension was circulated through the reactor and CFMFC by a peristaltic pump (MasterFlex EW-07553-80; Cole-Parmer Instrument Co.; IL, USA) at a flow rate of 6.0 L/h. All filtration experiments were carried out at room temperature (25 ± 2°C) with a constant permeate flux of 0.3 m/d, which was controlled by a digital peristaltic pump (ISM 936; IDEX Health & Science; Wertheim, Germany) mounted on the permeate line.

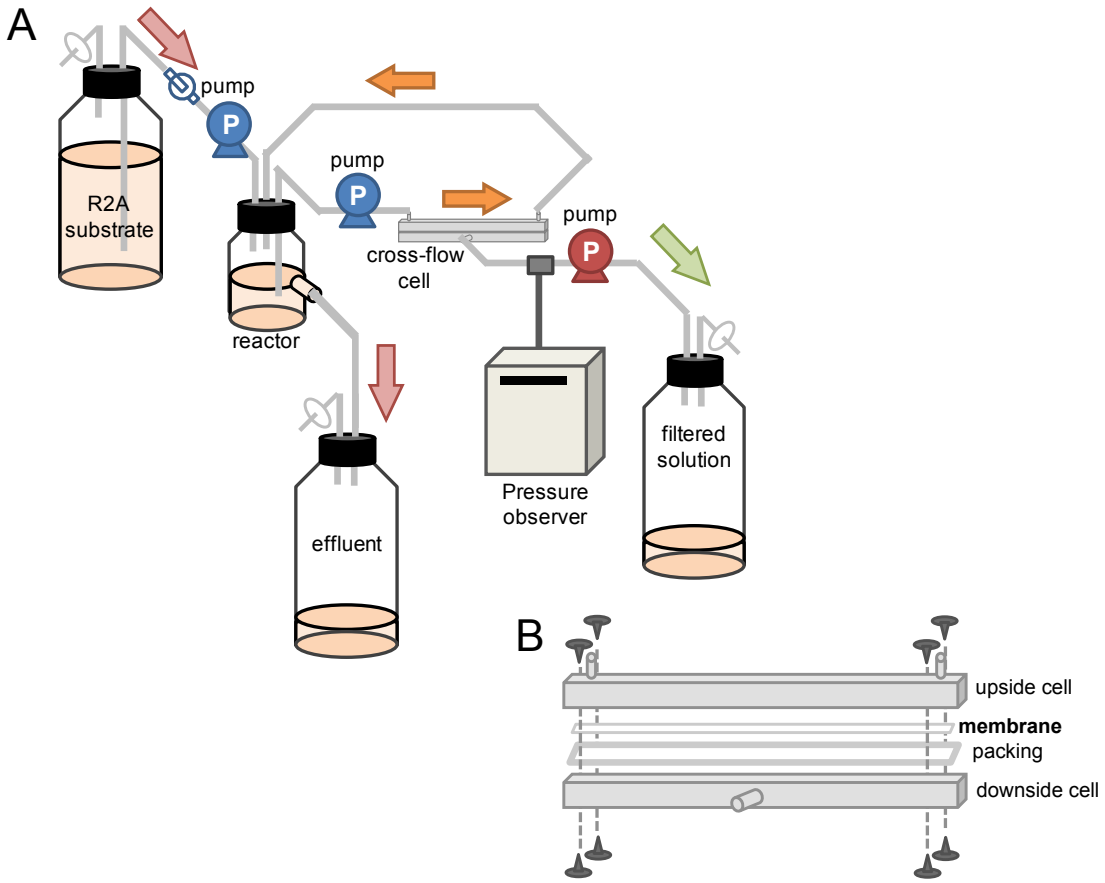

Figure 4.2 Illustrations of a bench-scale cross-flow membrane filtration system (CFMFS) (**A**) and a cross-flow membrane filtration cell (CFMFC) (**B**). Isolated bacteria were cultivated continuously in the "reactor" and circulated in the cross-flow cell as indicated with orange arrows. Fresh R2A broth medium (3.2 g/L) was fed to the reactor from a reservoir "R2A substrate" and the excess culture flowed to an "effluent" bottle as indicated with red arrows. The permeate was collected by a digital peristaltic pump as indicated with a green arrow.

The trans-membrane pressure (TMP) was continuously monitored and recorded with a data logger (midi logger GL220; Graphtec; Yokohama, Japan). Trans-membrane pressure after 4 hr (TMP_4) and 24 hr (TMP_{24}) of filtration were measured to characterize membrane fouling potential of isolated strains. After 24 hr of operation, the biomass concentration (OD_{600}) in the reactor and the biomass accumulated on the

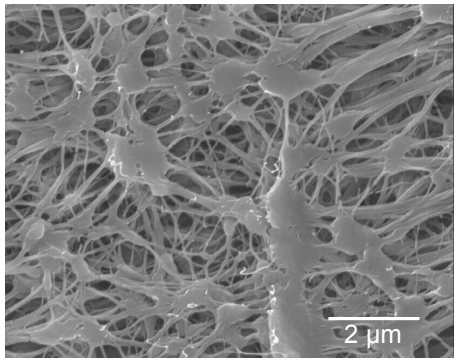

Figure 4.3 SEM image of PTFE membrane used in this study. The contact angle and surface charge of the membrane are 50° and -13 mV, respectively

membrane surface were measured with an optical absorbance meter (Smart Spec Plus; Bio-Rad; CA, USA). The biomass accumulated on the membrane was removed and suspended in 25 ml of 0.05% NaCl solution by vortexing for 1 min, and then OD_{600} was measured (described as OD_{600} of suspended BC). All apparatus except for the CFMFC and membrane were autoclaved, and the CFMFC and membrane were sterilized with sodium hypochlorite (3,000 ppm for 30 min) and rinsed well with sterilized MilliQ water.

4.2.4. Cellular characterization

Maximum specific growth rate (MGR) was determined by monitoring OD_{600} increase in walls of a 96-well microtiter plate. Each isolated strain (initial OD_{600} = 0.1) was incubated at 30°C, the OD_{600} was monitored every 1 hr for 24 hrs, and then the MGR was determined based on the OD_{600} growth curves.

Cell surface hydrophobicity was measured as described previously with minor changes (Pang et al., 2005a). Overnight grown cultures of each isolated strain in R2A broth (5 ml) were prepared, and then the cells were harvested by centrifuged at 4°C, 6,000 ×*g* for 15 min and washed twice with 0.85% NaCl solution. The washed cells were resuspended in 0.85% NaCl solution to OD_{600} of approximately 0.7. The washed

cell culture (3.0 ml) was mixed with 1.0 ml of xylene, vortexed for 1 min, and incubated for 10 min in a water bath at 37°C. Zeta potentials of the washed cells (OD_{600} = 0.1) were measured by using an electrophoretic light-scattering spectrophotometer (Zetasizer Nano ZS; Malvern Instruments; Malvern, Worcestershire, UK).

Biofilm formation potential was determined by quantifying the amount of biomass attached on walls of a 96-well microtiter plate as described previously (Burmølle et al., 2006). Briefly, 200 μl of each washed cell culture (OD_{600} = 0.1) was inoculated into each well and incubated at 30°C for 24 hr. After 24 hr of incubation, OD_{600} in the suspended culture was measured, and attached biomass (biofilm) was also measured after staining with 1% crystal violet (CV) solution for 30 min and resuspending into 220 μl of a mixed solution of ethanol and acetone (ethanol : acetone = 8:2). The biofilm formation potential was normalized by the growth of suspended cells and expressed as the ratio of CV value to OD_{600} value.

The biofilm firmly adhered on the walls of a 96-well microtiter plate was measured, which is defined as “rigid biofilm formation potential” in this study. Loosely attached biofilms were removed by ultrasonic treatment (400W for 30 min) followed by rigorous washing with MilliQ water, and thereafter the remaining biofilm was determined after staining with 1% crystal violet (CV) as described above.

Swimming and swarming motilities were measured as described previously with minor modification (Déziel et al., 2001;Rashid and Kornberg, 2000). For swimming and swarming motility, the strains were inoculated on the center of 0.3% and 0.5% (w/v) R2A agar plate, respectively. These plates were incubated at 30°C for 24 hr, and the diameter of each colony was measured.

In order to evaluate the degree of bacterial cell aggregation, particle size distributions of bacterial cells were measured by using Nano Sight NS500 (SALD-7100; Shimadzu Co., Kyoto, Japan). Overnight grown cultures of each isolated strain in R2A broth (10 ml) were prepared, and then the cells were harvested by centrifuged at 4°C, 6,000 ×*g* for 15 min and washed with 0.85% NaCl solution to

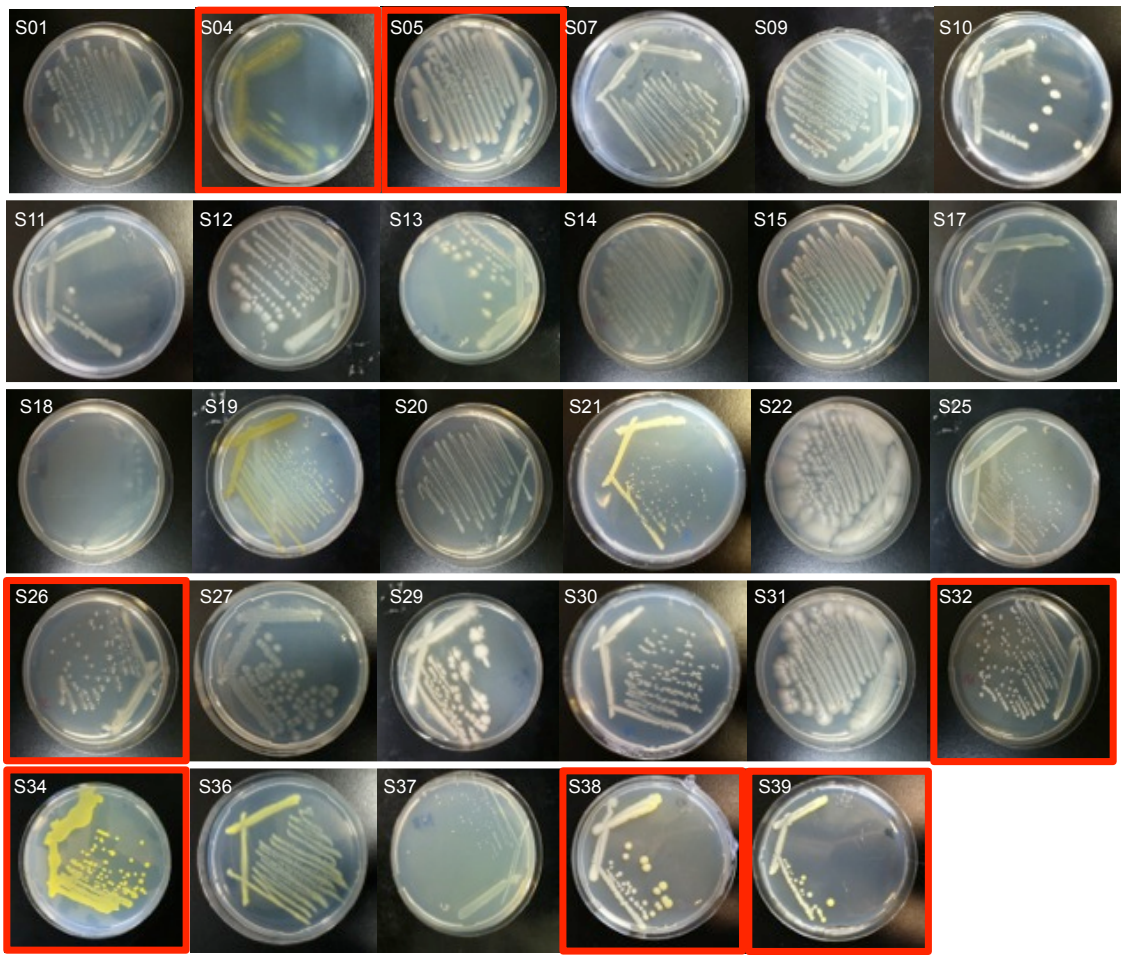

Figure 4.4 Photographs of the colonies of representative strains. The images of FCB were enclosed with red frames.

eliminate the influence of small particles contained in fresh R2A medium (**Fig. 4.4**). Five ml of the diluted washed bacterial cells was gently vortexed and loaded to the Nano Sight NS500.

All the statistical analyses were carried out with R 3.0.2 (R Development Core Team; Vienna, Austria). *P* values less than 0.05 were considered statistically significant in all analyses.

4.2.5. Colony water content

Colony water contents were quantified as follows. The representative strains were inoculated on R2A agar plates (1.5% (w/v)) and incubated for 3 days. Colonies formed on R2A agar plate were collected carefully with spatula in a 1.5 ml tube, and its weight was measured. After drying at 100°C for 24 hr, the weight was measured again. The colony water content was calculated as following:

$$\text{Water content (\%)} = (W_{initial} - W_{dried}) / W_{initial}$$

where, $W_{initial}$ (mg) and W_{dried} (mg) were the colony weight before and after dried, respectively. Photographs of each colony were taken after 3 days of incubation (**Fig. 4.4**).

4.2.6. Extraction of SMP and EPS

Soluble microbial product (SMP) and extracellular polymeric substance (EPS) in colony of isolated strains were extracted as described previously with minor modifications (Ramesh et al., 2007;Wang et al., 2009b). Briefly, colonies were collected from R2A agar plate (1.5% (w/v)), suspended in 0.05% NaCl solution, dispersed well by vortexing, and then diluted to OD_{600} = 0.3 to eliminate the concentration effect. The colony suspension was centrifuged at 4°C and 6,000 × *g* for 15 min. The supernatant was regarded as SMP. The remained pellet was suspended with 0.05% NaCl solution and then was subjected to heat treatment at 80°C and 1 hour. After dispersed well by vortexing, the suspension was centrifuged again at 4°C and 6,000 × *g* for 15 min. The supernatant was regarded as EPS.

Fractions of hydrophilic, hydrophobic, and neutral organic matter in SMP in colonies were obtained by using DAX-8 (Supelite™ DAX-8; Sigma-Aldrich Co.; MO, USA) and XAD-4 resin (Amberlite® XAD-4; Sigma-Aldrich Co.; MO, USA) as described previously with minor modifications (Aiken et al., 1992;Yamamura et al., 2014). The SMP was diluted to TOC concentration < 20 mg/L and acidified to pH 2 with 11.2 M HCl, and 5 ml of each solution was passed through DAX-8 and XAD-4 at

a flow rate of 200 mL/min in series. The fraction passed through both DAX-8 and XAD-4 resins was regarded as hydrophilic fraction, the fraction that was retained on the DAX-8 resin was designated as the hydrophobic fraction, and the fraction that was retained on the XAD-4 resin was designated as the neutral fraction, respectively. Hydrophobic and neutral fractions were collected by eluting each resin with 5 ml of NaOH (pH 12) at a flow rate of 120 mL/min. The amounts of each fraction were determined based on TOC concentration as follows:

$$\text{Hydrophilic organic matter content} = a \times TOC_{hydrophilic} / OD_{600}$$

$$\text{Hydrophobic organic matter content} = a \times TOC_{hydrophobic} / OD_{600}$$

$$\text{Neutral organic matter content} = a \times TOC_{neutral} / OD_{600}$$

where, a is dilution factor, OD_{600} is the value of OD_{600} of the colony suspension, and $TOC_{hydrophilic}$, $TOC_{hydrophobic}$, and $TOC_{neutral}$ are TOC concentration (mg/l) of hydrophilic, hydrophobic, and neutral fraction, respectively. The concentration of TOC was measured by using a TOC analyzer (TOC-V CSH; Shimadzu; Kyoto, Japan).

4.2.7. Chemical analysis

Carbohydrate and protein concentrations of the supernatant were measured with the phenol-sulfonic acid method with glucose as the standard and the Lowry method using BSA as the standard, respectively. The contents of carbohydrate and protein were determined as follows:

$$\text{Carbohydrate} = a \times C / OD_{600}$$

$$\text{Protein} = a \times P / OD_{600}$$

where, C and P are the carbohydrate and protein concentration of SMP and EPS (mg/l), respectively.

4.2.8. Dead-end filtration

Dead-end filtration test was performed to measure the fouling potential of SMP and EPS in colony of isolated strains as described previously with minor modification

(Kimura et al., 2012;Ramesh et al., 2007). Five ml of SMP or EPS was transferred to a stirred filtration unit (UHP-25K; Advantec Toyo; Tokyo, Japan) with a flat membrane filter (0.2 μm, hydrophilic PTFE; Advantec Toyo; Tokyo, Japan), and filtered under 50 kPa of ambient air. MilliQ water (approximately 10 mL) was added in the filtration unit and filtered again under the same pressure. The permeate flow rate of MilliQ water was measured, and the membrane resistance of the fouled membrane was calculated as follows;

$$\text{Membrane resistance } (m^{-1}) = PA/\mu Q$$

where, P is the pressure (Pa), A is the filtration area of membrane (m^2), μ is the dynamic viscosity of MilliQ water (Pa・s), and Q is the permeate flow rate of MilliQ water (m^3/s).

4.3. Results

4.3.1. Microbial community analysis

Bacterial diversity and composition of the gel layer (biofilm) formed on fouled MF hollow fiber membranes of a pilot-scale MBR treating real municipal wastewater was determined based on 16S rRNA gene sequences using next-generation sequencing (Illumina MiSeq) and compared with those of the ML (**Fig. 4.1**). Microbial community structure of the gel layer was basically similar to that of the mixed liquor. *Proteobacteria* and *Bacteroidetes* are dominant phyla in both ML and Gel, which agreed with the previous report (Duan et al. 2009) (**Fig. 4.1**). The *Xanthomonadaceae* and *Comamonadaceae*, which were frequently detected in MBRs treating municipal wastewater (Mulina-Munoz et al. 2009), were found to be dominant families in the gel layer and ML (approximately 2 - 5% of total reads) (**Table 4.1** and **Fig. 4.1D** and **4.1H**). Although many isolated strains were affiliated with the *Enterobacteriaceae* and *Microbacteriaceae* families (see below), which also often detected as dominant species in MBRs (Lim et al., 2012;Xia et al., 2010), both the families accounted for less than 0.17 % in both the gel layer and mixed liquor samples (**Table 4.1**).

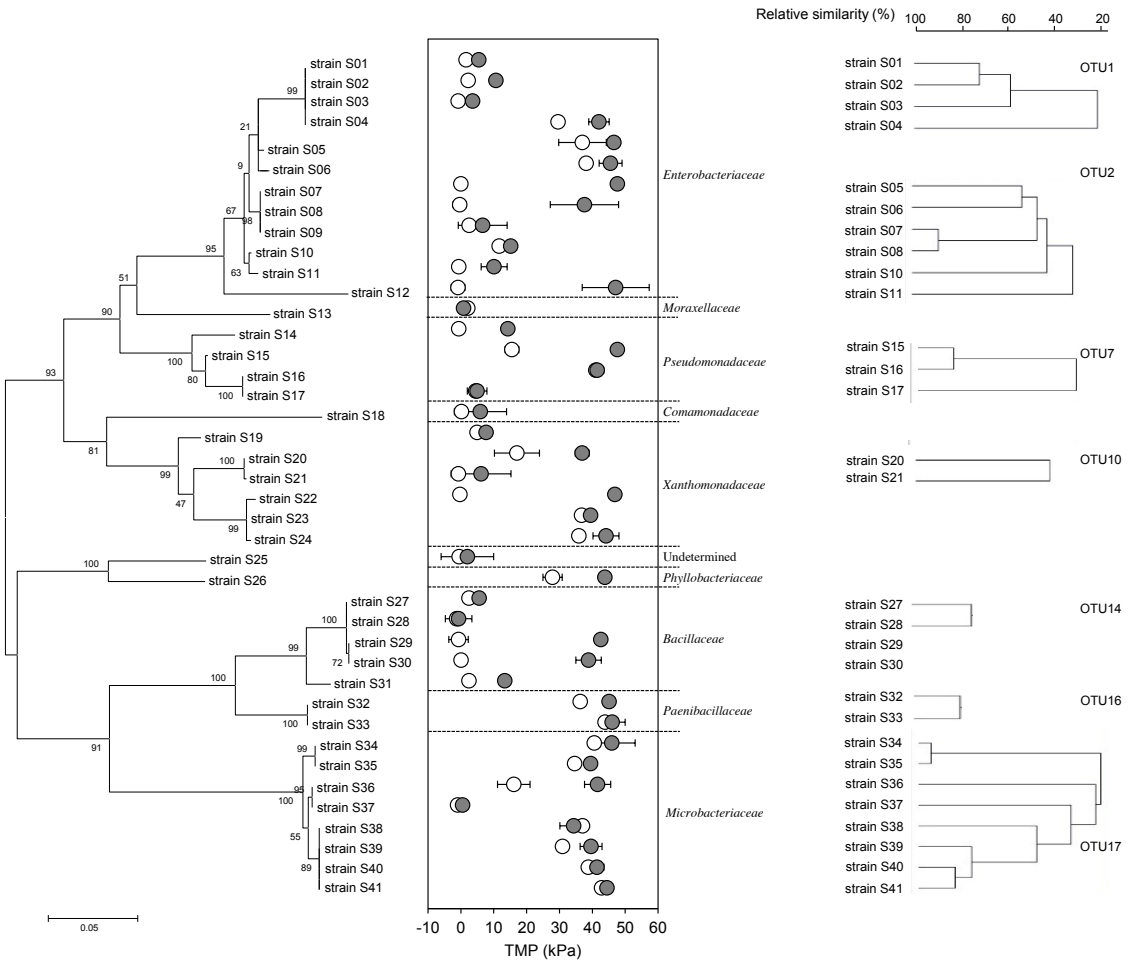

Figure 4.5 Phylogenetic relationships and membrane fouling potentials of the strains isolated fouled MF membranes. The fouling potential was determined using bench-scale cross-flow membrane filtration system (CFMFS) that was continuously operated for 24 hr. White and gray dots represent trans-membrane pressure at 4 hr (TMP_4) and 24 hr (TMP_{24}), respectively. The membrane filtration experiments were performed in duplicate and the error bars indicate the standard deviations. Isolated strains were identified based on 16S rRNA gene sequencing analysis (phylogenetic tree, left) and rep-PCR fingerprint analysis (dendrogram, right). OTUs were generated using 16S rRNA gene identity cut-offs of 97%. When isolates sheared >97% 16S rRNA gene sequence identity, rep-PCRs were performed to further differentiate the isolated strains.

4.3.2. Membrane fouling potential

Forty-one strains were isolated from the fouled MF membranes and identified based on ca. 1,352 bp of 16S rRNA gene sequences and rep-PCR DNA fingerprinting analyses (**Fig. 4.5**). These isolates were then tested for membrane fouling potentials using bench-scale cross-flow membrane filtration systems (CFMFSs). During filtration, the trans-membrane pressure after 4 hr (TMP_4) and 24 hr (TMP_{24}) of filtration were measured to characterize the fouling potentials of these isolated strains.

The isolated stains formed distinct phylogenetic clusters (families) based on ≥97% 16S rRNA gene sequence similarity; 12 isolates (4 OTUs) in *Enterobacteriaceae*, 1 isolate in *Moraxellaceae*, 4 isolates (2 OTUs) in *Pseudomonadaceae*, 1 isolate in *Comamonadaceae*, 6 isolates (3 OTUs) in *Xanthomonadaceae*, 1 isolate in *Phyllobacteriaceae*, 5 isolates (2 OTUs) in *Bacillaceae*, 2 isolates (1 OTU) in *Paenibacillaceae*, and 8 isolates (1 OTU) in *Microbacteriaceae* (**Table 4.1**). Strain S25 was affiliated with the order *Rhizobiales*, but did not have ≥97% 16S rRNA gene sequence similarity to any families. These families were frequently detected in various MBRs (Gao et al., 2014b;Guo et al., 2015;Lim et al., 2004;Lim et al., 2012;Molina-Muñoz et al., 2009;Oh et al., 2012;Shapiro et al., 2010).

Although 4 *Enterobacteriaceae* isolates (OTU 1), strains S01, S02, S03, and S04, had ≥99% 16S rRNA gene sequence similarity (**Table 4.2**), only strain S04 showed a significantly high fouling potential as compared with others (**Fig. 4.5**). A dendrogram generated from rep-PCR banding profiles revealed that the strain S04 differed from other three strains with the relative similarity of 20%, indicating a different strain (Healy et al., 2004). Similarly, although the *Microbacteriaceae* strains S36 and S37 shared ≥99% 16S rRNA gene sequence identity, rep-PCR analysis could discriminate the two strains which showed different fouling behavior. The similar results were obtained for the *Xanthomonadaceae* strains S20 and S21 and the *Pseudomonadaceae* strains S16 and S17.

Family	[a]OTU	[b]Strain	[c]Rep-PCR	Maximum growth rate (/h)	Swimming (mm)	Swariming (mm)	Zeta potential (mV)	Hydrophobicity (-)	Biofilm formation potential (-)	Rigid biofilm formation potential (-)	Median of particle size distribution (μm)	Water content (%)	Hydrophilic secretion in colony (mg/OD0.3)	Carbohydrate in colony (μg/OD0.3)	Protein in colony (μg/OD0.3)	Fouling-potential group	[d]ML (%)	[e]Gel (%)
Enterobacteriaceae	1	S01	+	0.107	80	3	-9.3	33.6	0.49	0.51	1.00	81.9	18.2	15.8	26.7	III	0.17	0.15
		S02	+	0.104	70	2	-5.7	46.1	1.26	0.81						III		
		S03	+	0.111	70	2	0.0	5.3	0.33	0.31						III		
		S04	+	0.052	2	1	-12.1	26.1	1.09	0.63	0.92	94.0	15.1	54.3	0.0	I		
	2	S05	+	0.084	3.5	8	-11.6	45.2	0.66	0.41	0.97	96.7	68.8	224.7	44.9	I		
		S06	+	0.068	3	8	-8.3	65.8	0.53	0.25						I		
		S07	+	0.082	7	2	-14.2	50.2	0.29	0.28	0.44	88.2	5.2	0.0	0.0	II		
		S08	+	0.113	5	2	-16.1	69.4	0.31	0.34						II		
		S10	+	0.100	25	3	-11.0	62.5	0.28	0.18	1.07	88.1	9.5	0.0	114.5	III		
		S11	+	0.119	55	0.5	-7.3	37.0	0.20	0.22	1.08	81.0	4.2	16.5	41.8	III		
	3	S09		0.088	70	2	-16.3	42.6	0.32	0.29	0.42	83.6	17.8	85.8	23.9	III		
	4	S12		0.099	4	2	-14.6	30.6	0.26	0.24	0.02	85.1	16.6	29.2	24.5	II		
Moraxellaceae	5	S13		0.101	1	2	-8.2	42.0	0.72	0.25	1.05	85.9	12.7	8.6	0.0	III	1.61	0.50
	6	S14		0.150	23	1	-13.0	35.0	2.18	0.55	0.02	85.1	17.7	22.5	69.1	III		
Pseudomonadaceae	7	S15	+	0.121	55	2	-17.9	9.5	1.45	0.66	1.13	85.6	19.1	52.5	14.3	II	0.08	0.30
		S16	+	0.091	15	5	-6.1	14.2	0.89	0.22						I		
		S17	+	0.209	23	40	-6.6	22.2	1.25	0.49	0.02	84.0	4.8	0.0	38.5	III		
Comamonadaceae	8	S18		0.131	3	2	-5.3	36.7	1.10	0.29	0.09	89.8	23.4	85.8	90.8	III	4.69	4.52
Xanthomonadaceae	9	S19		0.098	1	1	-5.9	25.0	0.63	0.22	2.00	83.3	32.3	0.0	114.0	III	2.73	4.21
	10	S20	+	0.129	2	3	-4.4	62.5	0.25	0.28	0.54	83.6	15.9	74.7	78.7	II		
		S21	+	0.127	8	2	-4.0	-1.4	0.27	0.20	0.02	82.0	13.0	13.1	1.9	III		
	11	S22	-	0.063	35	4	-24.0	42.4	0.93	0.16	0.02	89.8	23.4	58.0	15.5	II		
		S23	-	0.087	1	3	-12.8	-4.8	1.32	0.72						I		
		S24	-	0.091	0	1	-10.6	30.8	1.15	0.30						I		
Undetermined	12	S25		0.059	2	1	-5.8	6.4	0.49	0.30	0.15	82.5	51.2	24.4	0.0	III	0.00	0.00
Phyllobacteriaceae	13	S26		0.098	6	1	-10.9	21.6	1.02	0.97	0.02	97.4	109.2	2347.4	55.2	I	0.01	0.03
Bacillaceae	14	S27	+	0.106	14	10	-6.0	37.6	0.60	0.21	0.84	85.0	5.2	15.9	40.4	III	0.05	0.04
		S28	+	0.081	11	10	-7.4	-33.0	0.25	0.26						III		
		S29	-	0.071	20	5	-11.5	30.7	0.26	0.15	1.34	91.6	70.9	0.0	1.0	II		
		S30	-	0.104	40	5	-12.5	1.7	0.23	0.18	1.29	90.3	4.2	0.0	0.0	II		
	15	S31		0.119	10	10	-17.3	40.9	1.09	0.14	0.15	88.7	21.8	76.9	13.9	III		
Paenibacillaceae	16	S32	+	0.140	17	5	-18.4	4.0	0.27	0.18	0.96	95.3	43.3	984.8	57.4	I	0.00	0.01
		S33	+	0.084	12	3	-10.2	35.8	0.30	0.25						I		
Microbacteriaceae	17	S34	+	0.116	1.5	1	-12.2	12.9	0.25	0.23	0.02	95.0	16.1	10.4	0.0	I	0.17	0.02
		S35	+	0.132	1	1	-12.6	12.4	0.26	0.21						I		
		S36	+	0.031	1	2	-29.5	-2.3	0.92	0.71	0.02	92.1	23.3	0.0	0.0	II		
		S37	+	0.072	1	1	-4.1	24.7	2.20	1.71	0.02	80.1	28.7	2.1	4.3	III		
		S38	+	0.122	1.5	2	-10.6	41.5	2.41	2.18	0.47	94.4	71.2	18.8	7.6	I		
		S39	+	0.119	3	3	-10.3	22.2	2.46	1.20	0.36	95.2	28.6	58.0	18.1	I		
		S40	+	0.124	2	2	-11.0	33.8	3.50	3.29						I		
		S41	+	0.122	3	2	-11.3	40.2	2.46	2.87						I		

[a]Strains filled with dark gray boxes: representative strains of each OTU (differentiated with light gray and white colors, respectively), which were discriminated based on 60% DNA similarity of rep-PCR analysis. The colony properties (i.e., water content and hydrophilic organic matter content) were analyzed only for these representative strains.

[b]Rep-PCR: "+" and "-" indicated whether any amplicon was obtained by rep-PCR.

[c]Fouling-potential group: classification based on development of membrane fouling as shown in **Fig. 4.6**.

[d]Fouling potential of SMP and EPS in colony were measured by dead-end filtration.

[e]ML (%) and [f]Gel (%): the percentage of the 16S rRNA gene sequences affiliating with specific family in total sequence reads of Miseq analysis for the mixed liquor (ML) and gel layer (Gel) samples.

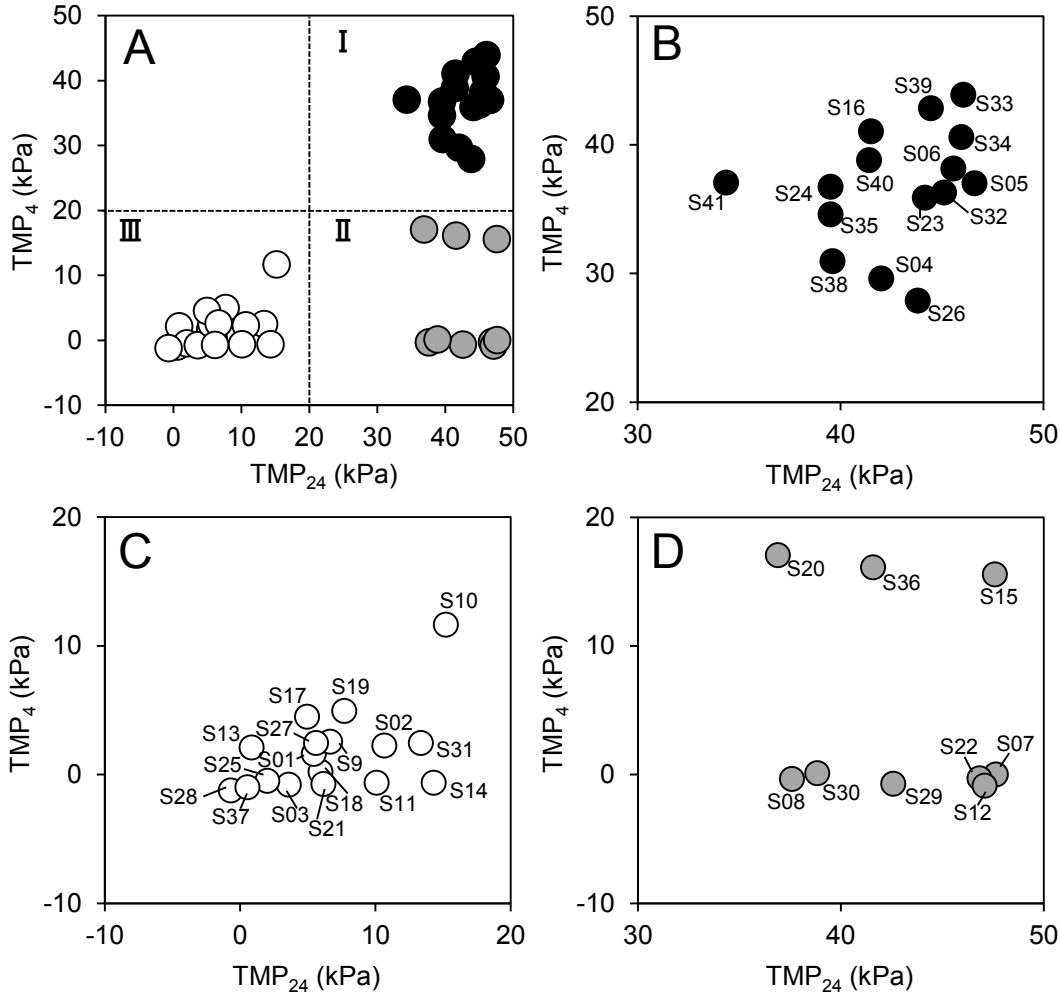

Figure 4.6 Classification of the isolated strains based on development of membrane fouling. (**A**) Relationship between TMP_4 and TMP_{24} shown in Figure 1. The fouling patterns could be classified into three groups; **I**. membrane fouling is quickly developed and reached TMP > 20 kPa within 24 hr (black) (**B**), **II**. membrane fouling is gradually developed but reached TMP > 20 kPa within 24 hr (light gray) (**D**), and **III**. membrane fouling is gradually developed and reached TMP < 20 kPa after 24 hr (white) (**C**). The region of each group was enlarged as **Fig. 4.6B**, **4.6D** and **4.6C**, respectively.

Overall, the isolated strains were grouped into three groups based on development of membrane fouling; **I**. membrane fouling is quickly developed and

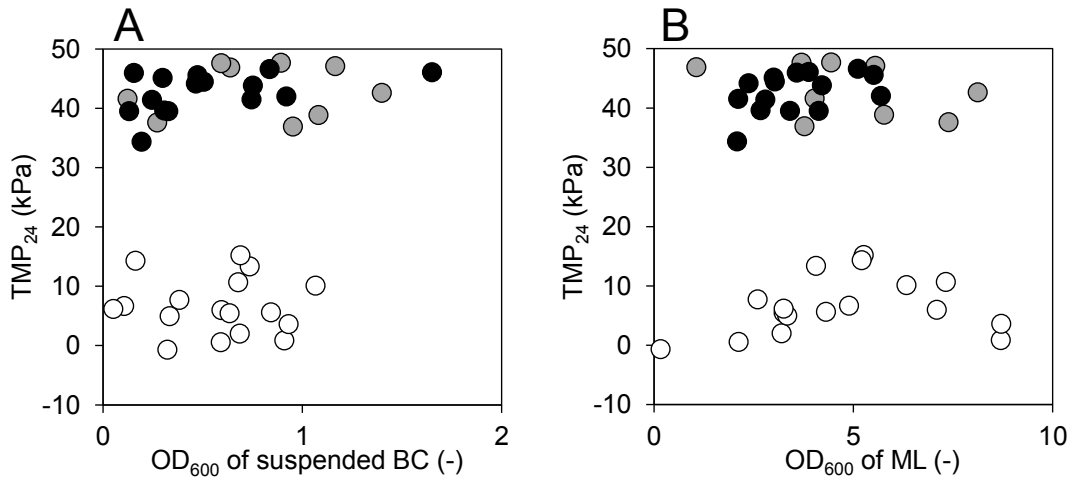

Figure 4.7 Relationships between fouling potentials (TMP_{24}) and the biomass accumulated on membrane (BC) (**A**) and the mixed liquor (**B**) in CFMFS. Biomass accumulated on membrane surfaces during 24 hr filtration was resuspended in NaCl solution, and its OD_{600} was measured (OD_{600} of BC). The biomass concentrations in the mixed liquor were measured after 24 hr filtration (OD_{600} of ML). Black, gray, and white dots represent the isolated strains in group **I**, **II** and **III**, respectively, as shown in **Figure 4.6.**

reached TMP > 20 kPa within 4 hr, **II**. Membrane fouling is gradually developed but reached TMP > 20 kPa within 24 hr, and **III**. Membrane fouling is gradually developed and reached TMP < 20 kPa after 24 hr (**Fig. 4.6**). The isolated strains classified into the group **I** were defined as fouling-causing bacteria (FCB) in this study, which includes the *Enterobacteriaceae* strains S04, S05, and S06, *Pseudomonadaceae* strain S16, *Xanthomonadaceae* strains S23 and S24, *Phyllobacteriaceae* strain S26, *Paenibacillaceae* strains S32 and S33, and *Microbacteriaceae* strains S34, S35, S38, S39, S40, and S41 (**Table 4.1** and **4.2**).

The different fouling patterns could be attributed to biomass concentrations (OD_{600}) in the mixed liquor during filtration, i.e., the growth rates of the isolated strains. However, there was no clear correlation between TMP_{24} and the biomass accumulated

Table 4.2 Similarities of 16S ribosomal RNA gene sequences of the isolated strains classified in *Enterobacteriaceae* (**A**), *Microbacteriaceae* (**B**), *Xanthomonadaceae* (**C**), *Bacillaceae* (**D**), *Pseudomonadaceae* (**E**), and *Paenibacillaceae* (**F**), respectively. (**G**) Summary of each OTU and isolated strains based on the results of **Table 4.2A** to **4.2F** and membrane fouling potentials (**Figure 4.6**).

A

Enterobacteriaceae

	S01	S02	S03	S04	S05	S06	S07	S08	S09	S10	S11	S12
S01		1.00	1.00	1.00	0.97	0.96	0.96	0.96	0.96	0.96	0.96	0.92
S02			1.00	1.00	0.96	0.97	0.96	0.96	0.96	0.96	0.96	0.92
S03				1.00	0.97	0.96	0.96	0.96	0.86	0.96	0.96	1.00
S04					0.96	0.96	0.96	0.96	0.96	0.96	0.96	0.92
S05						0.99	0.98	0.98	0.98	0.98	0.98	0.97
S06							0.98	0.98	0.98	0.98	0.98	0.93
S07								1.00	0.96	0.98	0.99	0.96
S08									0.96	0.98	0.99	0.96
S09										0.92	0.99	0.92
S10											0.99	0.96
S11												0.93
S12												

B

Pseudomonadaceae

	S14	S15	S16	S17
S14		0.87	0.95	0.95
S15			0.87	0.87
S16				0.97
S17				

C

Xanthomonadaceae

	S19	S20	S21	S22	S23	S24
S19		0.95	0.96	0.94	0.94	0.95
S20			1.00	0.94	0.95	0.94
S21				0.94	0.94	0.94
S22					0.99	0.99
S23						1.00
S24						

D

Bacillaceae

	S27	S28	S29	S30	S31
S27		0.94	1.00	0.99	1.00
S28			0.94	0.94	0.94
S29				1.00	1.00
S30					1.00
S31					

E

Paenibacillaceae

	S32	S33
S32		1.00
S33		

F

Microbacteriaceae

	S34	S35	S36	S37	S38	S39	S40	S41
S34		1.00	0.98	0.99	0.97	1.00	0.97	0.97
S35			0.98	0.99	0.97	0.97	0.97	0.97
S36				1.00	0.98	0.98	0.98	0.98
S37					0.99	0.99	0.99	0.99
S38						1.00	1.00	1.00
S39							1.00	1.00
S40								1.00
S41								

G

OTU	Closely-related family	Group I	Group II	Group III
1	*Enterobacteriaceae*	S04	-	S01, S02, S03
2	*Enterobacteriaceae*	S05, S06	S07, S08	S10, S11
3	*Enterobacteriaceae*	-	-	S09
4	*Enterobacteriaceae*	-	S12	-
5	*Moraxellaceae*	-	-	S13
6	*Pseudomonadaceae*	-	-	S14
7	*Pseudomonadaceae*	S16	S15	S17
8	*Comamonadaceae*	-	-	S18
9	*Xanthomonadaceae*	-	-	S19
10	*Xanthomonadaceae*	-	S20	S21
11	*Xanthomonadaceae*	S23, S24	S22	-
12	Undetermined	-	-	S25
13	*Phyllobacteriaceae*	S26	-	-
14	*Bacillaceae*	-	S29, S30	S27, S28
15	*Bacillaceae*	-	-	S31
16	*Paenibacillaceae*	S32, S33	-	-
17	*Microbacteriaceae*	S34, S35, S38, S39, S40, S41	S36	S37

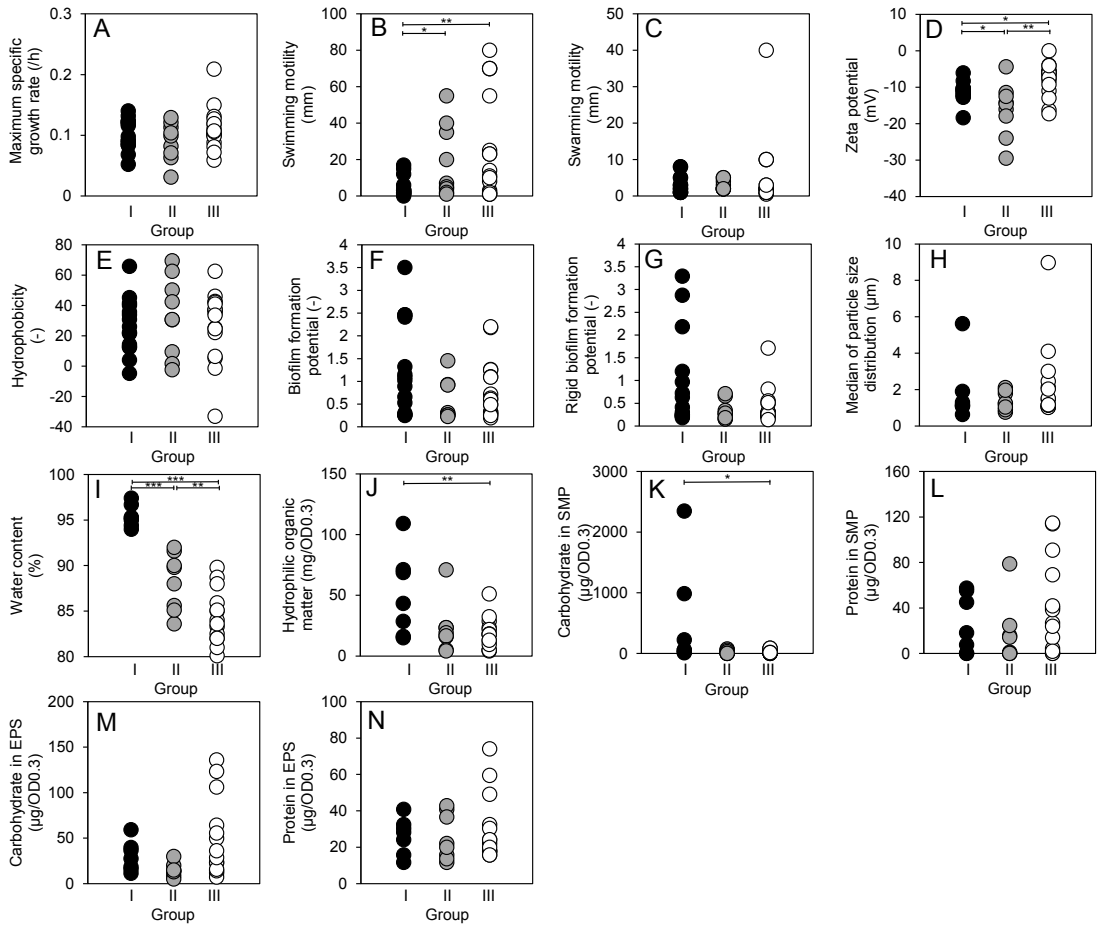

Figure 4.8 Comparison of cellular properties of isolated strains such as maximum specific growth rate (**A**), swimming motility (**B**), swarming motility (**C**), zeta potential (**D**), hydrophobicity (**E**), biofilm formation potential (**F**), rigid biofilm formation potential (**G**), median of particle size distribution (**H**), water content (**I**), hydrophilic organic matter content (**J**), carbohydrate content in SMP (**K**), and protein content in SMP (**L**), carbohydrate content in EPS (**M**), and protein content in EPS (**N**). The detail information is summarized in **Table 4.1**. Black, gray, and white dots represent the isolated strains in group **I**, **II** and **III**, respectively. Measurements of particle size distribution and water, hydrophilic organic matter, and carbohydrate and protein contents in colonies were performed for only representative strains. The bars with the following signs indicate statistically significant difference between two groups with respective *P* value: ***, $P<0.001$; **, $P<0.01$; *, $P<0.05$.

Table 4.3 Multiple linear regression analysis between TMP_4 and cellular properties of representative strains. The cellular properties of the isolated strains were summarized in **Table 4.1**. There is a significant linear relationship (p<0.01) between water content and fouling potential.

	p value
Maximum growth rate	0.70
Swimming motility	0.89
Swarming motility	0.99
Zeta potential	0.73
Hydrophobicity	0.78
Median of particle size distribution	0.74
Biofilm formation potential	0.48
Rigid biofilm formation potential	0.4
Water content	0.74
Hydrophilic organic matter	0.01
Carbohydrate in SMP in colony	0.94
Protein in SMP in colony	0.95
Carbohydrate in EPS in colony	0.41
Protein in EPS in colony	0.81
Adjusted determination coefficient	0.28

on the membrane after 24 hr of filtration (suspended BC: suspended biocake) (**Fig. 4.7A**) and biomass concentrations in the mixed liquor (ML) (**Fig. 4.7B**). These results indicate that membrane fouling was not mainly caused by accumulation of bacterial cells, instead probably caused by soluble microbial products (SMP) and/or extracellular polymeric substances (EPS) as previously reported (Guo et al., 2012;Lin et al., 2014). This also suggests that dominant species or faster-growing species in MBRs may not be necessarily FCB.

4.3.3. Cellular properties

Maximum specific growth rate, motility (swimming and swarming), zeta potential, cell surface hydrophobicity, particle size distributions of bacterial cultures, and biofilm formation potential (CV_{570}/OD_{600}) of the isolated strains were determined in details to evaluate the relevance of these cellular properties in their membrane fouling potentials

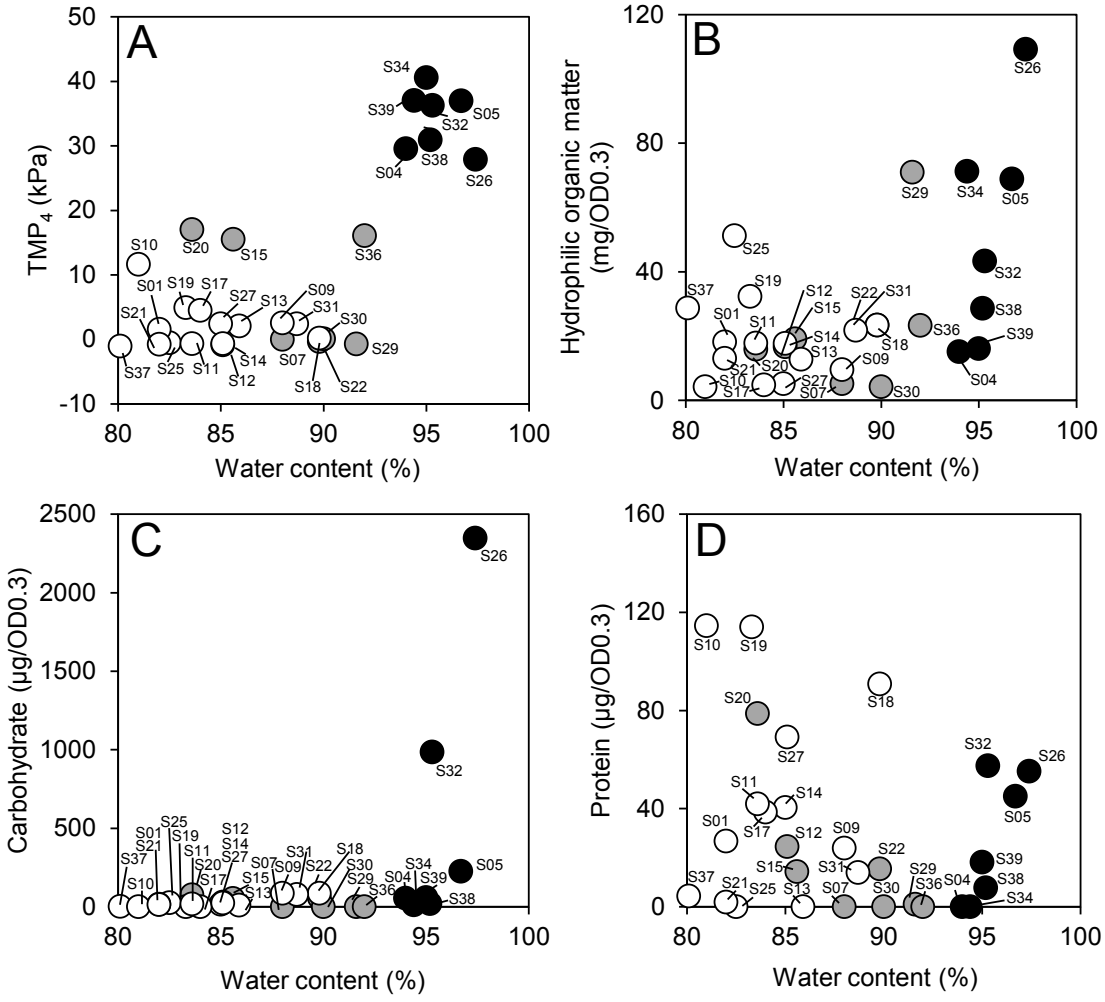

Figure 4.9 Relationships between fouling potentials (TMP_4) and colony water content (**A**) and between colony water content and hydrophilic organic matter content (**B**), carbohydrate content (**C**), and protein content (**D**) in the colonies of representative strains, respectively (**Table 4.1**). Black, gray, and white dots represent the isolated strains in group **I**, **II** and **III**, respectively (**Figure 4.6**).

(**Table 4.1**). The biofilm formation potential was normalized by the growth of suspended cells and expressed as CV_{570}/OD_{600}. Multiple linear regression analysis was performed to determine the most influential cellular property on membrane fouling (**Table 4.3**). As a result, FCB (group **I**) generally showed lower swimming motility than

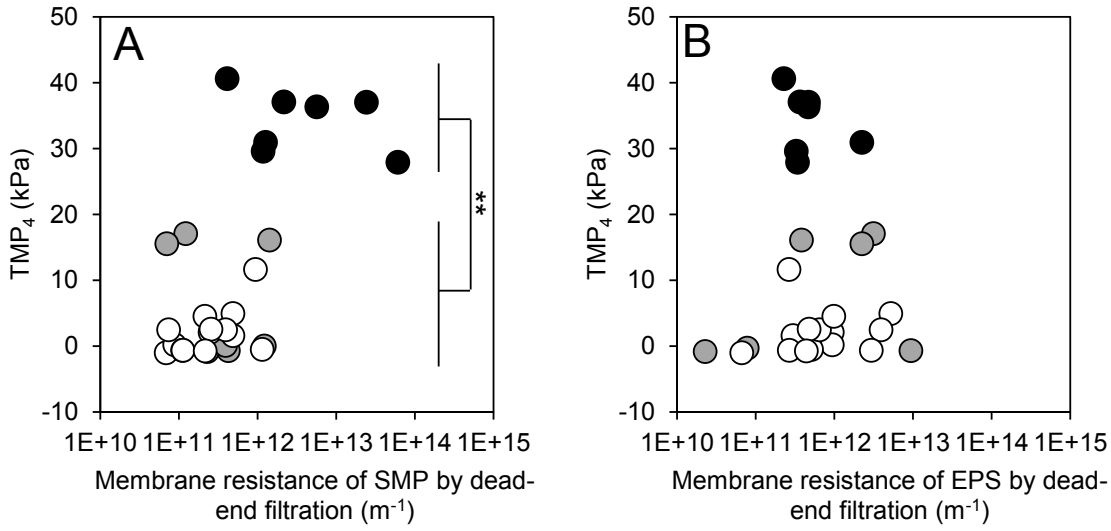

Figure 4.10 Fouling potentials of SMP (**A**) and EPS (**B**) in the representative strains were measured using dead-end filtration test, which were compared with TMP_4 measured in the CFMFS (**Figure 4.5**). Black, gray, and white dots represent the isolated strains in group **I**, **II** and **III**, respectively. The bar with the following sign indicates statistically significant difference between two group with respective *P* value: **, $P<0.01$.

other strains (group **II** and **III**) ($p<0.05$, **Fig. 4.8B**). There is, however, no clear explanation of the relationship between the lower swimming motility and higher fouling potential. Furthermore, biofilm formation potential was not related to the membrane fouling potential. Firmly attached (rigid) biofilm was also quantified (**Table 4.1**). However, the difference in rigid biofilm formation potential was not statistically significant among the isolated strains (**Fig. 4.8G**).

4.3.4. Colony characteristics

The most prominent feature of FCB was that FCB formed convex colonies having swollen podgy shape and smooth lustrous surfaces (swollen podgy colony) (**Fig. 4.9A**). In this study, the water contents of colonies were directly measured (**Table 4.1**). The

FCB in the group **I** showed significantly higher (>93%, **Fig. 4.9A**) colony water contents than isolated strains in other groups (p<0.001, **Fig. 4.8I**). In addition, FCB produced more soluble hydrophilic organic matter (p<0.01) and carbohydrate (p<0.01) in SMP than the other strains (**Fig. 4.8J** and **4.8K**, and **Fig. 4.9B** and **4.9C**). On the other hand, there was no significant difference between the amounts of protein in SMP, and both carbohydrate and protein in EPS in FCB and the other strain colonies (**Fig. 4.8L** to **Fig. 4.8N**, and **Fig. 4.9D**). Since hydrophilic material is known to have higher water-retention property than hydrophobic material (Fontani et al., 2013;Pandey et al., 2014), the higher water content of FCB colonies could be attributed to the higher content of soluble hydrophilic organic matter. Fouling potentials of SMP and EPS produced in colony of isolated strains were measured using dead-end filtration test to ensure the fouling behavior of colonies is similar to ones measured in the CFMFS (**Fig.4.10**). The SMP produced in colony by FCB showed significant membrane resistance than the other strains (p<0.01, **Fig.4.10**) and the resistance was in good agreement with TMP_4, whereas there was no clear tendency between the fouling potential of EPS produced in colony by FCB and TMP_4. These results indicated that the colony water and soluble microbial products can be used for evaluation of fouling potentials of isolated strains.

4.4 Discussion

The membrane fouling potentials of 41 bacterial strains isolated from fouled MF membranes in a MBR treating real municipal wastewater were determined and related to their cellular properties; cell surface properties, motility, biofilm formation potential, cell size, and colony characteristics. It was found that fouling causing bacteria (FCB) were affiliated with diverse families and the fouling potential was highly strain dependent; bacterial strains in the same family displayed different fouling potentials. This suggests that bacterial identification at the strain level is essential to identify key FCB. These FCB showed several common cellular properties; formation of swollen

podgy colonies with high water, hydrophilic organic matter, and carbohydrate contents. Major microbial species in MBRs have been frequently considered to be key bacteria responsible for membrane fouling. Although *Proteobacteria* have been considered to be one of dominant species and key FCB in MBRs (Lim et al., 2012;Miura et al., 2007c;Vanysacker et al., 2014a;Xia et al., 2010), only a few *Proteobacteria* strains were isolated and classified as FCB in our study. Similarly, *Xanthomonadaceae* constituted 2.73% and 4.21% in ML and Gel samples in this study, but less than half of the *Xanthomonadaceae* isolates (strains S23 and S24) were classified as FCB. In contrast, although *Microbacteriaceae* was one of minor groups in the MBR (0.17% and 0.02% in ML and Gel, respectively), 6 out of 8 strains (strains S34, S35, S38, S39, S40, and S41) caused severe membrane fouling. Based on these experimental results, dominant bacterial species are not always necessary to be FCB.

In this study, colony water content was clearly correlated to fouling potential, whereas general and rigid biofilm formation potential as determined with microtiter plates and cell surface properties (i.e., hydrophobicity and surface charge) did not reflect the fouling potential. Colony water content is easy to measure and thus could be a useful parameter to identify the potential FCB even for a large number of isolates. Colony morphology has been used to characterize bacterial properties (Yildiz and Visick, 2009). For example, bacteria that form wrinkled colonies were capable of producing more polysaccharides and more biofilm (Enos-Berlage and McCarter, 2000;Yildiz and Schoolnik, 1999). Based on such colony characteristics, mutant screening was also performed to identify biofilm-related genes ((Park et al., 2015).

In addition, the bacteria that form high water content colonies secret more soluble hydrophilic organic matters and carbohydrate. These characteristics were consistent with previous findings in which hydrophilic organic matters and carbohydrate were reported to cause severe membrane fouling, respectively (Kimura et al., 2012;Tran et al., 2015). However, the hydrophilic organic matter and carbohydrate content could not explain all the variation of membrane fouling (**Fig. 4.8J** and **Fig.**

4.8K), which may suggest that specific types and structures, but not amount (concentration), of hydrophilic organic matter are important for membrane fouling. This result is consistent with the previous report showing that specific polysaccharide fractions were responsible for significant membrane fouling of a pilot-scale MBR treating real municipal wastewater (Kimura et al., 2012). Further study is obviously required to investigate the compositions and properties of soluble hydrophilic organic matter excreted by the FCB in details and to relate to the degree of membrane fouling. Thermodynamic analysis will provide plausible explanations for the mechanism of membrane fouling by the soluble hydrophilic organic matter based on XDLVO theory (Hong et al. 2013). Furthermore, since membrane fouling is developed by multispecies of bacteria, not by a single of bacteria, the symbiotic interactions of bacteria should be investigated for better understanding about fouling mechanisms.

It should be noted that since the difference in experimental conditions (e.g., a cross flow velocity, permeate flux, substrates (medium) and so on) between the lab-scale CFMFS used in this study and pilot-scale MBR is large, species identified as FCB might not behave in the same way in the MBR. In particular, many researches have provided fruitful information on membrane fouling behavior by cultivate pure culture strain with medium containing rich nutrient (i.e. LB and R2A medium broth) such as the contribution of biofilm formation (Pang et al. 2005), membrane surface colonization (Choi et al. 2006), growth behavior in ML and on membrane (Chao et al. 2011), and specific polysaccharides (Yoshida et al. 2015) on membrane fouling. However, the fouling potential of bacteria might vary with the nutrient concentration and composition in substrate since it has been reported that type of substrate and food to microorganisms ratio affect the degree of membrane fouling (McAdam et al., 2007;Villain and Marrot, 2013;Villain et al., 2014). Furthermore, since it has been recognized that most of the bacteria present in wastewater could not be cultured and the number of isolates is limited in this study, the isolated strains might not reflect the microbial community of fouled membrane of MBR. However, the objective of this

study was to identify FCB and to evaluate the relevance of the cellular properties in their membrane fouling potentials. The common characteristics (i.e. high water, hydrophilic organic matter, and carbohydrate contents in their colonies) of FCB found in this study must be analyzed for FCB that will be isolated from other MBRs to justify as a useful universal parameter.

4.5. Conclusion

In summary, 41 bacterial strains were isolated from a pilot-scale MBR treating real municipal wastewater and tested for membrane fouling potentials. In addition, their cellular properties were characterized to evaluate the relevance of these cellular properties in their membrane fouling potentials. The fouling potential was highly strain dependent, suggesting that bacterial identification at the strain level is essential to identify key fouling-causing bacteria (FCB). The FCB showed some common cellular properties; they formed convex colonies having swollen podgy shape and smooth lustrous surfaces with high water, hydrophilic organic matter, and carbohydrate contents. Colony water content is easy to measure and therefore could be a useful parameter to identify the potential FCB even for a large number of samples.

CHAPTER 5

Membrane fouling induced by AHL-mediated soluble microbial product (SMP) formation by fouling-causing bacteria co-cultured with fouling-enhancing bacteria

5.1. Background and Objectives

Membrane bioreactor (MBR) is considered to be a core wastewater reclamation technology to fulfill our diverse water demand (Judd, 2008;Meng et al., 2009a). However, membrane fouling is still one of the main obstacles for its wider applications (Zuthi et al., 2013). Soluble microbial product (SMP) and extracellular polymeric substances (EPS) were considered to be main causes of membrane fouling in MBRs (Tran et al., 2015). Therefore, better understanding of the detailed mechanisms of SMP and EPS production is essential for membrane fouling mitigation and control strategies (Malaeb et al., 2013b).

Extensive studies have been conducted to isolate and characterize key bacteria responsible for membrane fouling (Choi et al., 2006;Ishizaki et al., 2016a;Juang et al., 2010b;Pang et al., 2005b). In our previous study, forty-one bacterial strains were isolated from a pilot-scale MBR treating municipal wastewater, tested for their fouling potentials using a cross-flow filtration unit, and related to their cellular properties (Ishizaki et al., 2016a). In this study, fifteen strains showed significant fouling potentials based on single-culture studies, and were considered as fouling-causing bacteria (FCB). Since bacteria were commonly present as mixed species in actual MBRs, the influence of microbial interaction of isolated bacterial strains on membrane fouling should be examined.

Several studies have revealed microbial interactions stimulated the formation of thicker biocake (Gao et al., 2013b;Vanysacker et al., 2014b). The bacteria initially colonized on membrane surface and their SMP and EPS secretion facilitated subsequent

bacterial attachment and growth, and eventually caused severe membrane fouling (Gao et al., 2013b;Vanysacker et al., 2014b). However, it is not clear how microbial interaction influences the production of SMP and EPS and consequently membrane fouling.

It is well known that a variety of bacteria are capable of producing signal molecules (i.e. *N*-acyl homoserine lactones (AHL)), communicating each other and regulating gene expression in response to population density, which is known as AHL-mediated quorum-sensing (QS) system (Fuqua et al., 1994). Several AHLs-producing bacteria were identified in MBRs (Lade et al., 2014b). Furthermore, several studies have revealed the links between the presence of various AHL signals with biocake formation and membrane fouling in MBRs (Huang et al., 2016;Lade et al., 2014a;Yeon et al., 2008;Yu et al., 2016). Although the amounts of SMP and EPS in both biocake and mixed liquor were related to the increase in AHL concentrations (Yeon et al., 2008;Yu et al., 2016), the exact role and mechanism of AHL-based QS in membrane fouling are not still clearly understood due to complex microbial interactions.

The aim of this study is, therefore, to investigate whether microbial interaction influences on the fouling potential. To achieve this goal, thirteen bacterial strains isolated in our previous study were tested for their fouling potentials when cultivated as single-culture and co-culture. As a result, three strains exhibited significant fouling potential as single-cultures, thus they were defined as fouling-causing bacteria (FCB). Furthermore, co-culturing strain S26, one of the FCB, with S22 dramatically increased the fouling potential, which was caused by AHL-mediated SMP production by S26. The SMP produced in the co-culture of FCB and fouling-enhancing bacteria (FEB, S22 in this study) was further characterized.

5.2. Materials and Methods

5.2.1. Bacterial strains

Thirteen strains were selected from each operational taxonomic unit (OTU) composed of bacterial strains isolated in previous our study (Ishizaki et al., 2016a) (**Table 5.1**). The degree of fouling potential of the isolated strains was categorized in three groups (high, I; moderate, II; low: III) (Ishizaki et al., 2016a) (**Table 5.1**). All the strains were cultivated with M9 medium containing 48 mM Na_2HPO_4, 22 mM KH_2PO_4, 8.5 mM NaCl, 19 mM NH_4Cl, 2 mM $MgSO_4$, 100 μM $CaCl_2$, 20 mM glucose, and trace element.

5.2.2. Measurement of membrane fouling potential

Membrane fouling potential of isolated strains was determined by dead-end filtration. For single-culture studies, each strain culture (0.5 mL, OD_{600} = 1.0) was incubated in 50 mL of M9 medium for 2 days at 30°C. For co-culture studies, two strain cultures (each 0.25 mL, OD_{600} = 1.0) out of thirteen strains were inoculated into 50 mL of M9 medium and incubated for 2 days at 30°C. For mixed population (sludge) study, S26 culture (0.05 mL, OD_{600} = 1.0) and mixed liquor (0.45 mL, OD_{600} = 1.0) of MBR treating municipal wastewater was inoculated into 50 mL of M9 medium and incubated for 2 days at 30°C (Kimura et al., 2005). OD_{600} value of all the culture was adjusted to approximately 0.3 with fresh M9 medium to eliminate cell concentration effect before extracting SMP.

After incubation, each culture medium was centrifuged (4°C, 6,000 × *g* for 15 min), and the supernatant was subjected to dead-end filtration test to evaluate the fouling potential. Five mL of the supernatant was transferred to a stirred filtration unit (UHP-25K; Advantec Toyo; Tokyo, Japan) with a flat membrane filter (0.2 μm, hydrophilic PTFE; Advantec Toyo; Tokyo, Japan), and filtered under 50 kPa of ambient air. Thereafter, MilliQ water (approximately 10 mL) was added in the filtration unit and filtered again under the same pressure (Kimura et al., 2012). The permeate flow rate of

Table 5.1 Bacterial strains used in this study.

Strain	Closest species	Sequence similarity (%)	[a]Fouling potential
S01	*Escherichia coli*	99.9	III
S05	*Klebsiella pneumoniae*	99.5	I
S09	*Enterobacter aerogenes*	98.6	III
S12	*Leclercia adecarboxylata*	97.1	II
S14	*Pseudomonas aeruginosa*	99.9	III
S15	*Pseudomonas alkylphenolia*	99.3	II
S18	*Acidovorax delafieldii*	98.8	III
S20	*Pseudoxanthomonas mexicana*	99.8	II
S22	*Thermomonas fusca*	98.5	II
S26	*Mesorhizobium ciceri*	98.4	I
S31	*Bacillus subtilis*	100.0	III
S32	*Paenibacillus polymyxa*	99.4	I
S40	*Microbacterium azadirachtae*	99.6	I

[a]Fouling potential: The degrees of fouling potential of the isolated strains were determined with cross-flow membrane filtration system (CFMFS) when cultivated as single-culture and categorized as follow: high, I; moderate, II; low: III. (Ishizaki et al., 2016a)

MilliQ water was measured, and the membrane resistance of the fouled membrane was calculated as follows;

$$\text{Membrane resistance } (m^{-1}) = PA/\mu Q$$

where, P is the pressure (Pa), A is the filtration area of membrane (m^2), μ is the dynamic viscosity of MilliQ water (Pa・s), and Q is the permeate flow rate of MilliQ water (m^3/s).

5.2.3. Effect of supernatant and AHL on fouling potential

To investigate the microbial interaction between fouling-causing bacteria (FCB) and fouling-enhancing bacteria (FEB), S26 was cultured with the supernatant of either S22 or S31, and its fouling potential was measured. For the cultivation of S26, M9 medium was made with the supernatant of culture media (OD_{600} = 0.3) sterilized with syringe

filter (0.2 μm, Mixed Cellulose Ester; Advantec Toyo; Tokyo, Japan). S22 and S31 were also cultured with M9 medium made with the supernatant of S26 to decide the effect of the supernatant of FEB.

In order to evaluate the effect of *N*-acyl-homoserine-lactone (AHL) on enhancement of fouling potential, S22 and S26 was cultivated with M9 medium containing 4.4 μM of *N*-octanoyl-L-homoserine lactone (C8-HSL). The bacterial cultivation and the fouling potential measurement were carried out as mentioned above.

5.2.4. Thin-layer chromatograph (TLC) assay for AHL

TLC assay was conducted to identify the AHL produced by isolated strains as described elsewhere in previous study with small modification (McClean et al., 1997;Shaw et al., 1997). Each culture medium of S22 and S26 was centrifuged (4°C, 6,000 × g, 15 min) and filtered with the sterilized syringe filter (0.45 μm, Mixed Cellulose Ester; Advantec Toyo; Tokyo, Japan) to remove bacterial cells. The supernatant (100 mL) was concentrated about 20 times by freeze-dry and AHL was extracted four times with 10 mL of ethyl acetate. The ethyl acetate was evaporated and the residual was dissolved with 10 μL of ethyl acetate. This solution and 5 μL of AHL standards were spotted on the C18 reversed-phase plate (TLC silica gel 60 RP-18 F254s; Merck, Germany) and the chromatogram was developed with methanol/water (60:40, v/v). The production of AHL was determined with *Chromobacterium violaceum* VIR24 (VIR24) (Someya et al., 2009). After dried in air, the plate was overlaid with thin film of the mixture of LB broth containing 0.6% (w/v) and an overnight culture of VIR24 at the ratio of 1:1. After the incubation overnight at 30°C, purple spot appeared in response to the presence of AHL on the plate. Based on the color development, R_f value of AHL standard and AHL produced by the strains were estimated as described elsewhere (Yeon et al., 2008).

5.2.5. Characterization of SMP

SMP extracted from culture medium was dialyzed to remove residual glucose as

described elsewhere (Miura et al., 2013). OD_{600} value of all the culture was adjusted to approximately 0.3 with fresh M9 medium to eliminate cell concentration effect before the dialysis. Carbohydrate and protein concentrations in dialyzed SMP were quantified with phenol-sulfonic acid method using glucose as the standard and Lowry method using BSA as the standard, respectively. The contents of carbohydrate and protein were determined as follows:

$$\text{Carbohydrate} = a \times C$$

$$\text{Protein} = a \times P$$

where, a is a dilution factor, and C and P are carbohydrate and protein concentration of SMP (mg/L), respectively. In order to estimate the quantities of SMP trapped on membrane, carbohydrate and protein in SMP before and after the dead-end filtration was measured (Ishizaki et al., 2016a).

SMP was also characterized by using fourier transform infrared (FTIR). The spectrum of the freeze-dried SMP was measured by a FTIR spectrometry (FT/IR-660 Plus; JASCO Co., Tokyo, Japan). The operating range was from 4000 to 600 cm^{-1} with a resolution of 10 cm^{-1}. Principle compartment analysis (PCA) was carried out with the normalized spectra (Lammers et al., 2009).

All the statistical analyses including PCA were carried out with R 3.0.2 (R Development Core Team; Vienna, Austria). *P* values less than 0.05 were considered statistically significant in all analyses.

5.3. Results

5.3.1. Fouling potentials of isolated strains as single-culture

Fouling potentials of 13 isolated strains were determined by dead-end filtration when they were cultivated as single-cultures (**Fig. 5.1**). Strain S05, S26, and S32 showed significantly high fouling potential as compared with other strains. Therefore, these strains were considered as FCB in this study.

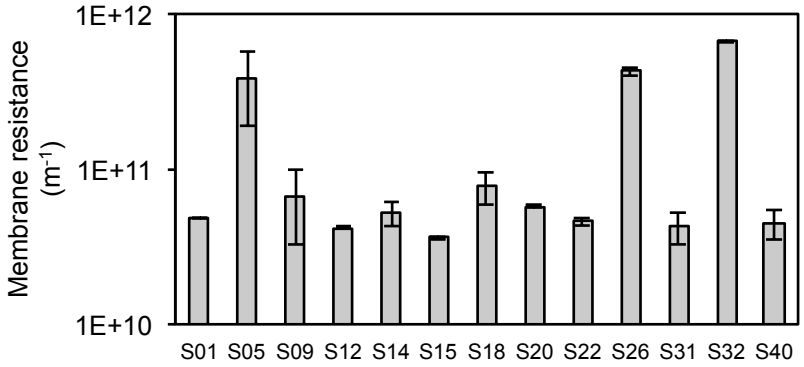

Figure 5.1 Fouling potentials of 13 isolated strains (see **Table 5.1**) cultivated as single-cultures. Since S05, S26, and S32 exhibited high fouling potentials, they were regarded as fouling-causing bacteria (FCB) in this study. The error bars indicate the standard deviations of two independent experiments.

5.3.2. Effect of co-cultivation on fouling potentials of isolated strains

1) Fouling potentials of isolated strains as co-culture

Fouling potentials of 13 isolated strains were determined by dead-end filtration when they were cultivated as co-cultures (**Fig. 5.2A**). There were 78 possible co-culture combinations of 13 isolated strains (the fouling potentials of all combinations were summarized in **Table 5.2**). The fouling potentials were elevated when all strains except for a few strains (S01, S12, and S14) were co-cultured with FCB (S05, S26, and S32). On the other hand, co-culturing with non-FCB did not significantly promote the fouling potential (**Fig. 5.2A**). These results suggest that membrane fouling was mainly caused by FCB, and some strains (S01, S12, and S14) might have capability to mitigate membrane fouling of FCB.

Furthermore, FCB were mixed with activated sludge and cultured for 2 days at 30°C, and then the fouling potential of culture medium was measured (**Fig. 5.2B**). The addition of all FCB significantly enhanced the fouling potential of activated sludge ($p < 0.05$), suggesting that FCB dominantly responsible for membrane fouling even in complex mixed populations.

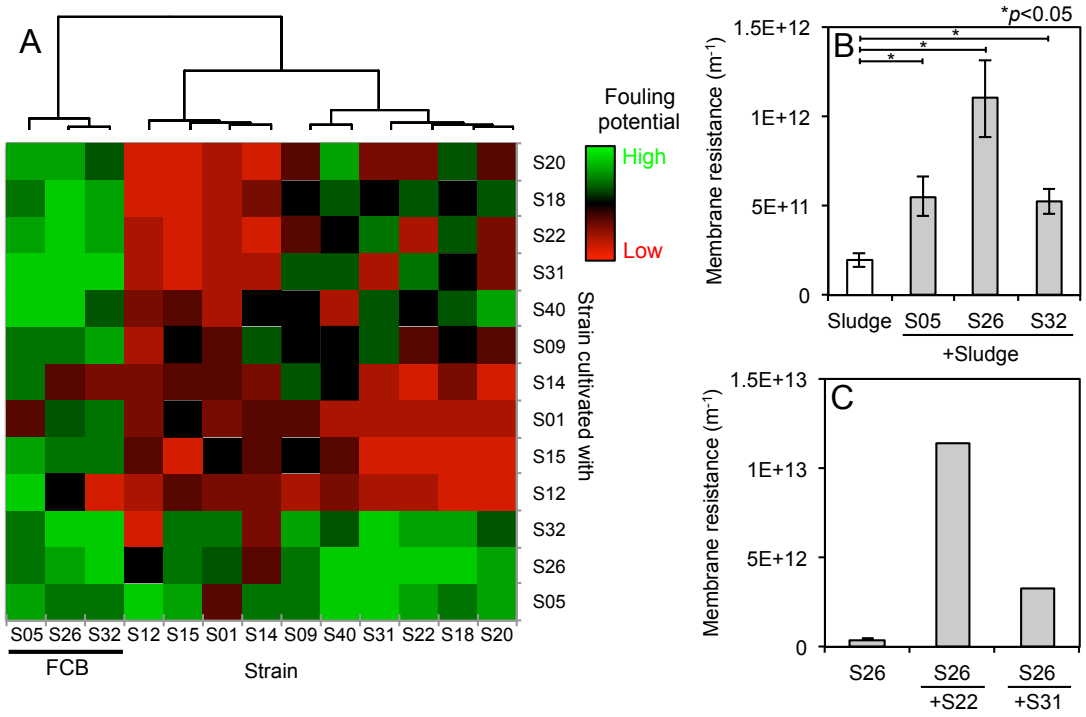

Figure 5.2 (**A**) Fouling potentials of co-cultures of 13 isolated strains (in total 78 combinations). (**B**) Effect of FCB (S05, S26, and S32) addition to activated sludge on fouling potential. The error bars indicate the standard deviations of two independent experiments. The bar following sign indicates statistical difference between two groups with respective *p* value: *, $P<0.05$. (**C**) Fouling potential of S26 as single-culture and co-culture with S22 or S31.

2) Effect of fouling-enhancing bacteria (FCB) on fouling potential of FCB

When S26 was co-cultured with S22 or S31, the fouling potentials increased to 1.1×10^{13} and 3.3×10^{12} (m^{-1}), respectively, which were 26.8 or 7.8 times greater than the one of S26 single-culture (4.3×10^{11} (m^{-1})) (**Table 5.2, Fig. 5.2C**). The growth of S26 was similar regardless of single and co-cultures (**Fig. 5.3**). Furthermore, the fouling potential of S26 was significantly increased when S26 was cultured in M9 medium made with the filter sterilized supernatant of S22 culture medium (9.6 times, $p < 0.05$) (**Fig. 5.4**). On the other hand, the fouling potentials of S22 and S31 remained

Table 5.2 Summary of fouling potential of all the combination of isolated strains.

Strain cultivated with \ Strain	S01	S05	S09	S12	S14	S15	S18	S20	S22	S26	S31	S32	S40
S01	5.E+10	6.E+10	6.E+10	5.E+10	6.E+10	6.E+10	4.E+10	4.E+10	5.E+10	8.E+10	5.E+10	1.E+11	5.E+10
S05	6.E+10	4.E+11	2.E+11	6.E+11	1.E+11	4.E+11	2.E+11	3.E+11	4.E+11	2.E+11	5.E+11	2.E+11	6.E+11
S09	6.E+10	2.E+11	7.E+10	4.E+10	1.E+11	7.E+10	8.E+10	6.E+10	6.E+10	2.E+11	1.E+11	3.E+11	6.E+10
S12	5.E+10	6.E+11	4.E+10	4.E+10	5.E+10	6.E+10	3.E+10	4.E+10	4.E+10	6.E+10	5.E+10	4.E+10	5.E+10
S14	6.E+10	1.E+11	1.E+11	5.E+10	5.E+10	6.E+10	5.E+10	4.E+10	4.E+10	6.E+10	5.E+10	5.E+10	6.E+10
S15	6.E+10	4.E+11	7.E+10	6.E+10	6.E+10	4.E+10	4.E+10	3.E+10	4.E+10	1.E+11	4.E+10	2.E+11	6.E+10
S18	4.E+10	2.E+11	8.E+10	3.E+10	5.E+10	4.E+10	8.E+10	9.E+10	9.E+10	6.E+11	7.E+10	2.E+11	1.E+11
S20	4.E+10	3.E+11	6.E+10	4.E+10	4.E+10	3.E+10	9.E+10	6.E+10	5.E+10	4.E+11	5.E+10	9.E+10	4.E+11
S22	5.E+10	4.E+11	6.E+10	4.E+10	4.E+10	4.E+10	9.E+10	5.E+10	5.E+10	1.E+13	1.E+11	5.E+11	8.E+10
S26	8.E+10	2.E+11	2.E+11	6.E+10	6.E+10	1.E+11	6.E+11	4.E+11	1.E+13	4.E+11	3.E+12	1.E+12	2.E+12
S31	5.E+10	5.E+11	1.E+11	5.E+10	5.E+10	4.E+10	7.E+10	5.E+10	1.E+11	3.E+12	4.E+10	1.E+12	1.E+11
S32	1.E+11	2.E+11	3.E+11	4.E+10	5.E+10	2.E+11	2.E+11	9.E+10	5.E+11	1.E+12	1.E+12	7.E+11	1.E+11
S40	5.E+10	6.E+11	6.E+10	5.E+10	6.E+10	6.E+10	1.E+11	4.E+11	8.E+10	2.E+12	1.E+11	1.E+11	4.E+10

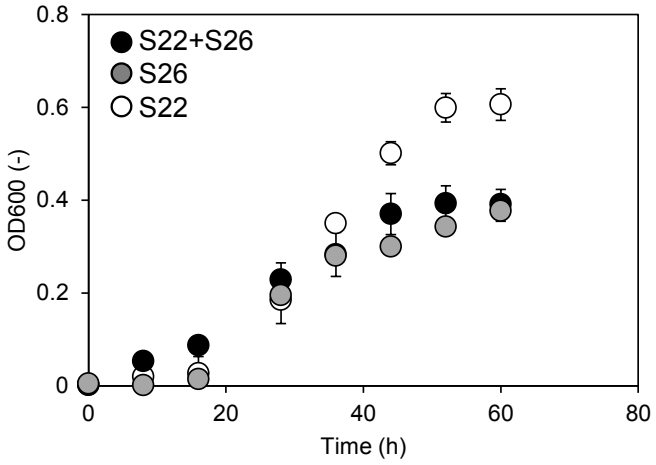

Figure 5.3 Growth curves of single-culture S22, S26, and co-culture of S22 and S26.

unchanged when S22 and S31 were cultured in the M9 medium made with the filter sterilized supernatant of S26 culture medium (**Fig. 5.4**). In addition, the fouling potential of the supernatant S26 remained unchanged when mixed with the supernatant of S22 or S31, indicating that abiotic interaction such as aggregation did not affect the membrane fouling (**Fig. 5.4**). These results suggest that production and secretion of fouling-causing matter, probably soluble microbial product (SMP), by S26 was enhanced by addition of the filter sterilized supernatant of S22 or S31 culture medium. Thus, S22 and S31 were considered as FEB in this manuscript.

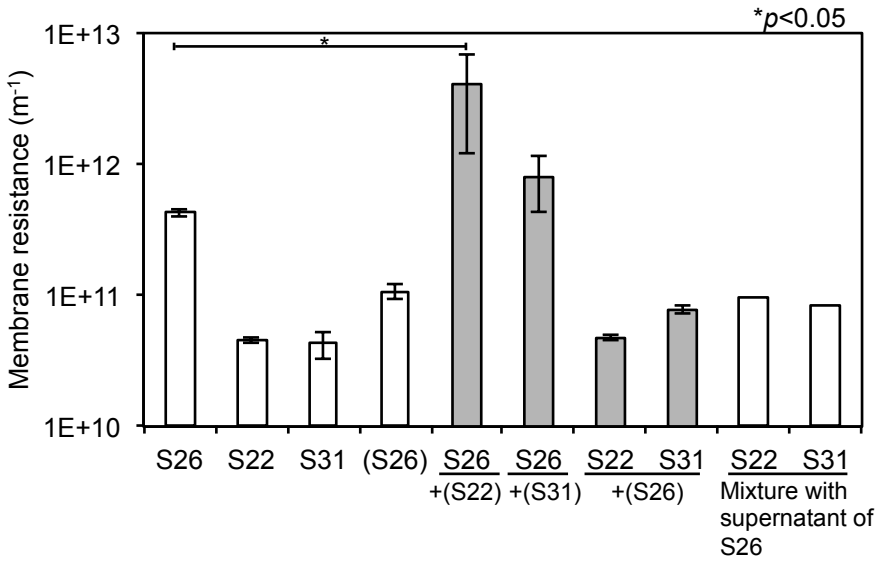

Figure 5.4 Effect of addition of the supernatants on fouling potential. The filter-sterilized supernatant of bacterial culture was added to M9 medium for cultivation of other strains. For example, S26 + (S22) indicates that S26 was cultured in the M9 medium with the filter-sterilized supernatant of S22 culture. The mixture of supernatants was also tested for fouling potential to assess abiotic effects by co-cultivating. The error bars indicate the standard deviations of two replicates except for the mixture of supernatants. The bar following sign indicates statistical difference between two groups with respective *p* value: *, $P<0.05$.

The S22 was affiliated with the Genus *Thermomonas* and shared 98.5% of 16S rRNA gene sequence with *Thermomonas fusca* DSM 15424 (Mergaert et al., 2003) (**Table 5.1**). The S26 was affiliated with the Genus *Mesorhizobium* and shared 98.4% of 16S rRNA gene sequence with *Mesorhizobium ciceri* biovar biserrulae WSM1271 (Nandasena et al., 2007) (**Table 5.1**). *Mesorhizobium* is known to produce AHL (Lade et al., 2014b). Although the ability of *Thermomonas* to produce AHL is not revealed in previous studies, the genus *Stenotrophomonas*, which is affiliated with the Family *Xanthomonadaceae*, is known to produce AHL (Valle et al., 2004). In addition, *Mesorhizobium* is known to possess LuxR/LuxI-type quorum-sensing regulatory system

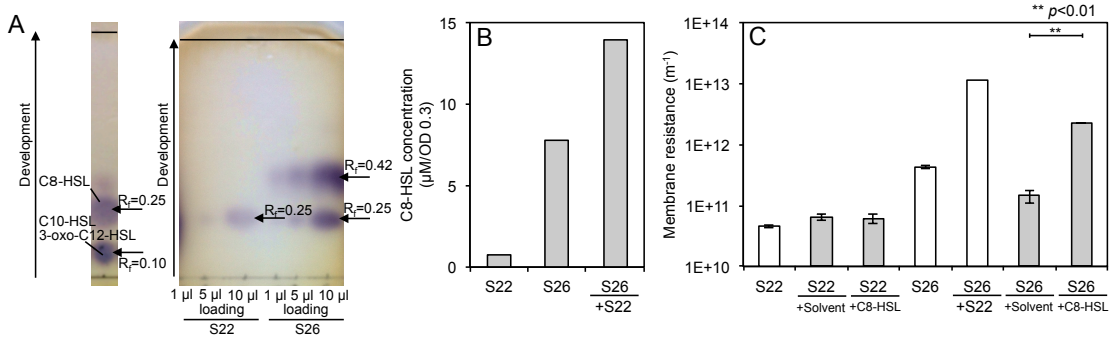

Figure 5.5 (**A**) Thin-layer chromatograph assay of *N*-acyl-homoserine-lactone (AHL) produced by S22 and S26. (**B**) *N*-octanoyl-L-homoserine lactone (C8-HSL) concentrations produced by single-culture of S22, S26, and co-culture of S22 and S26. (**C**) Effect of addition of C8-HSL on the fouling potential of S22 and S26 culture. The error bars indicate the standard deviations of two independent experiments. The bar following sign indicates statistical difference between two groups with respective *p* value: **, $P<0.01$.

(Ramsay et al., 2009;Zheng et al., 2006). Based on these evidences, it is speculated that the increased fouling potential of S26 is related to AHL-mediated processes.

3) Detection of C8-HSL in FCB and FEB and its role on fouling potential

TLC assay was performed to determine the production of AHL by S22 and S26. As a result, it was confirmed that both S22 and S26 produced most likely C8-HSL, but S26 produced more significantly than S22 (**Fig. 5.5A**). The C8-HSL production by S26 was increased by 78% when co-cultured with S22 (**Fig. 5.5B**). Furthermore, the fouling potential of S26 was significantly enhanced when S26 was co-cultured with S22 and cultured in M9 medium containing 4.4 µM C8-HSL for 2 day at 30°C (**Fig. 5.5C**). In contrast, addition of C8-HSL did not increase the fouling potential of S22 (**Fig. 5.5C**). These results indicated that C8-HSL production of S26 was significantly promoted by co-cultivating with S22, which stimulated the production and/or secretion of fouling-causing matter by S26 and consequently increased the fouling potential.

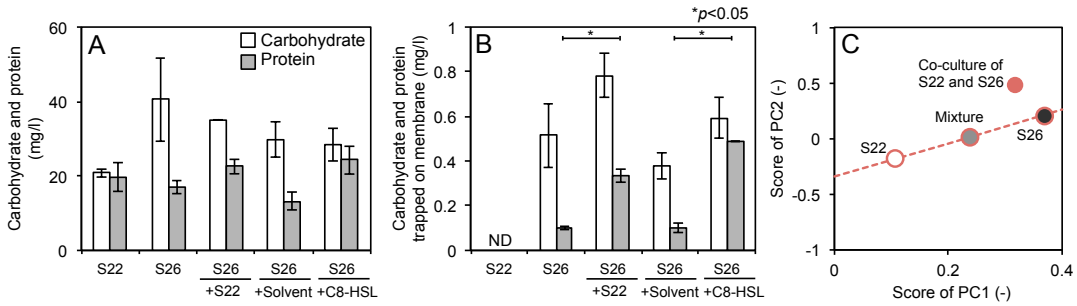

Figure 5.6 (**A**) Carbohydrate and protein contents in soluble microbial product (SMP) produced by S22, S26, S22+S26 (co-culture) and S26 cultured with C8-HSL (4.4 μM). (**B**) Carbohydrate and protein concentrations in SMP trapped on membrane surface in the dead-end filtration experiment for these cultures. The error bars indicate the standard deviations of two independent experiments. The bar following sign indicates statistical difference between two groups with respective *p* value: *, $P<0.05$. (**C**) Principal compartment analysis based on fourier transform infrared (FTIR) spectrum of SMP. "Mixture" indicates the mixture of the SMP produced by S22 and S26 with a ratio 1:1. The SMP produced by co-culture was close to the SMP produced by S26, indicating that the co-culture SMP was mostly produced by S26.

5.3.3. Characterization of SMP

1) Measurements of carbohydrate and protein contents in SMP

The carbohydrate content in SMP produced by S26 was higher than that of S22 (**Fig. 5.6A**), which might reflect the difference of fouling potential (**Fig. 5.5C**). Although total amount of SMP (carbohydrate and protein) remained unchanged when S26 was cultured with S22 and C8-HSL (**Fig. 5.6A**), the membrane fouling potential was significantly increased (**Fig. 5.5C**). However, amount of SMP trapped on the membrane surface after filtration was significant different. The more SMP was detected on the membrane surface when S26 was cultured with S22 and C8-HSL (**Fig. 5.6B**), which consisted with the increase in the fouling potential (**Fig. 5.5C**). In contrast, no accumulation of SMP was found for the S22 culture medium. These results might

indicate that the composition or characteristics, not total quantity, of SMP was an important factor determining membrane fouling and changed through C8-HSL produced by co-culturing with S22.

2) PCA analysis on the basis of FTIR

The composition of SMP was characterized with PCA based on the spectrum gained by a FTIR spectrometry (**Fig. 5.6C**). The SMPs produced by a single-culture S22 and S26 were plotted apart from each other, indicating different compositions. The mixture of the supernatants of single-culture S22 and S26 (1:1) was located in the middle of both plots (**Fig. 5.6C**). However, the plot representing co-culture of S22 and S26 located near the plot representing S26 rather than S22, suggesting the co-culture SMP was resemble the SMP produced by S26 (**Fig. 5.6C**).

5.4 Discussion

In our previous study, the fouling potentials of 41 phylogenetically distant strains that were previously isolated from the fouled membranes of a pilot-scale MBR treating real domestic wastewater were evaluated as single-culture(Ishizaki et al., 2016a). However, the effect of co-culturing these isolates on membrane fouling was unknown presently; therefore it was investigated in the present study. It was found that FCB induced sever membrane fouling even in co-cultures with non-FCB and complex microbial community (activated sludge) (**Fig. 5.2**). In particular, the fouling potential of S26, one of the FCB, was increased 26.8 times when cultivated with S22 that stimulated the production of fouling-causing SMP by S26. On the other hand, any co-cultures of non-FCB did not show higher fouling potentials than those of single non-FCB cultures (**Table 5.2**). It is, therefore, speculated that FCB could be responsible for membrane fouling in the pilot-scale MBRs treating domestic wastewater, suggesting that membrane fouling potentials of single-cultures of isolated strains provided useful, but limited information.

The microbial interaction that stimulated fouling-causing SMP production by S26 and consequently caused severe membrane fouling was further investigated in detail. The production of SMP was considered to be highly dependent on microbial populations in MBRs (Gao et al., 2013b;Lin et al., 2014). However, our findings demonstrated that SMP secretion was regulated by a signal molecule, C8-HS*L*, which is one of AHL. The secretion of C8-HSL molecule was significantly increased by co-culturing S26 and S22, which induced S26 to produce fouling-causing SMP (change the SMP composition), leading to severe membrane fouling.

Although many studies have examined the role of AHL-mediated QS in pure culture systems so far, available reports for co-culture or defined population systems are very limited. Given extensive studies so far, it is now conceivable that AHL-mediated QS system is important for biofilm formation. It is also known that EPS synthesis is subject to AHL molecules in both qualitative and quantitative manner (Marketon et al., 2003;Rinaudi and González, 2009;Sakuragi and Kolter, 2007). It was reported that the AHL-mediated QS was involved in production and secretion of hydrophobic extracellular proteins, which promote microbial aggregation of activated sludge (Lv et al., 2014). The carbohydrate and protein contents in EPS were also regulated by AHL (Lv et al., 2014;Tan et al., 2014). In MBRs, it was reported that the amounts of SMP and EPS in both biocake and mixed liquor were closely related to the increase in AHL concentration (Yeon et al., 2008;Yu et al., 2016). However, the exact mechanism of AHL in membrane fouling was not clearly revealed in these studies. To the best of our knowledge, the present study showed for the first time that AHL concentration was elevated by co-culturing FCB and FEB, which stimulated the production of fouling-causing SMP (induced the composition change) by FCB and consequently resulted in enhancement of membrane fouling.

Mesorhizobium and *Thermomonas* have been frequently detected in MBR (Shen et al., 2014;Silva et al., 2016;Tian et al., 2015a). They were also found in both mixed liquor (approximately 0.004% and 1.6% of total reads analyzed by

next-generation sequencing, respectively) and gel layer on fouled membrane (0.01% and 2.9% of the total reads, respectively) in the MBR where the bacterial strains were isolated(Ishizaki et al., 2016a). *Mesorhizobium* is capable of producing AHL (Zheng et al., 2006). *M. tianshanense* possess MtrI and MtrR, which is a homolog of LuxR and LuxI family proteins and acts as a QS regulatory system (Yang et al., 2009;Zheng et al., 2006). In this genus, QS system has been linked to the regulation of nodulation efficiency, growth rate, and exopolysaccharide production, and nitrogen fixation (Cao et al., 2009a). In contrast, there is limited information on the AHL-mediated QS of *Thermomonas* although it was reported that the growth was likely promoted by AHL (Hu et al., 2016).

In addition to AHL-mediated QS systems, existence and effects of quorum-quenching (QQ) systems that block the QS systems in MBRs have been extensively studied (Huang et al., 2016;Oh et al., 2012;Weerasekara et al., 2016). The present study clearly demonstrated that AHL-mediated QS was involved in the production of fouling-causing SMP, which consequently resulted in sever membrane fouling. Therefore, degradation and blocking of AHL by QQ enzymes, bacteria or fungus could be one of possible mitigation strategies of membrane fouling although the feasibility of this approach must be carefully examined (Lee et al., 2016;Oh et al., 2013). Furthermore, our results showed that FEB also played an important role in the AHL production by FCB. For better understanding of membrane fouling in MBRs, complex microbial interactions among QQ bacteria, FCB, and FEB must be taken into account in addition to the AHL-mediated QS and QQ systems (Huang et al., 2016). Therefore, possible combinations of QQ and other approaches such as chlorination (Weerasekara et al., 2016), enrichment of fouling-reducing bacteria (i.e. *Bacillus* and *Chloroflexi*) (Miura et al., 2007b;Zhang et al., 2014c), and anodic respiration (Ishizaki et al., 2016a) should be investigated for the efficacy of membrane fouling mitigation in future.

5.5. Conclusion

The effect of co-culturing bacterial strains isolated from a pilot-scale MBR on membrane fouling were investigated in the present study. It was found that FCB, especially S26 (closely related to *Mesorhizobium ciceri* (98.4%)), induced sever membrane fouling when co-cultured with non-FCB and activated sludge, suggesting that FCB were mainly responsible for membrane fouling in the pilot-scale MBRs treating domestic wastewater. In particular, the fouling potential of S26 was increased 26.8 times when cultivated with S22 (closely related to *Thermomonas fusca* (98.5%)). The mechanism enhancing membrane fouling in this co-culture was further investigated in detail. As a result, co-culturing with S22 induced S26 to produce more C8-HSL and thereby stimulated the production of fouling-causing SMP (induced the composition change) by S26, which consequently resulted in enhancement of membrane fouling. Taken together, AHL-mediated QS system was involved in SMP production and membrane fouling, which could not be revealed by single-culture studies.

CHAPTER 6

Effect of anodic respiration on fouling potential of fouling-causing bacteria

6.1. Background and Objectives

Integrated system of microbial fuel cell (MFC) and membrane bioreactor (MBR) was attractive as energy-efficient technique for wastewater treatment (Wang et al., 2011b;Yuan and He, 2015). Since MFC could achieve poor effluent quality, post-treatment was necessary to fulfill water quality standards for wastewater treatment (Wang et al., 2011a). In while, as mentioned above, MBR is capable of achieving high effluent quality, but its operation requires enormous energy for such as aeration (Gil et al., 2010;Kraume and Drews, 2010). Thus far, a variety type of the integrated system has been proposed (Yuan and He, 2015), and installing membrane module in or connected to anode chamber was likely effective for net positive energy generation (Katuri et al., 2014;Li et al., 2016;Ren et al., 2014).

Membrane fouling is of great concern to maximize the energy recovery, because aeration is not applied inside the anode chamber (Malaeb et al., 2013a). Aeration is a common technique to inhibit membrane fouling, but enormous energy is consumed, which accounted for 50% of total energy consumed to operate MBR (Gil et al., 2010;Kraume and Drews, 2010). Instead of aeration, it was thus proposed to install granular activated carbon into the anode chamber to reduce fouling potential (Li et al., 2014;Ren et al., 2014). Recently, our research group revealed that anodic reaction contributed to reduce membrane fouling (Ishizaki et al., 2016b). In this study, it was found that an enhancement of anodic respiration facilitated to reduce the production of biopolymer, which is well known as main foulant (Tian et al., 2013;Tran et al., 2015), and subsequently the fouling potential was reduced (Ishizaki et al., 2016b).

A variety of exoelectrogenic bacteria has been identified such as phylum

Proteobacteria, *Firmicutes*, and *Acidobacteria* (Huang et al., 2015;Logan, 2009). Although *Delta-Proteobacteria*, especially in *Geobacteraceae*, was observed predominantly in MFC at higher electrical current (Ishii et al., 2013;Torres et al., 2009), various bacteria must related to the generation of electricity, because high electrical current was observed in mixed-culture MFC reactor rather than pure-culture MFC reactor (Ishii et al., 2008). Furthermore, it was found that severe membrane fouling was caused by fouling-causing bacteria (FCB), which has significant fouling potential even in mixed-population and affiliated with a diverse of species (Ishizaki et al., 2016a;Ishizaki et al., *Submitted*). It is therefore speculated that anodic respiration influences on the fouling potential of exoelectrogenic FCB, and consequently the fouling potential is reduced in the integrated system: However, it is still unknown the effect of anodic respiration on the fouling potential of exoelectrogenic FCB.

Thus, the aim of this study is to evaluate the effect of various electron acceptors including with electrode on fouling potential of exoelectrgenic FCB. In this study, FCB was cultured with electrode, oxygen, and nitrate as sole external electron acceptor, and subjected to the measurements of fouling potential and bacterial secretion involving biopolymer.

6.2. Materials and Methods

6.2.1. Bacterial strain, reactor configuration and operational condition

The double-chamber MFC consisted of an anode chamber (250 ml) and a cathode chamber (250 ml) (Ishizaki et al., 2016b). The porous carbon (6 cm × 5 cm, Somerset; NJ, USA) and carbon cloth loaded with 0.5 mg/cm^2 of platinum (3 cm × 5 cm, E-TEK, Somerset; NJ, USA) were used as an anode electrode and a cathode electrode, respectively (Ishizaki et al., 2014). Each chamber was separated with a Nafion membrane (NafionTM 117, Dupont Co., DE, USA). Open circuit MFC was operated to test for oxygen and nitrate respirations. Ambient air was fed at a flow rate of 25 L/h and 2 ml of 20 mM $NaNO_3$ solution was fed per a day to supply with the same equivalent of

electron acceptor, respectively. Dissolved oxygen (DO) concentration and nitrate concentration were monitored to avoid the shortage of them, respectively. Open circuit MFC without any dissolved electron acceptor was also operated as a control. Anodic respiration was facilitated by regulating anodic electrode potential at +0.2 V (*vs*. Ag/AgCl) by using a potentiostat/galvanostat (HA-151B, Hokuto Denko Co., Tokyo, Japan). Closed-circuit reactor was equipped with external resistance of 1 ohm.

Strain S05, closely related to *Klebsiella pneumonia* (99.5%), was used in this study (Ishizaki et al., *Submitted*). After preincubated overnight, the culture washed twice with and incubated into a modified M9 medium with the following composition: 200 μM $(NH_4)_2SO_4$, 200 μM NaCl, 500 μM $CaCl_2$, 500 μM $MgCl_2 \cdot 6H_2O$, 27 mM K_2HPO_4, 55 mM KH_2PO_4 and 20 mM glucose (a sole energy source). The initial biomass concentration was approximately OD600 = 0.5. Each reactor was operated for 2 or 4 days as a batch mode at room temperature (25 ± 2˚C).

6.2.2. Measurement of membrane fouling potential

Dead-end filtration test was performed to evaluate the fouling potential as described elsewhere with minor modification (Kimura et al., 2012). After centrifugation at 4°C, 6000 × g for 15 min, 5 ml of the supernatant was transferred to a stirred filtration unit (UHP-25K; Advantec Toyo; Tokyo, Japan) with a flat membrane filter (0.2 μm, hydrophilic PTFE; Advantec Toyo; Tokyo, Japan). The permeate flow rate of MilliQ water was measured, and the membrane resistance of the fouled membrane was calculated as follows;

$$\text{Membrane resistance } (m^{-1}) = PA/\mu Q$$

where, P is the pressure (Pa), A is the filtration area of membrane (m^2), μ is the dynamic viscosity of MilliQ water (Pa・s), and Q is the permeate flow rate of MilliQ water (m^3/s).

6.2.3. Extraction of SMP and EPS

Soluble microbial product (SMP) and extracellular polymeric substance (EPS) in colony of isolated strains were extracted as described previously with minor modifications (Ramesh et al., 2007;Wang et al., 2009a). Briefly, mixed liquor was centrifuged at 4°C and 6,000 × *g* for 15 min. The supernatant was regarded as SMP. The remained pellet was suspended with 0.05% NaCl solution and then was subjected to heat treatment at 80°C and 1 hour. After dispersed well by vortexing, the suspension was centrifuged again at 4°C and 6,000 × *g* for 15 min. The supernatant was regarded as EPS.

6.2.4. Bacterial growth

Time variation in the biomass concentration (OD600) in each reactor was monitored for 2 or 4 days. The operation of each reactor was started at OD600 = approximately 0.1. OD600 value was measured by using an optical absorbance meter (Smart Spec Plus; Bio-Rad; CA, USA).

6.2.5. Chemical analysis

TOC concentration was measured using a TOC analyzer (TOC-V CSH; Shimadzu; Kyoto, Japan). COD concentration was measured following HACH COD method 8000 by using a HACH COD reactor and spectrophotometer DR/2400 (HACH Co.; CO, USA). The OD_{600} was measured by using an optical absorbance meter (Smart Spec Plus; Bio-Rad; CA, US). Carbohydrate and protein concentrations of the supernatant were measured with the phenol-sulfonic acid method with glucose as the standard and the Lowry method using BSA as the standard, respectively. Biopolymer concentration was determined by using Liquid chromatography with organic carbon detection (LC-OCD Model 8, DOC-LABOR; Karlsruhe, Germany). DO and nitrate concentrations were measured by using a DO meter (DO-5Z; Kasahara Chemical Instruments Co.; Saitama, Japan) and an ion-exchange chromatography (IC-2010,

TOSOH; Tokyo, Japan), respectively. The gas composite in anode chamber was measured by using Gas Chromatography (GC-14B; Shimadzu Co., Kyoto, Japan).

All the statistical analyses were carried out with R 3.0.2 (R Development Core Team; Vienna, Austria). *P* values less than 0.05 were considered statistically significant in all analyses.

6.3. Results

6.3.1. Fouling potentials with various electron acceptors

Strain S05, which is closely related to *Klebsiella pneumonia* (99.5%), was isolated in our previous study and categorized as FCB (Ishizaki et al., 2016a). S05 was cultured with electrode, oxygen, and nitrate as sole external electron acceptor for 2 days (**Table 6.1**). S05 was also cultured without any external electron acceptor as a control. Anodic respiration was enhanced by regulating anodic electrode potential at +0.2 V (*vs*. Ag/AgCl) to evaluate the effect of anodic respiration on the fouling potential of S05. The electrical current of S05 was enhanced from 0.64 ± 0.07 mA to 2.11 ± 0.26 mA by regulating the potential (**Table 6.1**).

Fouling potential of S05 was determined by dead-end filtration (**Fig. 6.1**). As shown in **Fig. 6.1**, the fouling potential remained unchanged regardless of external electron acceptor. In while, the fouling potential significantly increased when cultured without any external electron acceptor ($p<0.05$) (**Fig. 6.1**). In addition, the fouling potential significantly decreased when anodic respiration was enhanced ($p<0.05$) (**Fig. 6.1**). Enhancement of supplies of oxygen and nitrate were also effective to decrease the fouling potential, suggesting that the fouling potential of S05 was enhanced when small amount of electron acceptor was available regardless of the type of external electron acceptor (**Fig. 6.2**).

S05 was capable of producing hydrogen as fermentation, and less amount of hydrogen was produced when anodic respiration was enhanced (**Table 6.1**). This indicates that occurrence of fermentation could be inhibited when much more amount of

Table 6.1 Performance of strain S05 with various electron acceptors.

Electron acceptor	Electrode	Oxygen	Nitrate	Non	Electrode (+0.2V vs. Ag/AgCl)
COD removal rate (g/l/d)	0.814±0.023	1.884±0.017	1.824±0.008	0.377±0.061	0.847±0.104
Electrical current (mA)	0.64±0.07	-	-	-	2.11±0.26
Electrical transferred to Nitrate (mmol/d)	-	-	3.011±0.599	-	-
Coulomb efficiency (%)	2.9±0.5	-	-	-	9.3±0.6
Hydrogen production (mmol/d)	1.19	NA	NA	2.45	0.29

NA: Not analyzed

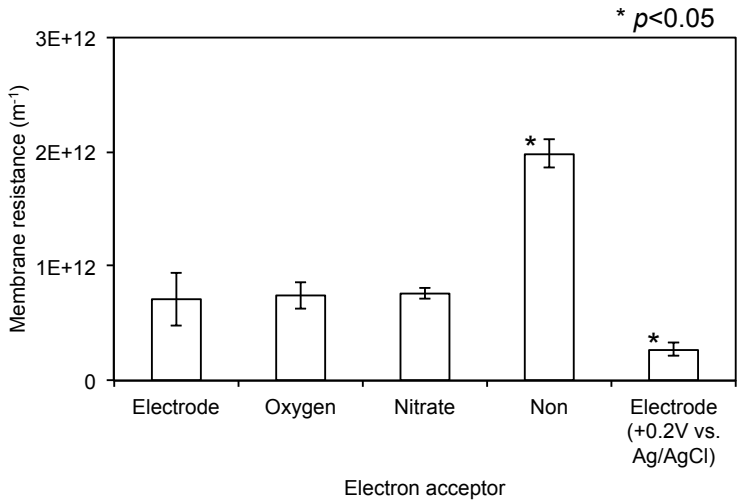

Figure 6.1 Fouling potential of strain S05 when cultured with various electron acceptors. The following sign indicates statistical difference as compared with the others with respective *p* value: *, *P*<0.05.

electron acceptor was available, which resulted in reducing the fouling potential. This also suggests that enhancement of anodic respiration by applying electric potential to anode electrode was effective to minimize fouling potential. Time variation in fouling potential of sterilized supernatant of S05 confirmed that abiotic reaction did not affect the fouling potential by regulating the anodic potential, suggesting that the reduction of the fouling potential is originated from anodic respiration by S05 (**Fig. 6.1.** and **6.3**).

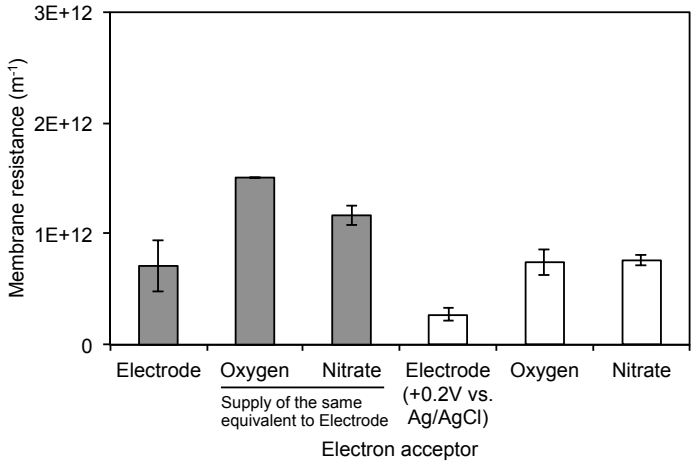

Figure 6.2 Fouling potential of strain S05 when cultured with limited amount of electron acceptors. Black bars indicate the fouling potential when fed with same equivalent of electron acceptor to Electrode (0.058 mmol/d).

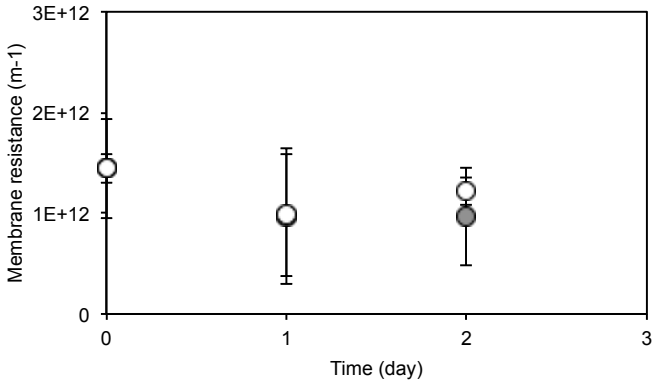

Figure 6.3 Abiotic effect of regulation of anodic electrode potential on fouling potential. Sterilized SMP of strain S05 was incubated in open circuit and closed circuit MFC reactor. The closed-circuit reactor was applied for +0.2 V (*vs.* Ag/AgCl). Open and filled circles were represented the fouling potential of SMP in open circuit and closed circuit, respectively.

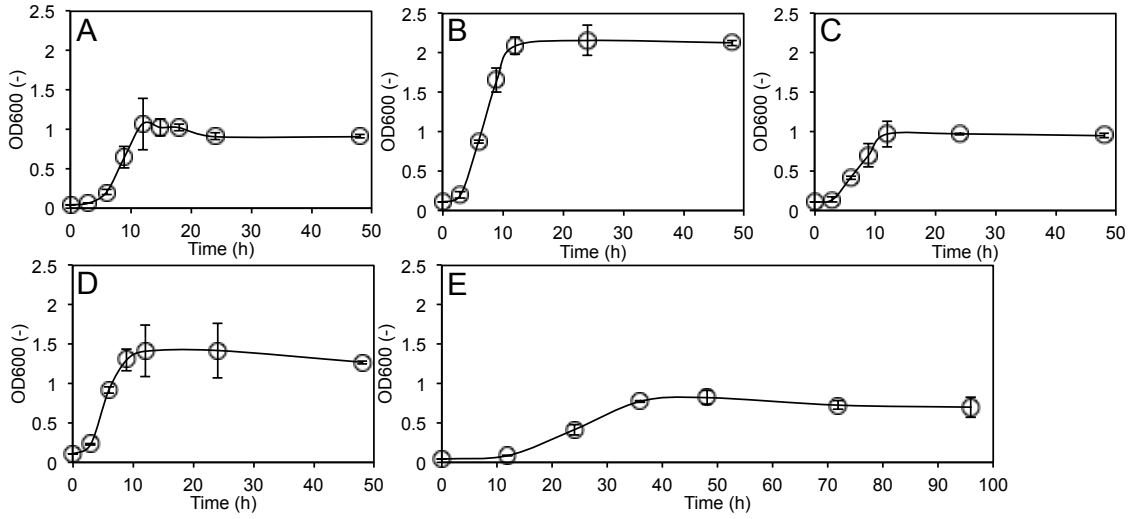

Figure 6.4 Growth curves of S05 when cultured with **A**) electrode, **B**) oxygen, **C**) nitrate, **D**) electrode (+0.2 V *vs.* Ag/AgCl) as sole electron acceptor. The growth curve without any electron acceptor was described in **Fig. 6.4E**

6.3.2. Bacterial growth

Time courses of OD600 of S05 with external electron acceptors were examined (**Fig. 6.4**). OD600 reached a plateau around 36 hours after the beginning of the cultivation without any external electron acceptor, whereas it reached a plateau around 12 hours after the beginning of the cultivation in the other conditions (**Fig. 6.4**). This indicates that S05 could grow slowly without any external electron acceptor.

Since the significant greater fouling potential of S05 without any external electron acceptor shown in **Fig. 6.1** was due to the slow growth, S05 was cultured without any external electron acceptor for 4 days, and subjected to the measurement of fouling potential (**Fig. 6.5**). However, the fouling potential of S05 at 4 day was still larger than that at 2 day. This means that the significant greater fouling potential was not attributable to time point of the measurement.

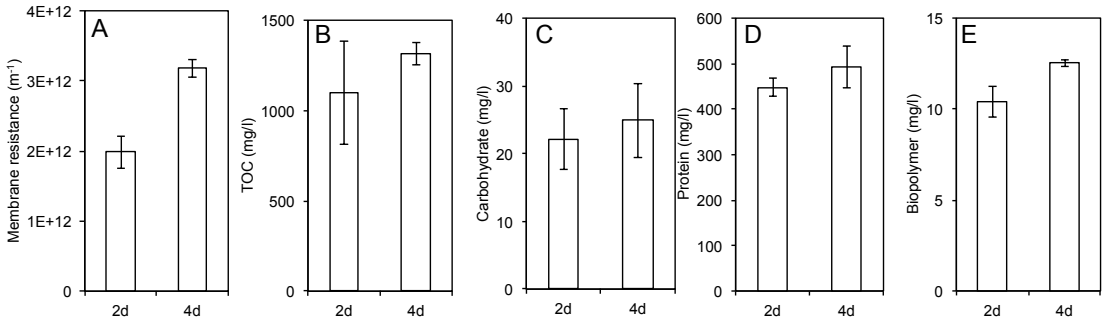

Figure 6.5 **A**) Fouling potential and **B**) TOC, **C**) carbohydrate, **D**) protein, and **E**) biopolymer in soluble microbial product (SMP) produced by strain S05 for 2 and 4 days without any electron acceptor.

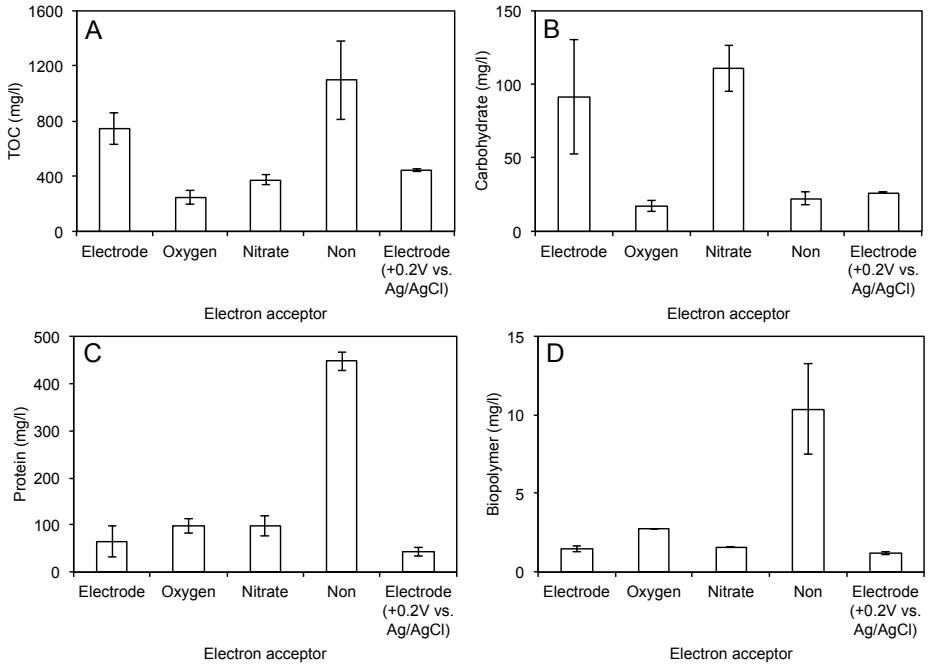

Figure 6.6 **A**) TOC, **B**) carbohydrate, **C**) protein, and **D**) biopolymer in soluble microbial product (SMP) produced by strain S05 with various electron acceptors.

6.3.3. Characterization in SMP

SMP and EPS produced by S05 were quantified in terms of TOC, carbohydrate, protein, and biopolymer concentrations (**Fig. 6.6** and **6.7**). As shown in **Fig. 6.6**, these concentrations differed depending on the type of external electron acceptor, implying

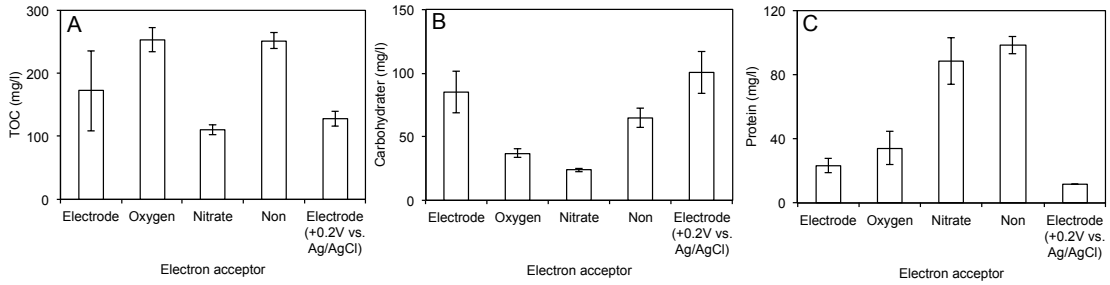

Figure 6.7 A) TOC, **B**) carbohydrate, and **C**) protein in extracellular polymeric substance (EPS) produced by strain S05 with various electron acceptors.

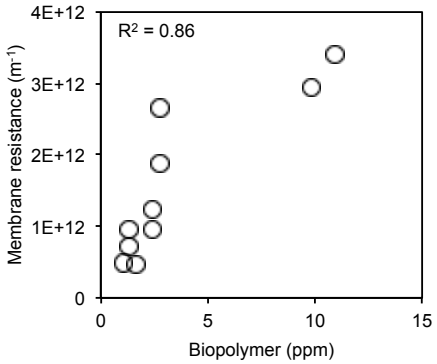

Figure 6.8 Correlation between the fouling potential and biopolymer of S05.

that the composition of both SMP and EPS was influenced on the external electron acceptors. In particular, protein and biopolymer concentrations in SMP were related to the fouling potential (**Fig. 6.1** and, **Fig. 6.6C** and **6.6D**). The fouling potential of S05 was closely correlated to the concentration of biopolymer (R^2 = 0.86, **Fig. 6.8**). These indicate that biopolymer was a main foulant of membrane fouling caused by S05, which was agreement with the previous studies (Ishizaki et al., 2016b;Kimura et al., 2014;Tian et al., 2013;Yamamura et al., 2014). Furthermore, the production of biopolymer was enhanced when cultured without any electron acceptor, namely at fermentation. Since biopolymer was considered as the macromolecules containing polysaccharides and protein and/or amino sugar, the biopolymer produced by S05 seemed to comprised much protein than carbohydrate (Tran et al., 2015).

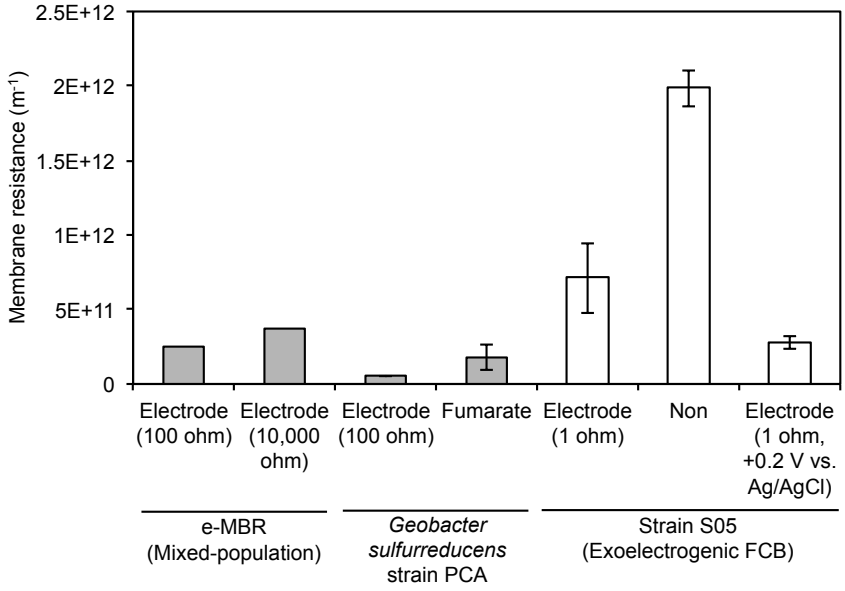

Figure 6.9 Fouling potential of e-MBR, *Geobacter sulfurreducens* strain PCA and strain S05 cultured with various electron acceptors. The data of e-MBR and strain PCA was referred to our previous study (Ishizaki et al., 2016b).

6.4. Discussion

The effects of various electron acceptors (electrode, oxygen, and nitrate) on the fouling potential and bacterial secretion of exoelectrogenic FCB were investigated. It was found that the fouling potential of FCB was remained unchanged regardless of electron acceptor, whereas a lack of electron acceptor enhanced fermentation and the fouling potential. The production of bacterial secretion including with biopolymer, which is known as main foulant in e-MBR, was increased without any external electron acceptor, and consequently severe membrane fouling occurred.

Integration of MFC to MBR has been known to effective for the mitigation of membrane fouling (Su et al., 2013;Yuan and He, 2015). Although several mechanisms for the membrane fouling mitigation were provided in previous studies (Liu et al., 2013;Wang et al., 2013;Xu et al., 2015), it was found that anodic respiration by exoelectrogenic bacteria also played important role on the mitigation in our previous study (Ishizaki et al., 2016b). This study revealed that the enhancement of anodic

respiration reduces the production of biopolymer, and subsequently reduced fouling potential in e-MBR established by mixed population (Ishizaki et al., 2016b). As like MBR, it seemed that membrane fouling was mainly caused by FCB in the e-MBR, because FCB dominantly responsible for membrane fouling even in complex mixed populations (Ishizaki et al., *Submitted*). Furthermore, since both FCB and exoelectrogenic bacteria were affiliated with a variety of species (Ishizaki et al., 2016a;Kumar et al., 2015;Logan, 2009), it could be speculated that the enhancement of anodic respiration primary contributes the reduction of the fouling potential of exoelectrogenic FCB. This study firstly accomplished to evaluate the fouling potential of exoelectrogenic FCB by cultivation with various electron acceptors. The fouling potential of strain S05 and *Geobacter sulfurreducens* strain PCA was compared in **Fig. 6.9**.

Enhancement of fermentation deteriorates membrane fouling. Several studies demonstrated that the fouling potential of the integration system did not reduced at further lower coulomb efficiency (Ishizaki et al., 2016b;Ma et al., 2015). In addition, anaerobic MBR generally causes severe membrane fouling as compared with aerobic MBR (Lin et al., 2013;Martin-Garcia et al., 2011). These agreed with our results that bacteria show severe fouling potential at the absence of external electron acceptor and occurrence of fermentation (**Fig. 6.1**). Martin-Garcia *et al.* observed significant increase in the protein concentration in SMP in anaerobic MBR, similar to our results (**Fig. 6.6**). Severe membrane fouling was also observed at lower DO concentration, which is also likely attributable to the absence of external electron acceptor (Gao et al., 2011a;Jin et al., 2006).

Increased production of protein and biopolymer might be caused by a reduction of biomass involving SMP. It is known that biomass can be utilized as electron acceptor (Parameswaran et al., 2009). In particular, much amount of electron is diverted to biomass at the absence of any external electron acceptor (Yu et al., 2015). Since biopolymer can be considered to be primary originated from bacterial cell and/or

EPS debris (Jiang et al., 2010b;Ni et al., 2011), the biopolymer might be produced by the change in composition and/or structure of the biomass involving SMP through the reductive reaction. In addition, slower degradation of SMP is also a possible reason for the increase in protein and biopolymer concentrations at the absence of external electron acceptor (Drews et al., 2007).

Klebsiella have frequently appeared in both MFCs and MBRs (Jia et al., 2013;Khan et al., 2013;Win et al., 2016;Yu et al., 2012). It was also found in both mixed liquor (in a range of 0.25% to 0.57% of total reads analyzed by next-generation sequencing, respectively) and anodic biofilm (in a range of 0.10 to 1.22% of the total reads, respectively) in e-MBR regardless of open- and closed-circuit in our previous study (Ishizaki et al., 2016b). *Klebsiella pneumonia* is known to be capable of the generation of electricity with recycle electron shuttle, indicating that it is able to generate electricity in both anodic biofilm and mixed liquor (Kumar et al., 2015;Zhang et al., 2008).

This study also demonstrated that enhancement of anodic respiration by regulating anodic potential is a promising technique for further mitigation of membrane fouling in the integrated system. When anodic potential was regulated at +0.2 V (*vs*. Ag/AgCl), the production of biopolymer was reduced (1.48 ± 0.18 *vs*. 1.17 ± 0.09 (mg/l)) and subsequently the fouling potential was mitigated (7.1 ± 2.3 *vs*. 2.7 ± 0.6 (10^{11} kPa)) (**Fig. 6.1** and **Fig. 6.6D**). Therefore, further investigation on the effect of anodic potential regulation on membrane fouling is necessary to maximize the net energy generation. In addition, the detail mechanism of the production of foulants (i.e. biopolymer) by various FCB at the absence of any external electron acceptor should be investigated for the better understanding of membrane fouling and the development of membrane fouling mitigation in future.

6.5. Conclusion

The effect of various electron acceptors (electrode, oxygen, and nitrate) on fouling potential of exoelectrogenic FCB was investigated in this study. Fouling potential of FCB, strain S05 (closely related to *Klebsiella pneumonia* (99.5%)) was remained unchanged regardless of electron acceptor. In while, a lack of electron acceptor enhanced fermentation and the production of bacterial secretion including with biopolymer, which is known as main foulant in e-MBR, and subsequently caused severe membrane fouling. Taken together, inhabitation of fermentation is essential to reduce fouling potential and an increase in anodic potential is promising for reducing fouling potential of FCB in e-MBR.

CHAPTER 7

Conclusion remarks

7.1. Impact of anodic respiration on biopolymer production and consequent membrane fouling in electrode-associated membrane bioreactor (e-MBR)

Microbial fuel cells (MFCs) have been recently integrated with membrane bioreactors (MBRs) for wastewater treatment and energy recovery. However, the impact of integration of the two reactors on membrane fouling of MBR has not been reported yet. In this study, MFCs equipped with different external resistances (1-10,000 ohm) were operated, and membrane-fouling potentials of the MFC anode effluents were directly measured to study the impact of anodic respiration by exoelectrogens on membrane fouling. It was found that although the COD removal efficiency was comparable, the fouling potential was significantly reduced due to less production of biopolymer (a major foulant) in MFCs equipped with lower external resistance (*i.e.*, with higher current generation) as compared with aerobic respiration. Furthermore, it was confirmed that *Geobacter sulfurreducens* strain PCA, a dominant exoelectrogen in anode biofilms of MFCs in this study, produced less biopolymer under anodic respiration condition than fumarate (anaerobic) respiration condition, resulting in lower membrane-fouling potential. Taken together, anodic respiration can mitigate membrane fouling of MBR due to less biopolymer production, suggesting that development of an electrode-assisted MBR (e-MBR) without aeration is feasible.

7.2. Membrane fouling potentials and cellular properties of bacteria isolated from fouled membranes in a MBR treating municipal wastewater

For better understanding and more effective control strategies of membrane fouling, it is important to identify and characterize the bacteria responsible for membrane fouling. In CHAPTER 4, 41 bacterial strains were isolated from fouled microfiltration membranes

in a pilot-scale MBR treating real municipal wastewater, and their membrane fouling potentials were directly measured using CFMFS and related to their cellular properties. As results, fifteen FCB were identified and their common cellular properties were revealed; they formed convex colonies having swollen podgy shape and smooth lustrous surfaces with high water, hydrophilic organic matter, and carbohydrate contents. Colony water content is easy to measure and therefore could be a useful parameter to identify the potential FCB even for a large number of samples.

7.3. Membrane fouling induced by AHL-mediated soluble microbial product (SMP) formation by fouling-causing bacteria co-cultured with fouling-enhancing bacteria

Since bacteria were commonly present as mixed species in actual MBRs, the influence of microbial interaction of isolated bacterial strains on membrane fouling should be examined. Thus, in CHAPTER 5, the effect of co-culturing bacterial strains isolated from a pilot-scale MBR on membrane fouling were investigated. It was found that FCB were mainly responsible for membrane fouling in the pilot-scale MBRs. In particular, the fouling potential of S26 (closely related to *Mesorhizobium ciceri* (98.4%)) was increased 26.8 times when cultivated with S22 (closely related to *Thermomonas fusca* (98.5%)). The mechanism enhancing membrane fouling in this co-culture was further investigated in detail. As a result, co-culturing with S22 induced S26 to produce more C8-HSL and thereby stimulated the production of fouling-causing SMP (induced the composition change) by S26, which consequently resulted in enhancement of membrane fouling.

7.4. Effect of anodic respiration on fouling potential of fouling-causing bacteria

It could be speculated that FCB also plays dominant role on membrane fouling in e-MBR and the enhancement of anodic respiration contributes to reduce the fouling potential of FCB which is capable of the generation of electricity. In this study, the

effect of various electron acceptors (electrode, oxygen, and nitrate) on fouling potential of exoelectrogenic FCB, strain S05 (closely related to *Klebsiella pneumonia* (99.5%)), was investigated. As results, the fouling potential was remained unchanged regardless of electron acceptor. However, a lack of electron acceptor enhanced fermentation and the production of bacterial secretion including with biopolymer, which is known as main foulant in e-MBR, and subsequently caused severe membrane fouling. In addition, it is also demonstrated that the enhancement of anodic respiration by anodic potential regulation is a promising technique for further membrane fouling mitigation in e-MBR.

7.5. Future outlooks

In this study, the effect of anodic respiration on membrane fouling in e-MBR was investigated for better operation of e-MBR in CHAPTER 3. For better operation of e-MBR, further investigation on the operation e-MBR at lower temperature is required, because it is known that the generation of electricity and membrane fouling become lower and severe at lower temperature, respectively (see CHAPTER 2.2.2 and 2.4.4.). As demonstrated in CHAPTER 6, the application of anodic potential regulation should be attempted to enhance anodic respiration and mitigate membrane fouling at lower temperature. In addition, the identification and characterization of FCB were accomplished in CHAPTER 4 and 5, but the fouling potential was evaluated at the same condition in these chapters. Since the fouling potential and their secretion seems to vary with culture condition (i.e. temperature and incubation time (see CHAPTER 2.4.4)), the identification and characterization of FCB should be continue at various culture condition. In particular, it should be noted that dissolved oxygen concentration might be more important parameter to determine the fouling potential of FCB (see CHAPTER 6). Thus, the investigation of the mechanism of biopolymer production at the absence of any external electron acceptor is recommended on transcriptomic and proteomic basis. Finally, application of only one technology might be inefficient for membrane fouling mitigation, because a variety of bacteria likely

related to cause severe membrane fouling as described in CHAPTER 4 to 6. For further membrane fouling mitigation, the combination of the techniques of membrane fouling mitigation (i.e. anodic respiration, quorum-quenching, enrichment of fouling-reducing bacteria) should be investigated on the basis of the study with pure culture and actual MBR to gain fundamental and applicative information in future.

Reference

Abegglen, C., Ospelt, M., Siegrist, H., 2008. Biological nutrient removal in a small-scale MBR treating household wastewater. Water Res 42(1), 338-346.

Aelterman, P., Versichele, M., Marzorati, M., Boon, N., Verstraete, W., 2008. Loading rate and external resistance control the electricity generation of microbial fuel cells with different three-dimensional anodes. Bioresource technology 99(18), 8895-8902.

Aiken, G.R., McKnight, D.M., Thorn, K., Thurman, E., 1992. Isolation of hydrophilic organic acids from water using nonionic macroporous resins. Organic Geochemistry 18(4), 567-573.

Akamatsu, K., Lu, W., Sugawara, T., Nakao, S.-i., 2010. Development of a novel fouling suppression system in membrane bioreactors using an intermittent electric field. Water Res 44(3), 825-830.

Al-Halbouni, D., Traber, J., Lyko, S., Wintgens, T., Melin, T., Tacke, D., Janot, A., Dott, W., Hollender, J., 2008. Correlation of EPS content in activated sludge at different sludge retention times with membrane fouling phenomena. Water Res 42(6), 1475-1488.

Altschul, S.F., Madden, T.L., Schäffer, A.A., Zhang, J., Zhang, Z., Miller, W., Lipman, D.J., 1997. Gapped BLAST and PSI-BLAST: a new generation of protein database search programs. Nucleic acids research 25(17), 3389-3402.

Apha, A. (1998) WEF (1998) Standard methods for the examination of water and wastewater, American Public Health Association, Washington, DC.

Ashida, N., Ishii, S., Hayano, S., Tago, K., Tsuji, T., Yoshimura, Y., Otsuka, S., Senoo, K., 2010. Isolation of functional single cells from environments using a micromanipulator: application to study denitrifying bacteria. Appl Microbiol Biotechnol 85(4), 1211-1217.

Barker, D.J., Stuckey, D.C., 1999. A review of soluble microbial products (SMP) in wastewater treatment systems. Water Res 33(14), 3063-3082.

Brown, R.K., Harnisch, F., Dockhorn, T., Schröder, U., 2015. Examining sludge production in bioelectrochemical systems treating domestic wastewater. Bioresource technology 198, 913-917.

Burmølle, M., Webb, J.S., Rao, D., Hansen, L.H., Sørensen, S.J., Kjelleberg, S., 2006. Enhanced biofilm formation and increased resistance to antimicrobial agents and

bacterial invasion are caused by synergistic interactions in multispecies biofilms. Appl Environ Microbiol 72(6), 3916-3923.

Calderón, K., Rodelas, B., Cabirol, N., González-López, J., Noyola, A., 2011. Analysis of microbial communities developed on the fouling layers of a membrane-coupled anaerobic bioreactor applied to wastewater treatment. Bioresource technology 102(7), 4618-4627.

Cao, H., Yang, M., Zheng, H., Zhang, J., Zhong, Z., Zhu, J., 2009a. Complex quorum-sensing regulatory systems regulate bacterial growth and symbiotic nodulation in Mesorhizobium tianshanense. Archives of microbiology 191(3), 283-289.

Cao, X., Huang, X., Liang, P., Xiao, K., Zhou, Y., Zhang, X., Logan, B.E., 2009b. A new method for water desalination using microbial desalination cells. Environmental Science & Technology 43(18), 7148-7152.

Caporaso, J.G., Lauber, C.L., Walters, W.A., Berg-Lyons, D., Huntley, J., Fierer, N., Owens, S.M., Betley, J., Fraser, L., Bauer, M., 2012. Ultra-high-throughput microbial community analysis on the Illumina HiSeq and MiSeq platforms. The ISME journal 6(8), 1621-1624.

Chae, K.J., Choi, M.J., Lee, J.W., Kim, K.Y., Kim, I.S., 2009. Effect of different substrates on the performance, bacterial diversity, and bacterial viability in microbial fuel cells. Bioresource technology 100(14), 3518-3525.

Chao, Y., Zhang, T., 2011. Growth behaviors of bacteria in biofouling cake layer in a dead-end microfiltration system. Bioresource technology 102(2), 1549-1555.

Chen, J.P., Yang, C.Z., Zhou, J.H., Wang, X.Y., 2007. Study of the influence of the electric field on membrane flux of a new type of membrane bioreactor. Chemical Engineering Journal 128(2), 177-180.

Chen, W., Westerhoff, P., Leenheer, J.A., Booksh, K., 2003. Fluorescence excitation-emission matrix regional integration to quantify spectra for dissolved organic matter. Environmental Science & Technology 37(24), 5701-5710.

Cheng, K.Y., Ho, G., Cord-Ruwisch, R., 2009a. Anodophilic biofilm catalyzes cathodic oxygen reduction. Environmental Science & Technology 44(1), 518-525.

Cheng, S., Xing, D., Call, D.F., Logan, B.E., 2009b. Direct biological conversion of electrical current into methane by electromethanogenesis. Environmental Science & Technology 43(10), 3953-3958.

Cheng, S., Xing, D., Logan, B.E., 2011. Electricity generation of single-chamber

microbial fuel cells at low temperatures. Biosensors and Bioelectronics 26(5), 1913-1917.

Choi, H., Zhang, K., Dionysiou, D.D., Oerther, D.B., Sorial, G.A., 2006. Effect of activated sludge properties and membrane operation conditions on fouling characteristics in membrane bioreactors. Chemosphere 63(10), 1699-1708.

Chung, K., Okabe, S., 2009. Continuous power generation and microbial community structure of the anode biofilms in a three-stage microbial fuel cell system. Appl Microbiol Biotechnol 83(5), 965-977.

Davis, F., Higson, S.P., 2007. Biofuel cells—recent advances and applications. Biosensors and Bioelectronics 22(7), 1224-1235.

Déziel, E., Comeau, Y., Villemur, R., 2001. Initiation of biofilm formation byPseudomonas aeruginosa 57RP correlates with emergence of hyperpiliated and highly adherent phenotypic variants deficient in swimming, swarming, and twitching motilities. Journal of Bacteriology 183(4), 1195-1204.

Dolch, K., Danzer, J., Kabbeck, T., Bierer, B., Erben, J., Förster, A.H., Maisch, J., Nick, P., Kerzenmacher, S., Gescher, J., 2014. Characterization of microbial current production as a function of microbe–electrode-interaction. Bioresource technology 157, 284-292.

Drews, A., Mante, J., Iversen, V., Vocks, M., Lesjean, B., Kraume, M., 2007. Impact of ambient conditions on SMP elimination and rejection in MBRs. Water Res 41(17), 3850-3858.

Drews, A., 2010. Membrane fouling in membrane bioreactors—characterisation, contradictions, cause and cures. Journal of Membrane Science 363(1), 1-28.

Du, Z., Li, H., Gu, T., 2007. A state of the art review on microbial fuel cells: a promising technology for wastewater treatment and bioenergy. Biotechnology advances 25(5), 464-482.

Duan, L., Moreno-Andrade, I., Huang, C.L., Xia, S., Hermanowicz, S.W., 2009. Effects of short solids retention time on microbial community in a membrane bioreactor. Bioresource technology 100(14), 3489-3496.

Duan, L., Song, Y., Yu, H., Xia, S., Hermanowicz, S.W., 2014. The effect of solids retention times on the characterization of extracellular polymeric substances and soluble microbial products in a submerged membrane bioreactor. Bioresource technology 163, 395-398.

Eboigbodin, K.E., Biggs, C.A., 2008. Characterization of the extracellular polymeric substances produced by Escherichia coli using infrared spectroscopic, proteomic, and aggregation studies. Biomacromolecules 9(2), 686-695.

Elshahed, M.S., Youssef, N.H., Spain, A.M., Sheik, C., Najar, F.Z., Sukharnikov, L.O., Roe, B.A., Davis, J.P., Schloss, P.D., Bailey, V.L., 2008. Novelty and uniqueness patterns of rare members of the soil biosphere. Appl Environ Microbiol 74(17), 5422-5428.

Enos-Berlage, J.L., McCarter, L.L., 2000. Relation of capsular polysaccharide production and colonial cell organization to colony morphology in Vibrio parahaemolyticus. Journal of Bacteriology 182(19), 5513-5520.

Fan, Y., Hu, H., Liu, H., 2007. Sustainable power generation in microbial fuel cells using bicarbonate buffer and proton transfer mechanisms. Environmental Science & Technology 41(23), 8154-8158.

Farias, E.L., Howe, K.J., Thomson, B.M., 2014. Effect of membrane bioreactor solids retention time on reverse osmosis membrane fouling for wastewater reuse. Water Res 49, 53-61.

Feng, L., Li, X., Du, G., Chen, J., 2009. Characterization and fouling properties of exopolysaccharide produced by Klebsiella oxytoca. Bioresource technology 100(13), 3387-3394.

Fontani, G., Gaspari, R., Spencer, N.D., Passerone, D., Crockett, R., 2013. Adsorption and Friction Behavior of Amphiphilic Polymers on Hydrophobic Surfaces. Langmuir 29(15), 4760-4771.

Fornero, J.J., Rosenbaum, M., Cotta, M.A., Angenent, L.T., 2010. Carbon dioxide addition to microbial fuel cell cathodes maintains sustainable catholyte pH and improves anolyte pH, alkalinity, and conductivity. Environmental Science & Technology 44(7), 2728-2734.

Freguia, S., Rabaey, K., Yuan, Z., Keller, J.r., 2008. Syntrophic processes drive the conversion of glucose in microbial fuel cell anodes. Environmental Science & Technology 42(21), 7937-7943.

Gajaraj, S., Hu, Z., 2014. Integration of microbial fuel cell techniques into activated sludge wastewater treatment processes to improve nitrogen removal and reduce sludge production. Chemosphere 117, 151-157.

Gao, D., Fu, Y., Ren, N., 2013a. Tracing biofouling to the structure of the microbial

community and its metabolic products: A study of the three-stage MBR process. Water Res 47(17), 6680-6690.
Gao, D.W., Fu, Y., Tao, Y., Li, X.X., Xing, M., Gao, X.H., Ren, N.Q., 2011a. Linking microbial community structure to membrane biofouling associated with varying dissolved oxygen concentrations. Bioresource technology 102(10), 5626-5633.
Gao, D.W., Wen, Z.D., Li, B., Liang, H., 2013b. Membrane fouling related to microbial community and extracellular polymeric substances at different temperatures. Bioresource technology 143, 172-177.
Gao, D.W., Wang, X.L., Xing, M., 2014a. Dynamic variation of microbial metabolites and community involved in membrane fouling in A/O-MBR. Journal of Membrane Science 458, 157-163.
Gao, D.W., Wen, Z.D., Li, B., Liang, H., 2014b. Microbial community structure characteristics associated membrane fouling in A/O-MBR system. Bioresource technology 154, 87-93.
Gao, W., Leung, K., Qin, W., Liao, B., 2011b. Effects of temperature and temperature shock on the performance and microbial community structure of a submerged anaerobic membrane bioreactor. Bioresource technology 102(19), 8733-8740.
Ge, Z., Ping, Q., He, Z., 2013. Hollow-fiber membrane bioelectrochemical reactor for domestic wastewater treatment. Journal of Chemical Technology and Biotechnology 88(8), 1584-1590.
Gil, J., Túa, L., Rueda, A., Montaño, B., Rodríguez, M., Prats, D., 2010. Monitoring and analysis of the energy cost of an MBR. Desalination 250(3), 997-1001.
Goodfellow, M., Stackebrandt, E. (1991) Nucleic acid techniques in bacterial systematics, J. Wiley.
Guo, W., Ngo, H.H., Li, J., 2012. A mini-review on membrane fouling. Bioresource technology 122, 27-34.
Guo, X., Miao, Y., Wu, B., Ye, L., Yu, H., Liu, S., Zhang, X.X., 2015. Correlation between microbial community structure and biofouling as determined by analysis of microbial community dynamics. Bioresource technology 197, 99-105.
Haberkamp, J., Ruhl, A.S., Ernst, M., Jekel, M., 2007. Impact of coagulation and adsorption on DOC fractions of secondary effluent and resulting fouling behaviour in ultrafiltration. Water Res 41(17), 3794-3802.
Habimana, O., Semião, A., Casey, E., 2014. The role of cell-surface interactions in

bacterial initial adhesion and consequent biofilm formation on nanofiltration/reverse osmosis membranes. Journal of Membrane Science 454, 82-96.
Harnisch, F., Schröder, U., Scholz, F., 2008. The suitability of monopolar and bipolar ion exchange membranes as separators for biological fuel cells. Environmental Science & Technology 42(5), 1740-1746.
Harnisch, F., Schröder, U., 2009. Selectivity versus mobility: separation of anode and cathode in microbial bioelectrochemical systems. ChemSusChem 2(10), 921-926.
Harnisch, F., Warmbier, R., Schneider, R., Schröder, U., 2009. Modeling the ion transfer and polarization of ion exchange membranes in bioelectrochemical systems. Bioelectrochemistry 75(2), 136-141.
Healy, M., Reece, K., Walton, D., Huong, J., Shah, K., Kontoyiannis, D., 2004. Identification to the species level and differentiation between strains of Aspergillus clinical isolates by automated repetitive-sequence-based PCR. Journal of Clinical Microbiology 42(9), 4016-4024.
Herlemann, D.P., Labrenz, M., Jürgens, K., Bertilsson, S., Waniek, J.J., Andersson, A.F., 2011. Transitions in bacterial communities along the 2000 km salinity gradient of the Baltic Sea. The ISME journal 5(10), 1571-1579.
Hu, J., Li, H., Li, H., Liuacd, Y., Song, S., 2016. Role of N-acyl-homoserine lactone (AHL) based quorum sensing on biofilm formation on packing media in wastewater treatment process. RSC Advances 6, 11128-11139.
Huang, J., Zhu, N., Cao, Y., Peng, Y., Wu, P., Dong, W., 2015. Exoelectrogenic Bacterium Phylogenetically Related to Citrobacter freundii, Isolated from Anodic Biofilm of a Microbial Fuel Cell. Applied biochemistry and biotechnology 175(4), 1879-1891.
Huang, J., Shi, Y., Zeng, G., Gu, Y., Chen, G., Shi, L., Hu, Y., Tang, B., Zhou, J., 2016. Acyl-homoserine lactone-based quorum sensing and quorum quenching hold promise to determine the performance of biological wastewater treatments: An overview. Chemosphere 157, 137-151.
Huang, L., Lee, D.J., 2015. Membrane bioreactor: A mini review on recent R&D works. Bioresource technology 194, 383-388.
Huang, L.N., De Wever, H., Diels, L., 2008. Diverse and distinct bacterial communities induced biofilm fouling in membrane bioreactors operated under different conditions. Environmental Science & Technology 42(22), 8360-8366.

Huber, S.A., Balz, A., Abert, M., Pronk, W., 2011. Characterisation of aquatic humic and non-humic matter with size-exclusion chromatography–organic carbon detection–organic nitrogen detection (LC-OCD-OND). Water Res 45(2), 879-885.

Ichihashi, O., Hirooka, K., 2012. Removal and recovery of phosphorus as struvite from swine wastewater using microbial fuel cell. Bioresource technology 114, 303-307.

Ishii, S., Sadowsky, M.J., 2009. Applications of the rep-PCR DNA fingerprinting technique to study microbial diversity, ecology and evolution. Environmental microbiology 11(4), 733-740.

Ishii, S.i., Watanabe, K., Yabuki, S., Logan, B.E., Sekiguchi, Y., 2008. Comparison of electrode reduction activities of Geobacter sulfurreducens and an enriched consortium in an air-cathode microbial fuel cell. Appl Environ Microbiol 74(23), 7348-7355.

Ishii, S.i., Logan, B.E., Sekiguchi, Y., 2012. Enhanced electrode-reducing rate during the enrichment process in an air-cathode microbial fuel cell. Appl Microbiol Biotechnol 94(4), 1087-1094.

Ishii, S.i., Suzuki, S., Norden-Krichmar, T.M., Wu, A., Yamanaka, Y., Nealson, K.H., Bretschger, O., 2013. Identifying the microbial communities and operational conditions for optimized wastewater treatment in microbial fuel cells. Water Res 47(19), 7120-7130.

Ishizaki, S., Fujiki, I., Sano, D., Okabe, S., 2014. External CO2 and Water Supplies for Enhancing Electrical Power Generation of Air-Cathode Microbial Fuel Cells. Environmental Science & Technology 48(19), 11204-11210.

Ishizaki, S., Fukushima, T., Ishii, S., Okabe, S., 2016a. Membrane fouling potentials and cellular properties of bacteria isolated from fouled membranes in a MBR treating municipal wastewater. Water Res 100, 448-457.

Ishizaki, S., Terada, K., Miyake, H., Okabe, S., 2016b. Impact of anodic respiration on biopolymer production and consequent membrane fouling. Environmental Science & Technology.

Ishizaki, S., Ryoichi, S., Okabe, S., *Submitted*. Membrane fouling induced by AHL-mediated soluble microbial product (SMP) formation by fouling-causing bacteria co-cultured with fouling-enhancing bacteria. Submitted.

Jadhav, G., Ghangrekar, M., 2009. Performance of microbial fuel cell subjected to variation in pH, temperature, external load and substrate concentration. Bioresource technology 100(2), 717-723.

Jafary, T., Daud, W.R.W., Ghasemi, M., Kim, B.H., Jahim, J.M., Ismail, M., Lim, S.S., 2015. Biocathode in microbial electrolysis cell; present status and future prospects. Renewable and Sustainable Energy Reviews 47, 23-33.

Jarusutthirak, C., Amy, G., 2006. Role of soluble microbial products (SMP) in membrane fouling and flux decline. Environmental Science & Technology 40(3), 969-974.

Jia, J., Tang, Y., Liu, B., Wu, D., Ren, N., Xing, D., 2013. Electricity generation from food wastes and microbial community structure in microbial fuel cells. Bioresource technology 144, 94-99.

Jiang, T., Kennedy, M.D., Schepper, V.D., Nam, S. N., Nopens, I., Vanrolleghem, P.A., Amy, G., 2010a. Characterization of soluble microbial products and their fouling impacts in membrane bioreactors. Environmental Science & Technology 44(17), 6642-6648.

Jiang, T., Kennedy, M.D., Schepper, V.D., Nam, S.N., Nopens, I., Vanrolleghem, P.A., Amy, G., 2010b. Characterization of soluble microbial products and their fouling impacts in membrane bioreactors. Environmental Science & Technology 44(17), 6642-6648.

Jin, Y.L., Lee, W.N., Lee, C.H., Chang, I.S., Huang, X., Swaminathan, T., 2006. Effect of DO concentration on biofilm structure and membrane filterability in submerged membrane bioreactor. Water Res 40(15), 2829-2836.

Juang, R.S., Chen, H.L., Chen, Y.S., 2008a. Resistance-in-series analysis in cross-flow ultrafiltration of fermentation broths of Bacillus subtilis culture. Journal of Membrane Science 323(1), 193-200.

Juang, R.S., Chen, H.L., Chen, Y.S., 2008b. Membrane fouling and resistance analysis in dead-end ultrafiltration of Bacillus subtilis fermentation broths. Separation and Purification Technology 63(3), 531-538.

Juang, Y.-C., Adav, S.S., Lee, D.-J., 2010a. Strains of internal biofilm in aerobic granular membrane bioreactors. Appl Microbiol Biotechnol 86(6), 1987-1993.

Juang, Y.C., Adav, S.S., Lee, D.J., 2010b. Strains of internal biofilm in aerobic granular membrane bioreactors. Appl Microbiol Biotechnol 86(6), 1987-1993.

Judd, S., 2008. The status of membrane bioreactor technology. Trends in biotechnology 26(2), 109-116.

Jung, S., Regan, J.M., 2011. Influence of external resistance on electrogenesis,

methanogenesis, and anode prokaryotic communities in microbial fuel cells. Appl Environ Microbiol 77(2), 564-571.

Katuri, K.P., Scott, K., Head, I.M., Picioreanu, C., Curtis, T.P., 2011. Microbial fuel cells meet with external resistance. Bioresource technology 102(3), 2758-2766.

Katuri, K.P., Werner, C.M., Jimenez-Sandoval, R.J., Chen, W., Jeon, S., Logan, B.E., Lai, Z., Amy, G.L., Saikaly, P.E., 2014. A novel anaerobic electrochemical membrane bioreactor (AnEMBR) with conductive hollow-fiber membrane for treatment of low-organic strength solutions. Environmental Science & Technology 48(21), 12833-12841.

Khan, S.J., Parveen, F., Ahmad, A., Hashmi, I., Hankins, N., 2013. Performance evaluation and bacterial characterization of membrane bioreactors. Bioresource technology 141, 2-7.

Kim, H.W., Oh, H.S., Kim, S.R., Lee, K.B., Yeon, K.M., Lee, C.H., Kim, S., Lee, J.K., 2013. Microbial population dynamics and proteomics in membrane bioreactors with enzymatic quorum quenching. Appl Microbiol Biotechnol 97(10), 4665-4675.

Kimura, K., Yamato, N., Yamamura, H., Watanabe, Y., 2005. Membrane fouling in pilot-scale membrane bioreactors (MBRs) treating municipal wastewater. Environmental Science & Technology 39(16), 6293-6299.

Kimura, K., Naruse, T., Watanabe, Y., 2009. Changes in characteristics of soluble microbial products in membrane bioreactors associated with different solid retention times: Relation to membrane fouling. Water Res 43(4), 1033-1039.

Kimura, K., Tanaka, I., Nishimura, S., Miyoshi, R., Miyoshi, T., Watanabe, Y., 2012. Further examination of polysaccharides causing membrane fouling in membrane bioreactors (MBRs): Application of lectin affinity chromatography and MALDI-TOF/MS. Water Res 46(17), 5725-5734.

Kimura, K., Tanaka, K., Watanabe, Y., 2014. Microfiltration of different surface waters with/without coagulation: Clear correlations between membrane fouling and hydrophilic biopolymers. Water Res 49, 434-443.

Kimura, K., Nishimura, S.-I., Miyoshi, R., Hoque, A., Miyoshi, T., Watanabe, Y., 2015. Application of glyco-blotting for identification of structures of polysaccharides causing membrane fouling in a pilot-scale membrane bioreactor treating municipal wastewater. Bioresource technology 179, 180-186.

Kobayashi, A., Sano, D., Taniuchi, A., Ishii, S., Okabe, S., 2013. Use of a

genetically-engineered Escherichia coli strain as a sample process control for quantification of the host-specific bacterial genetic markers. Appl Microbiol Biotechnol 97(20), 9165-9173.

Kraume, M., Drews, A., 2010. Membrane bioreactors in waste water treatment–status and trends. Chemical Engineering & Technology 33(8), 1251-1259.

Krieg, T., Sydow, A., Schröder, U., Schrader, J., Holtmann, D., 2014. Reactor concepts for bioelectrochemical syntheses and energy conversion. Trends in biotechnology 32(12), 645-655.

Kumar, R., Singh, L., Wahid, Z.A., Din, M.F.M., 2015. Exoelectrogens in microbial fuel cells toward bioelectricity generation: a review. International Journal of Energy Research 39(8), 1048-1067.

Lade, H., Paul, D., Kweon, J.H., 2014a. Quorum quenching mediated approaches for control of membrane biofouling. Int J Biol Sci 10(5), 550-565.

Lade, H., Paul, D., Kweon, J.H., 2014b. Quorum quenching mediated approaches for control of membrane biofouling. Int J Biol Sci 10(5), 550-565.

Lammers, K., Arbuckle-Keil, G., Dighton, J., 2009. FT-IR study of the changes in carbohydrate chemistry of three New Jersey pine barrens leaf litters during simulated control burning. Soil Biology and Biochemistry 41(2), 340-347.

Le-Clech, P., Chen, V., Fane, T.A., 2006. Fouling in membrane bioreactors used in wastewater treatment. Journal of Membrane Science 284(1), 17-53.

Lee, J., Ahn, W.Y., Lee, C.H., 2001. Comparison of the filtration characteristics between attached and suspended growth microorganisms in submerged membrane bioreactor. Water Res 35(10), 2435-2445.

Lee, K., Lee, S., Lee, S.H., Kim, S.R., Oh, H.S., Park, P.K., Choo, K.H., Kim, Y.W., Lee, J.K., Lee, C.H., 2016. Fungal Quorum Quenching: A Paradigm Shift for Energy Savings in Membrane Bioreactor (MBR) for Wastewater Treatment. Environmental Science & Technology 50(20), 10914-10922.

Lee, S.H., Hong, T.I., Kim, B., Hong, S., Park, H.D., 2014. Comparison of bacterial communities of biofilms formed on different membrane surfaces. World Journal of Microbiology and Biotechnology 30(2), 777-782.

Lee, W., Kang, S., Shin, H., 2003. Sludge characteristics and their contribution to microfiltration in submerged membrane bioreactors. Journal of Membrane Science 216(1), 217-227.

Li, J., Ge, Z., He, Z., 2014. A fluidized bed membrane bioelectrochemical reactor for energy-efficient wastewater treatment. Bioresource technology 167, 310-315.
Li, J., He, Z., 2015. Optimizing the performance of a membrane bio-electrochemical reactor using an anion exchange membrane for wastewater treatment. Environmental Science: Water Research & Technology 1(3), 355-362.
Li, J., Rosenberger, G., He, Z., 2016. Integrated experimental investigation and mathematical modeling of a membrane bioelectrochemical reactor with an external membrane module. Chemical Engineering Journal 287, 321-328.
Li, L., Sun, Y., Yuan, Z., Kong, X., Li, Y., 2013a. Effect of temperature change on power generation of microbial fuel cell. Environmental technology 34(13-14), 1929-1934.
Li, X., Yang, S., 2007. Influence of loosely bound extracellular polymeric substances (EPS) on the flocculation, sedimentation and dewaterability of activated sludge. Water Res 41(5), 1022-1030.
Li, X., Zhu, N., Wang, Y., Li, P., Wu, P., Wu, J., 2013b. Animal carcass wastewater treatment and bioelectricity generation in up-flow tubular microbial fuel cells: effects of HRT and non-precious metallic catalyst. Bioresource technology 128, 454-460.
Lim, B.R., Ahn, K.H., Songprasert, P., Cho, J.W., Lee, S.H., 2004. Microbial community structure of membrane fouling film in an intermittently and continuously aerated submerged membrane bioreactor treating domestic wastewater. Water science and technology 49(2), 255-261.
Lim, S., Kim, S., Yeon, K.M., Sang, B.I., Chun, J., Lee, C.H., 2012. Correlation between microbial community structure and biofouling in a laboratory scale membrane bioreactor with synthetic wastewater. Desalination 287, 209-215.
Lin, H., Peng, W., Zhang, M., Chen, J., Hong, H., Zhang, Y., 2013. A review on anaerobic membrane bioreactors: applications, membrane fouling and future perspectives. Desalination 314, 169-188.
Lin, H., Zhang, M., Wang, F., Meng, F., Liao, B.Q., Hong, H., Chen, J., Gao, W., 2014. A critical review of extracellular polymeric substances (EPSs) in membrane bioreactors: characteristics, roles in membrane fouling and control strategies. Journal of Membrane Science 460, 110-125.
Liu, H., Logan, B.E., 2004. Electricity generation using an air-cathode single chamber microbial fuel cell in the presence and absence of a proton exchange membrane.

Environmental Science & Technology 38(14), 4040-4046.
Liu, H., Cheng, S., Logan, B.E., 2005. Power generation in fed-batch microbial fuel cells as a function of ionic strength, temperature, and reactor configuration. Environmental Science & Technology 39(14), 5488-5493.
Liu, J., Liu, L., Gao, B., Yang, F., 2013. Integration of bio-electrochemical cell in membrane bioreactor for membrane cathode fouling reduction through electricity generation. Journal of Membrane Science 430, 196-202.
Liu, J., Liu, L., Gao, B., Yang, F., Crittenden, J., Ren, N., 2014. Integration of microbial fuel cell with independent membrane cathode bioreactor for power generation, membrane fouling mitigation and wastewater treatment. international journal of hydrogen energy 39(31), 17865-17872.
Liu, L., Tsyganova, O., Lee, D.J., Su, A., Chang, J.S., Wang, A., Ren, N., 2012. Anodic biofilm in single-chamber microbial fuel cells cultivated under different temperatures. international journal of hydrogen energy 37(20), 15792-15800.
Liu, Y., Bond, D.R., 2012. Long-Distance Electron Transfer by G. sulfurreducens Biofilms Results in Accumulation of Reduced c-Type Cytochromes. ChemSusChem 5(6), 1047-1053.
Logan, B.E., Hamelers, B., Rozendal, R., Schröder, U., Keller, J., Freguia, S., Aelterman, P., Verstraete, W., Rabaey, K., 2006. Microbial fuel cells: methodology and technology. Environmental Science & Technology 40(17), 5181-5192.
Logan, B.E., 2009. Exoelectrogenic bacteria that power microbial fuel cells. Nature Reviews Microbiology 7(5), 375-381.
Lorite, G.S., Rodrigues, C.M., De Souza, A.A., Kranz, C., Mizaikoff, B., Cotta, M.A., 2011. The role of conditioning film formation and surface chemical changes on Xylella fastidiosa adhesion and biofilm evolution. Journal of colloid and interface science 359(1), 289-295.
Lovley, D.R., 2012. Electromicrobiology. Annual review of microbiology 66, 391-409.
Lv, J., Wang, Y., Zhong, C., Li, Y., Hao, W., Zhu, J., 2014. The effect of quorum sensing and extracellular proteins on the microbial attachment of aerobic granular activated sludge. Bioresource technology 152, 53-58.
Lyon, D.Y., Buret, F., Vogel, T.M., Monier, J.M., 2010. Is resistance futile? Changing external resistance does not improve microbial fuel cell performance. Bioelectrochemistry 78(1), 2-7.

Ma, J., Wang, Z., Yang, Y., Mei, X., Wu, Z., 2013a. Correlating microbial community structure and composition with aeration intensity in submerged membrane bioreactors by 454 high-throughput pyrosequencing. Water Res 47(2), 859-869.

Ma, J., Wang, Z., He, D., Li, Y., Wu, Z., 2015. Long-term investigation of a novel electrochemical membrane bioreactor for low-strength municipal wastewater treatment. Water Res 78, 98-110.

Ma, Z., Wen, X., Zhao, F., Xia, Y., Huang, X., Waite, D., Guan, J., 2013b. Effect of temperature variation on membrane fouling and microbial community structure in membrane bioreactor. Bioresource technology 133, 462-468.

Malaeb, L., Katuri, K.P., Logan, B.E., Maab, H., Nunes, S.P., Saikaly, P.E., 2013a. A hybrid microbial fuel cell membrane bioreactor with a conductive ultrafiltration membrane biocathode for wastewater treatment. Environmental Science & Technology 47(20), 11821-11828.

Malaeb, L., Le-Clech, P., Vrouwenvelder, J.S., Ayoub, G.M., Saikaly, P.E., 2013b. Do biological-based strategies hold promise to biofouling control in MBRs? Water Res 47(15), 5447-5463.

Malamis, S., Andreadakis, A., 2009. Fractionation of proteins and carbohydrates of extracellular polymeric substances in a membrane bioreactor system. Bioresource technology 100(13), 3350-3357.

Malvankar, N.S., Vargas, M., Nevin, K.P., Franks, A.E., Leang, C., Kim, B.C., Inoue, K., Mester, T., Covalla, S.F., Johnson, J.P., 2011. Tunable metallic-like conductivity in microbial nanowire networks. nature nanotechnology 6(9), 573-579.

Malvankar, N.S., Lovley, D.R., 2014. Microbial nanowires for bioenergy applications. Current opinion in biotechnology 27, 88-95.

Marketon, M.M., Glenn, S.A., Eberhard, A., González, J.E., 2003. Quorum sensing controls exopolysaccharide production in Sinorhizobium meliloti. Journal of Bacteriology 185(1), 325-331.

Martin-Garcia, I., Monsalvo, V., Pidou, M., Le-Clech, P., Judd, S., McAdam, E., Jefferson, B., 2011. Impact of membrane configuration on fouling in anaerobic membrane bioreactors. Journal of Membrane Science 382(1), 41-49.

McAdam, E.J., Judd, S.J., Cartmell, E., Jefferson, B., 2007. Influence of substrate on fouling in anoxic immersed membrane bioreactors. Water Res 41(17), 3859-3867.

McClean, K.H., Winson, M.K., Fish, L., Taylor, A., Chhabra, S.R., Camara, M., Daykin,

M., Lamb, J.H., Swift, S., Bycroft, B.W., 1997. Quorum sensing and Chromobacterium violaceum: exploitation of violacein production and inhibition for the detection of N-acylhomoserine lactones. Microbiology 143(12), 3703-3711.

McLean, J.S., Wanger, G., Gorby, Y.A., Wainstein, M., McQuaid, J., Ishii, S.i., Bretschger, O., Beyenal, H., Nealson, K.H., 2010. Quantification of electron transfer rates to a solid phase electron acceptor through the stages of biofilm formation from single cells to multicellular communities. Environmental Science & Technology 44(7), 2721-2727.

Meng, F., Chae, S.-R., Drews, A., Kraume, M., Shin, H.-S., Yang, F., 2009a. Recent advances in membrane bioreactors (MBRs): membrane fouling and membrane material. Water Res 43(6), 1489-1512.

Meng, F., Chae, S.R., Drews, A., Kraume, M., Shin, H.S., Yang, F., 2009b. Recent advances in membrane bioreactors (MBRs): membrane fouling and membrane material. Water Res 43(6), 1489-1512.

Meng, F., Drews, A., Mehrez, R., Iversen, V., Ernst, M., Yang, F., Jekel, M., Kraume, M., 2009c. Occurrence, source, and fate of dissolved organic matter (DOM) in a pilot-scale membrane bioreactor. Environmental Science & Technology 43(23), 8821-8826.

Mergaert, J., Cnockaert, M.C., Swings, J., 2003. Thermomonas fusca sp. nov. and Thermomonas brevis sp. nov., two mesophilic species isolated from a denitrification reactor with poly (ε-caprolactone) plastic granules as fixed bed, and emended description of the genus Thermomonas. International Journal of Systematic and Evolutionary Microbiology 53(6), 1961-1966.

Michie, I.S., Kim, J.R., Dinsdale, R.M., Guwy, A.J., Premier, G.C., 2011a. The influence of psychrophilic and mesophilic start-up temperature on microbial fuel cell system performance. Energy & Environmental Science 4(3), 1011-1019.

Michie, I.S., Kim, J.R., Dinsdale, R.M., Guwy, A.J., Premier, G.C., 2011b. Operational temperature regulates anodic biofilm growth and the development of electrogenic activity. Appl Microbiol Biotechnol 92(2), 419-430.

Min, B., Román, Ó.B., Angelidaki, I., 2008. Importance of temperature and anodic medium composition on microbial fuel cell (MFC) performance. Biotechnology letters 30(7), 1213-1218.

Miura, T., Sano, D., Suenaga, A., Yoshimura, T., Fuzawa, M., Nakagomi, T., Nakagomi,

O., Okabe, S., 2013. Histo-blood group antigen-like substances of human enteric bacteria as specific adsorbents for human noroviruses. Journal of virology 87(17), 9441-9451.

Miura, Y., Hiraiwa, M.N., Ito, T., Itonaga, T., Watanabe, Y., Okabe, S., 2007a. Bacterial community structures in MBRs treating municipal wastewater: relationship between community stability and reactor performance. Water Res 41(3), 627-637.

Miura, Y., Watanabe, Y., Okabe, S., 2007b. Significance of Chloroflexi in performance of submerged membrane bioreactors (MBR) treating municipal wastewater. Environmental Science & Technology 41(22), 7787-7794.

Miura, Y., Watanabe, Y., Okabe, S., 2007c. Membrane biofouling in pilot-scale membrane bioreactors (MBRs) treating municipal wastewater: impact of biofilm formation. Environmental Science & Technology 41(2), 632-638.

Miura, Y., Okabe, S., 2008. Quantification of cell specific uptake activity of microbial products by uncultured Chloroflexi by microautoradiography combined with fluorescence in situ hybridization. Environmental Science & Technology 42(19), 7380-7386.

Miyahara, M., Hashimoto, K., Watanabe, K., 2013. Use of cassette-electrode microbial fuel cell for wastewater treatment. Journal of bioscience and bioengineering 115(2), 176-181.

Miyoshi, T., Tsuyuhara, T., Ogyu, R., Kimura, K., Watanabe, Y., 2009. Seasonal variation in membrane fouling in membrane bioreactors (MBRs) treating municipal wastewater. Water Res 43(20), 5109-5118.

Miyoshi, T., Aizawa, T., Kimura, K., Watanabe, Y., 2012. Identification of proteins involved in membrane fouling in membrane bioreactors (MBRs) treating municipal wastewater. International Biodeterioration & Biodegradation 75, 15-22.

Molina-Muñoz, M., Poyatos, J., Sánchez-Peinado, M., Hontoria, E., González-López, J., Rodelas, B., 2009. Microbial community structure and dynamics in a pilot-scale submerged membrane bioreactor aerobically treating domestic wastewater under real operation conditions. Science of The Total Environment 407(13), 3994-4003.

Nandasena, K.G., O'Hara, G.W., Tiwari, R.P., Willlems, A., Howieson, J.G., 2007. Mesorhizobium ciceri biovar biserrulae, a novel biovar nodulating the pasture legume Biserrula pelecinus L. International Journal of Systematic and Evolutionary Microbiology 57(5), 1041-1045.

Nevin, K.P., Kim, B.C., Glaven, R.H., Johnson, J.P., Woodard, T.L., Methé, B.A., DiDonato Jr, R.J., Covalla, S.F., Franks, A.E., Liu, A., 2009. Anode biofilm transcriptomics reveals outer surface components essential for high density current production in Geobacter sulfurreducens fuel cells.

Ng, H.Y., Tan, T.W., Ong, S.L., 2006. Membrane fouling of submerged membrane bioreactors: impact of mean cell residence time and the contributing factors. Environmental Science & Technology 40(8), 2706-2713.

Ng, T.C.A., Ng, H.Y., 2010. Characterisation of initial fouling in aerobic submerged membrane bioreactors in relation to physico-chemical characteristics under different flux conditions. Water Res 44(7), 2336-2348.

Ni, B.J., Rittmann, B.E., Yu, H.Q., 2011. Soluble microbial products and their implications in mixed culture biotechnology. Trends in biotechnology 29(9), 454-463.

Oh, H.S., Yeon, K.M., Yang, C.S., Kim, S.R., Lee, C.H., Park, S.Y., Han, J.Y., Lee, J.K., 2012. Control of membrane biofouling in MBR for wastewater treatment by quorum quenching bacteria encapsulated in microporous membrane. Environ Sci Technol 46(9), 4877-4884.

Oh, H.S., Kim, S.R., Cheong, W.S., Lee, C.H., Lee, J.K., 2013. Biofouling inhibition in MBR by Rhodococcus sp. BH4 isolated from real MBR plant. Appl Microbiol Biotechnol 97(23), 10223-10231.

Pandey, R.P., Thakur, A.K., Shahi, V.K., 2014. Sulfonated polyimide/acid-functionalized graphene oxide composite polymer electrolyte membranes with improved proton conductivity and water-retention properties. ACS applied materials & interfaces 6(19), 16993-17002.

Pang, C.M., Hong, P., Guo, H., Liu, W.-T., 2005a. Biofilm formation characteristics of bacterial isolates retrieved from a reverse osmosis membrane. Environmental Science & Technology 39(19), 7541-7550.

Pang, C.M., Hong, P., Guo, H., Liu, W.T., 2005b. Biofilm formation characteristics of bacterial isolates retrieved from a reverse osmosis membrane. Environmental Science & Technology 39(19), 7541-7550.

Pang, C.M., Liu, W.T., 2007. Community structure analysis of reverse osmosis membrane biofilms and the significance of Rhizobiales bacteria in biofouling. Environmental Science & Technology 41(13), 4728-4734.

Pant, D., Van Bogaert, G., Diels, L., Vanbroekhoven, K., 2010. A review of the

substrates used in microbial fuel cells (MFCs) for sustainable energy production. Bioresource technology 101(6), 1533-1543.
Parameswaran, P., Torres, C.I., Lee, H.S., Krajmalnik-Brown, R., Rittmann, B.E., 2009. Syntrophic interactions among anode respiring bacteria (ARB) and Non-ARB in a biofilm anode: electron balances. Biotechnology and Bioengineering 103(3), 513-523.
Park, J.H., Jo, Y., Jang, S.Y., Kwon, H., Irie, Y., Parsek, M.R., Kim, M.H., Choi, S.H., 2015. The cabABC Operon Essential for Biofilm and Rugose Colony Development in Vibrio vulnificus. PLoS Pathog 11(9), e1005192.
Patil, S.A., Harnisch, F., Kapadnis, B., Schröder, U., 2010. Electroactive mixed culture biofilms in microbial bioelectrochemical systems: the role of temperature for biofilm formation and performance. Biosensors and Bioelectronics 26(2), 803-808.
Penteado, E.D., Fernandez-Marchante, C.M., Zaiat, M., Cañizares, P., Gonzalez, E.R., Rodrigo, M.A., 2016. Influence of sludge age on the performance of MFC treating winery wastewater. Chemosphere 151, 163-170.
Pfeffer, C., Larsen, S., Song, J., Dong, M., Besenbacher, F., Meyer, R.L., Kjeldsen, K.U., Schreiber, L., Gorby, Y.A., El-Naggar, M.Y., 2012. Filamentous bacteria transport electrons over centimetre distances. Nature 491(7423), 218-221.
Pham, T., Rabaey, K., Aelterman, P., Clauwaert, P., De Schamphelaire, L., Boon, N., Verstraete, W., 2006. Microbial fuel cells in relation to conventional anaerobic digestion technology. Engineering in Life Sciences 6(3), 285-292.
Pinto, R., Srinivasan, B., Guiot, S., Tartakovsky, B., 2011. The effect of real-time external resistance optimization on microbial fuel cell performance. Water Res 45(4), 1571-1578.
Popat, S.C., Torres, C.I., 2016. Critical transport rates that limit the performance of microbial electrochemistry technologies. Bioresource technology 215, 265-273.
Pribyl, M., Tucek, F., Wilderer, P., Wanner, J., 1997. Amount and nature of soluble refractory organics produced by activated sludge micro-organisms in sequencing batch and continuous flow reactors. Water science and technology 35(1), 27-34.
Qu, Y., Feng, Y., Wang, X., Liu, J., Lv, J., He, W., Logan, B.E., 2012. Simultaneous water desalination and electricity generation in a microbial desalination cell with electrolyte recirculation for pH control. Bioresource technology 106, 89-94.
Rabaey, K., Verstraete, W., 2005. Microbial fuel cells: novel biotechnology for energy generation. Trends in biotechnology 23(6), 291-298.

Rabaey, K., Butzer, S., Brown, S., Keller, J.r., Rozendal, R.A., 2010. High current generation coupled to caustic production using a lamellar bioelectrochemical system. Environmental Science & Technology 44(11), 4315-4321.

Ramesh, A., Lee, D., Lai, J., 2007. Membrane biofouling by extracellular polymeric substances or soluble microbial products from membrane bioreactor sludge. Appl Microbiol Biotechnol 74(3), 699-707.

Ramsay, J.P., Sullivan, J.T., Jambari, N., Ortori, C.A., Heeb, S., Williams, P., Barrett, D.A., Lamont, I.L., Ronson, C.W., 2009. A LuxRI-family regulatory system controls excision and transfer of the Mesorhizobium loti strain R7A symbiosis island by activating expression of two conserved hypothetical genes. Molecular microbiology 73(6), 1141-1155.

Rashid, M.H., Kornberg, A., 2000. Inorganic polyphosphate is needed for swimming, swarming, and twitching motilities of Pseudomonas aeruginosa. Proceedings of the National Academy of Sciences 97(9), 4885-4890.

Rathnayake, R.M., Oshiki, M., Ishii, S., Segawa, T., Satoh, H., Okabe, S., 2015. Effects of dissolved oxygen and pH on nitrous oxide production rates in autotrophic partial nitrification granules. Bioresource technology.

Reguera, G., Nevin, K.P., Nicoll, J.S., Covalla, S.F., Woodard, T.L., Lovley, D.R., 2006. Biofilm and nanowire production leads to increased current in Geobacter sulfurreducens fuel cells. Appl Environ Microbiol 72(11), 7345-7348.

Ren, L., Ahn, Y., Logan, B.E., 2014. A two-stage microbial fuel cell and anaerobic fluidized bed membrane bioreactor (MFC-AFMBR) system for effective domestic wastewater treatment. Environmental Science & Technology 48(7), 4199-4206.

Ren, Z., Ramasamy, R.P., Cloud-Owen, S.R., Yan, H., Mench, M.M., Regan, J.M., 2011a. Time-course correlation of biofilm properties and electrochemical performance in single-chamber microbial fuel cells. Bioresource technology 102(1), 416-421.

Ren, Z., Yan, H., Wang, W., Mench, M.M., Regan, J.M., 2011b. Characterization of microbial fuel cells at microbially and electrochemically meaningful time scales. Environmental Science & Technology 45(6), 2435-2441.

Rickard, A.H., McBain, A.J., Stead, A.T., Gilbert, P., 2004. Shear rate moderates community diversity in freshwater biofilms. Appl Environ Microbiol 70(12), 7426-7435.

Rinaudi, L.V., González, J.E., 2009. The low-molecular-weight fraction of

exopolysaccharide II from Sinorhizobium meliloti is a crucial determinant of biofilm formation. Journal of Bacteriology 191(23), 7216-7224.

Rismani-Yazdi, H., Carver, S.M., Christy, A.D., Tuovinen, O.H., 2008. Cathodic limitations in microbial fuel cells: an overview. Journal of Power Sources 180(2), 683-694.

Rismani-Yazdi, H., Christy, A.D., Carver, S.M., Yu, Z., Dehority, B.A., Tuovinen, O.H., 2011. Effect of external resistance on bacterial diversity and metabolism in cellulose-fed microbial fuel cells. Bioresource technology 102(1), 278-283.

Rosenberger, S., Evenblij, H., Te Poele, S., Wintgens, T., Laabs, C., 2005. The importance of liquid phase analyses to understand fouling in membrane assisted activated sludge processes—six case studies of different European research groups. Journal of Membrane Science 263(1), 113-126.

Rosenberger, S., Laabs, C., Lesjean, B., Gnirss, R., Amy, G., Jekel, M., Schrotter, J.C., 2006. Impact of colloidal and soluble organic material on membrane performance in membrane bioreactors for municipal wastewater treatment. Water Res 40(4), 710-720.

Rozendal, R.A., Hamelers, H.V., Buisman, C.J., 2006. Effects of membrane cation transport on pH and microbial fuel cell performance. Environmental Science & Technology 40(17), 5206-5211.

Rozendal, R.A., Hamelers, H.V., Rabaey, K., Keller, J., Buisman, C.J., 2008. Towards practical implementation of bioelectrochemical wastewater treatment. Trends in biotechnology 26(8), 450-459.

Ruiz-Martinez, A., Garcia, N.M., Romero, I., Seco, A., Ferrer, J., 2012. Microalgae cultivation in wastewater: nutrient removal from anaerobic membrane bioreactor effluent. Bioresource technology 126, 247-253.

Saitou, N., Nei, M., 1987. The neighbor-joining method: a new method for reconstructing phylogenetic trees. Molecular biology and evolution 4(4), 406-425.

Sakuragi, Y., Kolter, R., 2007. Quorum-sensing regulation of the biofilm matrix genes (pel) of Pseudomonas aeruginosa. Journal of Bacteriology 189(14), 5383-5386.

Schröder, U., 2007. Anodic electron transfer mechanisms in microbial fuel cells and their energy efficiency. Physical Chemistry Chemical Physics 9(21), 2619-2629.

Shapiro, O.H., Kushmaro, A., Brenner, A., 2010. Bacteriophage predation regulates microbial abundance and diversity in a full-scale bioreactor treating industrial wastewater. The ISME journal 4(3), 327-336.

Sharma, V., Kundu, P., 2010. Biocatalysts in microbial fuel cells. Enzyme and Microbial Technology 47(5), 179-188.

Shaw, P.D., Ping, G., Daly, S.L., Cha, C., Cronan, J.E., Rinehart, K.L., Farrand, S.K., 1997. Detecting and characterizing N-acyl-homoserine lactone signal molecules by thin-layer chromatography. Proceedings of the National Academy of Sciences 94(12), 6036-6041.

Shen, L., Yao, Y., Meng, F., 2014. Reactor performance and microbial ecology of a nitritation membrane bioreactor. Journal of Membrane Science 462, 139-146.

Shen, Y.X., Xiao, K., Liang, P., Sun, J.Y., Sai, S.J., Huang, X., 2012. Characterization of soluble microbial products in 10 large-scale membrane bioreactors for municipal wastewater treatment in China. Journal of Membrane Science 415, 336-345.

Shimoyama, T., Komukai, S., Yamazawa, A., Ueno, Y., Logan, B.E., Watanabe, K., 2008. Electricity generation from model organic wastewater in a cassette-electrode microbial fuel cell. Appl Microbiol Biotechnol 80(2), 325-330.

Shrout, J.D., Nerenberg, R., 2012. Monitoring bacterial twitter: does quorum sensing determine the behavior of water and wastewater treatment biofilms? Environmental Science & Technology 46(4), 1995-2005.

Silva, A.F., Antunes, S., Saunders, A., Freitas, F., Vieira, A., Galinha, C.F., Nielsen, P.H., Crespo, M.T.B., Carvalho, G., 2016. Impact of sludge retention time on the fine composition of the microbial community and extracellular polymeric substances in a membrane bioreactor. Appl Microbiol Biotechnol 100(19), 8507-8521.

Sleutels, T.H., Hamelers, H.V., Rozendal, R.A., Buisman, C.J., 2009. Ion transport resistance in microbial electrolysis cells with anion and cation exchange membranes. international journal of hydrogen energy 34(9), 3612-3620.

Snider, R.M., Strycharz-Glaven, S.M., Tsoi, S.D., Erickson, J.S., Tender, L.M., 2012. Long-range electron transport in Geobacter sulfurreducens biofilms is redox gradient-driven. Proceedings of the National Academy of Sciences 109(38), 15467-15472.

Someya, N., Morohoshi, T., Okano, N., Otsu, E., Usuki, K., Sayama, M., Sekiguchi, H., Ikeda, T., Ishida, S., 2009. Distribution of N-acylhomoserine lactone-producing fluorescent pseudomonads in the phyllosphere and rhizosphere of potato (Solanum tuberosum L.). Microbes and environments 24(4), 305-314.

Su, X., Tian, Y., Sun, Z., Lu, Y., Li, Z., 2013. Performance of a combined system of

microbial fuel cell and membrane bioreactor: wastewater treatment, sludge reduction, energy recovery and membrane fouling. Biosensors and Bioelectronics 49, 92-98.

Sun, D., Wang, A., Cheng, S., Yates, M., Logan, B.E., 2014a. Geobacter anodireducens sp. nov., an exoelectrogenic microbe in bioelectrochemical systems. International Journal of Systematic and Evolutionary Microbiology 64(Pt 10), 3485-3491.

Sun, D., Cheng, S., Wang, A., Li, F., Logan, B.E., Cen, K., 2015. Temporal-spatial changes in viabilities and electrochemical properties of anode biofilms. Environmental Science & Technology 49(8), 5227-5235.

Sun, D., Chen, J., Huang, H., Liu, W., Ye, Y., Cheng, S., 2016. The effect of biofilm thickness on electrochemical activity of Geobacter sulfurreducens. international journal of hydrogen energy.

Sun, J., Xiao, K., Mo, Y., Liang, P., Shen, Y., Zhu, N., Huang, X., 2014b. Seasonal characteristics of supernatant organics and its effect on membrane fouling in a full-scale membrane bioreactor. Journal of Membrane Science 453, 168-174.

Sweity, A., Ying, W., Ali-Shtayeh, M.S., Yang, F., Bick, A., Oron, G., Herzberg, M., 2011. Relation between EPS adherence, viscoelastic properties, and MBR operation: Biofouling study with QCM-D. Water Res 45(19), 6430-6440.

Tan, C.H., Koh, K.S., Xie, C., Tay, M., Zhou, Y., Williams, R., Ng, W.J., Rice, S.A., Kjelleberg, S., 2014. The role of quorum sensing signalling in EPS production and the assembly of a sludge community into aerobic granules. The ISME journal 8(6), 1186-1197.

Tang, S., Wang, Z., Wu, Z., Zhou, Q., 2010. Role of dissolved organic matters (DOM) in membrane fouling of membrane bioreactors for municipal wastewater treatment. Journal of hazardous materials 178(1), 377-384.

Tian, H.L., Zhao, J.Y., Zhang, H.Y., Chi, C.Q., Li, B.A., Wu, X.L., 2015a. Bacterial community shift along with the changes in operational conditions in a membrane-aerated biofilm reactor. Appl Microbiol Biotechnol 99(7), 3279-3290.

Tian, J.Y., Ernst, M., Cui, F., Jekel, M., 2013. Correlations of relevant membrane foulants with UF membrane fouling in different waters. Water Res 47(3), 1218-1228.

Tian, Y., Chen, L., Jiang, T., 2011a. Characterization and modeling of the soluble microbial products in membrane bioreactor. Separation and Purification Technology 76(3), 316-324.

Tian, Y., Chen, L., Zhang, S., Zhang, S., 2011b. A systematic study of soluble

microbial products and their fouling impacts in membrane bioreactors. Chemical Engineering Journal 168(3), 1093-1102.

Tian, Y., Ji, C., Wang, K., Le-Clech, P., 2014. Assessment of an anaerobic membrane bio-electrochemical reactor (AnMBER) for wastewater treatment and energy recovery. Journal of Membrane Science 450, 242-248.

Tian, Y., Li, H., Li, L., Su, X., Lu, Y., Zuo, W., Zhang, J., 2015b. In-situ integration of microbial fuel cell with hollow-fiber membrane bioreactor for wastewater treatment and membrane fouling mitigation. Biosensors and Bioelectronics 64, 189-195.

Torres, C.I., Kato Marcus, A., Rittmann, B.E., 2008a. Proton transport inside the biofilm limits electrical current generation by anode-respiring bacteria. Biotechnology and Bioengineering 100(5), 872-881.

Torres, C.I., Lee, H.S., Rittmann, B.E., 2008b. Carbonate species as OH^- carriers for decreasing the pH gradient between cathode and anode in biological fuel cells. Environmental Science & Technology 42(23), 8773-8777.

Torres, C.I., Krajmalnik-Brown, R., Parameswaran, P., Marcus, A.K., Wanger, G., Gorby, Y.A., Rittmann, B.E., 2009. Selecting anode-respiring bacteria based on anode potential: phylogenetic, electrochemical, and microscopic characterization. Environmental Science & Technology 43(24), 9519-9524.

Torres, C.I., Marcus, A.K., Lee, H.S., Parameswaran, P., Krajmalnik-Brown, R., Rittmann, B.E., 2010. A kinetic perspective on extracellular electron transfer by anode-respiring bacteria. FEMS Microbiology Reviews 34(1), 3-17.

Tran, N.H., Ngo, H.H., Urase, T., Gin, K.Y.H., 2015. A critical review on characterization strategies of organic matter for wastewater and water treatment processes. Bioresource technology 193, 523-533.

Valle, A., Bailey, M.J., Whiteley, A.S., Manefield, M., 2004. N-acyl-L-homoserine lactones (AHLs) affect microbial community composition and function in activated sludge. Environmental microbiology 6(4), 424-433.

van den Brink, P., Satpradit, O.A., van Bentem, A., Zwijnenburg, A., Temmink, H., van Loosdrecht, M., 2011. Effect of temperature shocks on membrane fouling in membrane bioreactors. Water Res 45(15), 4491-4500.

Vanysacker, L., Boerjan, B., Declerck, P., Vankelecom, I.F., 2014a. Biofouling ecology as a means to better understand membrane biofouling. Appl Microbiol Biotechnol 98(19), 8047-8072.

Vanysacker, L., Declerck, P., Bilad, M., Vankelecom, I., 2014b. Biofouling on microfiltration membranes in MBRs: Role of membrane type and microbial community. Journal of Membrane Science 453, 394-401.

Villain, M., Marrot, B., 2013. Influence of sludge retention time at constant food to microorganisms ratio on membrane bioreactor performances under stable and unstable state conditions. Bioresource technology 128, 134-144.

Villain, M., Bourven, I., Guibaud, G., Marrot, B., 2014. Impact of synthetic or real urban wastewater on membrane bioreactor (MBR) performances and membrane fouling under stable conditions. Bioresource technology 155, 235-244.

Wang, H., Park, J.D., Ren, Z.J., 2015. Practical Energy Harvesting for Microbial Fuel Cells: A Review. Environmental Science & Technology 49(6), 3267-3277.

Wang, J., Zheng, Y., Jia, H., Zhang, H., 2014. Bioelectricity generation in an integrated system combining microbial fuel cell and tubular membrane reactor: Effects of operation parameters performing a microbial fuel cell-based biosensor for tubular membrane bioreactor. Bioresource technology 170, 483-490.

Wang, Y.-K., Sheng, G.-P., Li, W.-W., Huang, Y.-X., Yu, Y.-Y., Zeng, R.J., Yu, H.-Q., 2011a. Development of a novel bioelectrochemical membrane reactor for wastewater treatment. Environmental Science & Technology 45(21), 9256-9261.

Wang, Y.K., Sheng, G.P., Li, W.W., Huang, Y.X., Yu, Y.Y., Zeng, R.J., Yu, H.Q., 2011b. Development of a novel bioelectrochemical membrane reactor for wastewater treatment. Environmental Science & Technology 45(21), 9256-9261.

Wang, Y.K., Li, W.W., Sheng, G.P., Shi, B.J., Yu, H.Q., 2013. In-situ utilization of generated electricity in an electrochemical membrane bioreactor to mitigate membrane fouling. Water Res 47(15), 5794-5800.

Wang, Y.P., Liu, X.W., Li, W.W., Li, F., Wang, Y.K., Sheng, G.P., Zeng, R.J., Yu, H.Q., 2012a. A microbial fuel cell–membrane bioreactor integrated system for cost-effective wastewater treatment. Applied Energy 98, 230-235.

Wang, Z., Chu, J., Song, Y., Cui, Y., Zhang, H., Zhao, X., Li, Z., Yao, J., 2009a. Influence of operating conditions on the efficiency of domestic wastewater treatment in membrane bioreactors. Desalination 245(1), 73-81.

Wang, Z., Wu, Z., Tang, S., 2009b. Extracellular polymeric substances (EPS) properties and their effects on membrane fouling in a submerged membrane bioreactor. Water Res 43(9), 2504-2512.

Wang, Z., Wu, Z., Tang, S., 2009c. Characterization of dissolved organic matter in a submerged membrane bioreactor by using three-dimensional excitation and emission matrix fluorescence spectroscopy. Water Res 43(6), 1533-1540.

Wang, Z., Wu, Z., Tang, S., 2010. Impact of temperature seasonal change on sludge characteristics and membrane fouling in a submerged membrane bioreactor. Separation Science and Technology 45(7), 920-927.

Wang, Z., Mei, X., Ma, J., Wu, Z., 2012b. Recent advances in microbial fuel cells integrated with sludge treatment. Chemical Engineering & Technology 35(10), 1733-1743.

Weerasekara, N.A., Choo, K.H., Lee, C.H., 2016. Biofouling control: Bacterial quorum quenching versus chlorination in membrane bioreactors. Water Res 103, 293-301.

Werner, C.M., Katuri, K.P., Hari, A.R., Chen, W., Lai, Z., Logan, B.E., Amy, G.L., Saikaly, P.E., 2016. Graphene-coated hollow fiber membrane as the cathode in anaerobic electrochemical membrane bioreactors–Effect of configuration and applied voltage on performance and membrane fouling. Environmental Science & Technology 50(8), 4439-4447.

Win, T.T., Kim, H., Cho, K., Song, K.G., Park, J., 2016. Monitoring the microbial community shift throughout the shock changes of hydraulic retention time in an anaerobic moving bed membrane bioreactor. Bioresource technology 202, 125-132.

Wu, B., Yi, S., Fane, A.G., 2011. Microbial behaviors involved in cake fouling in membrane bioreactors under different solids retention times. Bioresource technology 102(3), 2511-2516.

Xia, S., Duan, L., Song, Y., Li, J., Piceno, Y.M., Andersen, G.L., Alvarez-Cohen, L., Moreno-Andrade, I., Huang, C.L., Hermanowicz, S.W., 2010. Bacterial community structure in geographically distributed biological wastewater treatment reactors. Environmental Science & Technology 44(19), 7391-7396.

Xiong, Y., Liu, Y., 2010. Biological control of microbial attachment: a promising alternative for mitigating membrane biofouling. Appl Microbiol Biotechnol 86(3), 825-837.

Xu, L., Zhang, G.Q., Yuan, G.E., Liu, H.Y., Liu, J.D., Yang, F.L., 2015. Anti-fouling performance and mechanism of anthraquinone/polypyrrole composite modified membrane cathode in a novel MFC–aerobic MBR coupled system. RSC Advances 5(29), 22533-22543.

Yamamura, H., Kimura, K., Watanabe, Y., 2007. Mechanism involved in the evolution of physically irreversible fouling in microfiltration and ultrafiltration membranes used for drinking water treatment. Environmental Science & Technology 41(19), 6789-6794.
Yamamura, H., Okimoto, K., Kimura, K., Watanabe, Y., 2014. Hydrophilic fraction of natural organic matter causing irreversible fouling of microfiltration and ultrafiltration membranes. Water Res 54, 123-136.
Yang, M., Sun, K., Zhou, L., Yang, R., Zhong, Z., Zhu, J., 2009. Functional analysis of three AHL autoinducer synthase genes in Mesorhizobium loti reveals the important role of quorum sensing in symbiotic nodulation. Canadian journal of microbiology 55(2), 210-214.
Yang, Y., Xiang, Y., Sun, G., Wu, W.-M., Xu, M., 2014. Electron acceptor-dependent respiratory and physiological stratifications in biofilms. Environmental Science & Technology 49(1), 196-202.
Yeon, K.M., Cheong, W.S., Oh, H.S., Lee, W.N., Hwang, B.K., Lee, C.H., Beyenal, H., Lewandowski, Z., 2008. Quorum sensing: a new biofouling control paradigm in a membrane bioreactor for advanced wastewater treatment. Environmental Science & Technology 43(2), 380-385.
Yildiz, F.H., Schoolnik, G.K., 1999. Vibrio cholerae O1 El Tor: identification of a gene cluster required for the rugose colony type, exopolysaccharide production, chlorine resistance, and biofilm formation. Proceedings of the National Academy of Sciences 96(7), 4028-4033.
Yildiz, F.H., Visick, K.L., 2009. Vibrio biofilms: so much the same yet so different. Trends in microbiology 17(3), 109-118.
Yoshida, K., Tashiro, Y., May, T., Okabe, S., 2015. Impacts of hydrophilic colanic acid on bacterial attachment to microfiltration membranes and subsequent membrane biofouling. Water Res 76, 33-42.
You, S.J., Ren, N.Q., Zhao, Q.L., Kiely, P.D., Wang, J.Y., Yang, F.L., Fu, L., Peng, L., 2009. Improving phosphate buffer-free cathode performance of microbial fuel cell based on biological nitrification. Biosensors and Bioelectronics 24(12), 3698-3701.
Yu, H., Xu, G., Qu, F., Li, G., Liang, H., 2016. Effect of solid retention time on membrane fouling in membrane bioreactor: from the perspective of quorum sensing and quorum quenching. Appl Microbiol Biotechnol 100(18), 7887-7897.
Yu, J., Seon, J., Park, Y., Cho, S., Lee, T., 2012. Electricity generation and microbial

community in a submerged-exchangeable microbial fuel cell system for low-strength domestic wastewater treatment. Bioresource technology 117, 172-179.
Yu, J., Park, Y., Lee, T., 2015. Electron flux and microbial community in microbial fuel cells (open-circuit and closed-circuit modes) and fermentation. J Ind Microbiol Biotechnol 42(7), 979-983.
Yuan, H., He, Z., 2015. Integrating Membrane Filtration into Bioelectrochemical Systems as Next Generation Energy-Efficient Wastewater Treatment Technologies for Water Reclamation: a Review. Bioresource technology.
Zaky, A., Escobar, I., Motlagh, A.M., Gruden, C., 2012. Determining the influence of active cells and conditioning layer on early stage biofilm formation using cellulose acetate ultrafiltration membranes. Desalination 286, 296-303.
Zhang, F., Ge, Z., Grimaud, J., Hurst, J., He, Z., 2013. Long-term performance of liter-scale microbial fuel cells treating primary effluent installed in a municipal wastewater treatment facility. Environmental Science & Technology 47(9), 4941-4948.
Zhang, G., Zhang, H., Ma, Y., Yuan, G., Yang, F., Zhang, R., 2014a. Membrane filtration biocathode microbial fuel cell for nitrogen removal and electricity generation. Enzyme and Microbial Technology 60, 56-63.
Zhang, K., Choi, H., Dionysiou, D.D., Sorial, G.A., Oerther, D.B., 2006. Identifying pioneer bacterial species responsible for biofouling membrane bioreactors. Environmental microbiology 8(3), 433-440.
Zhang, L., Zhou, S., Zhuang, L., Li, W., Zhang, J., Lu, N., Deng, L., 2008. Microbial fuel cell based on Klebsiella pneumoniae biofilm. Electrochemistry communications 10(10), 1641-1643.
Zhang, L., Zhu, X., Li, J., Liao, Q., Ye, D., 2011. Biofilm formation and electricity generation of a microbial fuel cell started up under different external resistances. Journal of Power Sources 196(15), 6029-6035.
Zhang, L., Shen, J., Wang, L., Ding, L., Xu, K., Ren, H., 2014b. Stable operation of microbial fuel cells at low temperatures (5–10° C) with light exposure and its anodic microbial analysis. Bioprocess and biosystems engineering 37(5), 819-827.
Zhang, X., Bishop, P.L., 2003. Biodegradability of biofilm extracellular polymeric substances. Chemosphere 50(1), 63-69.
Zhang, Y., Yu, X., Gong, S., Ye, C., Fan, Z., Lin, H., 2014c. Antibiofilm activity of Bacillus pumilus SW9 against initial biofouling on microfiltration membranes. Appl

Microbiol Biotechnol 98(3), 1309-1320.
Zheng, H., Zhong, Z., Lai, X., Chen, W.X., Li, S., Zhu, J., 2006. A LuxR/LuxI-type quorum-sensing system in a plant bacterium, Mesorhizobium tianshanense, controls symbiotic nodulation. Journal of Bacteriology 188(5), 1943-1949.
Zhou, G., Zhou, Y., Zhou, G., Lu, L., Wan, X., Shi, H., 2015a. Assessment of a novel overflow-type electrochemical membrane bioreactor (EMBR) for wastewater treatment, energy recovery and membrane fouling mitigation. Bioresource technology 196, 648-655.
Zhou, Z., Meng, F., Liang, S., Ni, B.J., Jia, X., Li, S., Song, Y., Huang, G., 2012. Role of microorganism growth phase in the accumulation and characteristics of biomacromolecules (BMM) in a membrane bioreactor. RSC Advances 2(2), 453-460.
Zhou, Z., Meng, F., He, X., Chae, S.R., An, Y., Jia, X., 2015b. Metaproteomic Analysis of Biocake Proteins To Understand Membrane Fouling in a Submerged Membrane Bioreactor. Environmental Science & Technology 49(2), 1068-1077.
Zuo, K., Wang, Z., Chen, X., Zhang, X., Zuo, J., Liang, P., Huang, X., 2016. Self-driven desalination and advanced treatment of wastewater in a modularized filtration air cathode microbial desalination cell. Environmental Science & Technology.
Zuthi, M.F.R., Guo, W., Ngo, H., Nghiem, L., Hai, F., 2013. Enhanced biological phosphorus removal and its modeling for the activated sludge and membrane bioreactor processes. Bioresource technology 139, 363-374.